POLITECNICO DI TORINO

Corso di Laurea Magistrale in Ingegneria Biomedica

Master Thesis

Assessment of the swallowing function through High-Density surface EMG

Advisors:

Eng. Alberto Botter
Prof. Marco Gazzoni
Dr. Mauro Viganò

Candidate:

Alessandra Giangrande

Academic Year 2018/2019

To my loving Parents,

my greatest source of inspiration.

To my Grandmothers,

the mentors of my self-improvement.

Acknowledgments

First of all, I would like to express my sincere gratitude to the Casa di Cura Privata del Policlinico di Milano for their professionalism and complete availability to carry out the present project. Thanks to my supervisor, Mauro, for the continuous guidance during this work. It has been a pleasure to work with a so efficient multidisciplinary team.

I am sincerely thankful to my temporary-research group: the Laboratory for Engineering of the Neuromuscular System. I would like to give special attention to my advisors: Marco Gazzoni and Alberto Botter. Thanks for giving me the opportunity to take part of such a wonderful team. I'm especially grateful to my tutor, who taught me so much. Thank you for your precious support, your encouragement and critical comments. Thanks for gradually introducing me in this unknown, but extraordinary world. Above all, thanks for your guidance in the life choices of this difficult period. You have been more than a tutor. My gratitude is also extended to Giacinto Luigi Cerone and Davide Mastrapasqua for their technical and moral support and to the other LISiN people for sharing with me this journey.

Ringraziamenti

Ed anche questa esperienza, così travolgente ed emozionante, volge al termine. Sono stati mesi di duro lavoro, di crescita personale, oltre che professionale. Al termine di questo intenso viaggio, credo sia doveroso esprimere la mia gratitudine verso chi mi ha supportato e sopportato in questo capitolo della mia vita.

Come non iniziare da lui, la mia certezza, la mia spalla, la mia ossimorica unità complementare. Grazie, Fabio, per non avermi mai fatto sentire sola, dove ci sei tu c'è sempre stata casa, anche quando una casa effettivamente non ce l'ho avuta. Stare lontano dai propri cari non è facile, ma tu hai sempre cercato di colmare tutte le assenze ed io ti sono grata per questo. Grazie per essermi stato accanto in questo percorso senza mai esitare, per aver sempre creduto in me, incoraggiandomi in ogni mia scelta. Mi dici che la cosa che più ti piace è la mia capacità portare il sorriso dovunque, ma non sai che quel sorriso è anche merito tuo. Iniziare questo percorso mano nella mano è stato un privilegio e non vedo l'ora di affrontare tutto ciò che la vita ci sta riservando, insieme. D'altronde, niente potrà essere speciale, se non condiviso.

Grazie mamma e papà per aver permesso di realizzare i miei sogni. Non ho mai visto due fari così luminosi come voi. Grazie per essermi stati vicino, sempre in

punta di piedi, grazie ai vostri Whatsapp post-esame, grazie alla vostra tempestività in ogni momento di bisogno.
A mio padre, la cui calma e fermezza sono quotidianamente fonte di ispirazione per me. Grazie per essere il mio complice perfetto, non smettere mai di farmi sentire la bimba che giocava con i tuoi capelli.
A mia madre, una Donna con la D maiuscola. Alla sua forza, alla sua compostezza, alla sua capacità di spronarmi continuamente. Se sono arrivata fin qui, è soprattutto grazie a questo.
Grazie per tutto l'amore incondizionato. Il vero traguardo lo raggiungo ogni volta che riesco a mettere in pratica almeno un terzo di quanto mi avete insegnato.

A mia sorella Francesca, ai nostri battibecchi, ai nostri punti di vista così diversi. È vero, a volte siamo proprio come cane e gatto, ma io con te e tu con me. Grazie per aver condiviso gioie e dolori di questo percorso, grazie per essermi stata accanto sempre, ma soprattutto in questo periodo. Grazie per i pranzi, le cene, le chiamate alla guardia medica.. Ah no, forse quelle no. Lo sai che anche se ti abbraccio poco e non te lo dico mai, ti voglio un bene infinito.

Alla mia saggia zia Carla, alla sua interminabile pazienza. Le giornate non sono mai iniziate davvero senza il suo "Buongiorno". Grazie per la carica che mi hai sempre trasmesso, per avermi fatto capire che, in fondo, gli ostacoli esistono soltanto per essere superati.

A mia nonna Chicca. Grazie per lo stupore in videochiamata, per la gioia incontenibile nel rivedermi e per le lacrime nel vedermi andare via. Grazie, nonna, per avermi chiesto se avevo mangiato prima ancora di chiedermi come stessi perché "il sacco vuoto non si regge da solo". Custodisco gelosamente il nostro legame, è la cosa più preziosa che ho.
A mia nonna Tetta, presente nonostante la fisica assenza. Sarà sempre la mia silenziosa guida.

Ai miei zii, a mio cugino. Grazie per esservi sempre presi cura di me, anche a distanza, per aver sempre fatto il tifo per me, spronandomi a non mollare.

A Cristina, Paolo e Federica. Grazie per la vostra premura, per il vostro affetto, per la vostra vicinanza. Grazie per avermi accolto come una figlia, siete diventati la mia seconda famiglia.

A Beatrice, la mia migliore amica since 2001, così lontana, ma così vicina. Anche se non ha mai trovato un giorno per venirmi a trovare, non posso dire nulla su come sia riuscita ad abbattere le distanze. 1100 km sono tantissimi, ma la sua disponibilità ad ascoltarmi ad ogni ora del giorno e della notte ha saputo superarli tutti. Grazie per avermi fatto sentire sempre un po' meno esaurita di te (della serie: non c'è mai fine al peggio), per aver razionalizzato insieme a me ogni problema che mi sembrava insormontabile. Grazie per aver creduto in me più di quanto ci credessi io. Sei la mia ancora di salvezza, in ogni momento. Grazie per esserci stata senza che te lo chiedessi.

Alle mie amiche Nora e Marta, agli stickers della prima e alle lunghe note audio della seconda. Grazie per aver trovato sempre il modo di farmi sorridere e di essere presenti anche se sparse per l'Italia. Grazie per avermi dato la certezza di poter contare sempre su di voi, per aver condiviso con me ogni piccolo nostro traguardo. Scusate l'assenza dell'ultimo periodo, ricordatevi sempre di essere le mie migliori amiche, non potrò mai fare a meno di voi.

Al mio toothbrush-group: i pezzi perfetti di un meraviglioso puzzle.

Ad Enrica, più di una collega, la mia amica sincera, pura e generosa. Sei sempre stata la piccola Eri, così dolce ed educata, ma altrettanto forte, determinata ed ambiziosa. Grazie per essere stata il mio punto di riferimento, non solo in questa esperienza, ma in tutto il nostro percorso accademico. Sei stata la ragione dell'utilizzo improprio della prima persona plurale in ogni discorso, lo sai che, per me, è sempre stato un noi. Grazie per tutti i saggi consigli, le lunghe chiacchierate, le complesse organizzazioni delle sessioni. Senza di te non sarebbe

stato (e soprattutto non sarà) lo stesso. Sono convinta che questa esperienza sia solo il punto di partenza di una vita piena di soddisfazioni e successi, lo meriti davvero.

A Daria, una bomba di allegria. La spontaneità con cui è nato il nostro rapporto è l'eccezione che conferma la regola per cui "gli opposti si attraggono". Grazie per esserci stata in questo percorso, ascoltando ogni mia ansia, comprendendomi sempre, anche solo dandomi un forte abbraccio. Grazie per la sensibilità con cui hai condiviso ogni mio punto di vista. Grazie per la nostra complicità, per i nostri sguardi carichi di significato, grazie per aver reso più leggeri i miei problemi. D'altronde, forse, sei davvero un po' una specie di terapista. Grazie per aver costruito così tanto in così poco, le risate con te hanno un altro sapore.

A Marco, l'amico-ing-dottorando migliore che si potesse desiderare. Grazie per avermi GUIdato in questo travolgente percorso. Grazie per avermi sempre accolto in sala relax, per esserti interessato dei miei stati d'animo, per avermi aperto gli occhi nei momenti di massima esagerazione. Grazie per avermi teso sempre una mano, facendo un po' tuoi i miei problemi. Grazie, soprattutto, per essere stato un compagno di scherzi perfetto, riuscendo a strapparmi un sorriso anche quando non vedevo vie di fuga. Non è vero che non sei un bravo insegnante, devi solo crederci di più.

Grazie a tutti dal profondo del cuore per aver contribuito al raggiungimento di questo traguardo. Se oggi sono come mi vedete, è anche merito (o forse colpa) vostro.

Summary

Swallowing is one of the most important human functions in our daily life consisting in a coordinated sequence of events aimed at moving nutrients from the mouth to the stomach. Despite its relevance, it has been less investigated than other motor activities. This is likely due to the complexity of this sensorimotor task. Indeed, a single swallow involves the coordination of more than 30 muscles within 1 second, including voluntary and reflexive activities: manipulation of food, displacements of the hyoid bone, hyolaringeal elevation and tilting of the epiglottis. All these events are possible because of the contraction of specific muscles of the submental region and in the anterior portion of the neck, controlled by swallowing center of the brainstem. Any structural or neurological impairment along the swallowing pathway is referred to as dysphagia, a pathology with high impact on the quality of life. An objective evaluation of the swallowing disorders is potentially relevant to identify and classify the type of dysfunction and to evaluate the outcome of treatments. Nevertheless, the evaluation of disorders of swallowing has to be preceded by a correct understanding of the normal physiology of swallowing. Currently, several technologies can be used in order to assess different aspects (e.g. mechanical or electrophysiological) of the swallowing function: videofluoroscopy (VFSS), endoscopy (FEES), manometry, electromyography. In this study we designed an integrated measurement framework for non-invasive assessment of the

swallowing function of healthy subjects. Specifically, the proposed experimental setup includes high-density surface electromyography (HD-sEMG) for a spatio-temporal evaluation of the electrical muscular activity and accelerometry for the temporal segmentation of swallowing phases based on hyolaringeal excursion. To the best of our knowledge, previous analyses on swallowing assessment were carried out without performing a swallowing segmentation. Here we propose an acceleromter-based segmentation. An experimental study was carried-out: (i) to assess the validity of this innovative setup by comparing the accelerometer-based task segmentation with that obtained with the clinical standard (FEES), (ii) to identify the possible contribution of HD sEMG in the refinement of phase-related symmetry indexes, (iii) to evaluate the sequential muscular activation across swallowing phases. The study was conducted on a group of 10 healthy subjects performing 15 swallowing tasks with 5 types of bolus: saliva (dry swallow), 3 and 10 ml of water, 3 and 10 ml of gelled water.

Results indicated (i) a good intra-subject consistency between the accelerometer- and FEES-based identification of the swallowing onset. In fact, the accelerometer-based onset occurred, on average, 250 ms before that obtained with FEES, with an inter-subject variability of 300 ms (interquartile range), regardless to the type of bolus. No significant differences were found in EMG symmetry indexes estimated considering the FEES-based and accelerometer-based segmentation. (ii) Phase-related symmetry indexes, and barycenter of the amplitude maps showed a good correlation in finding muscular activation symmetry. (iii) HD-sEMG technique allowed a detailed evaluation of the spatiotemporal variation of EMG activity. Results of muscular activation patterns derived from the accelerometer-based segmentation were consistent among healthy subjects.

A preliminary application of the proposed methods on subjects with swallowing impairments suggested the potentiality of the proposed methods in detecting deviations from the physiological trends. Clinical studies on a large population of dysphagic subjects are required to ascertain whether these initial and very

preliminary results can be generalized to dysphagic patients with different pathologies.

In conclusion, the present study proposed a possible, alternative method for the evaluation of swallowing function with a non invasive, easy to use and innovative setup.

Table of Contents

List of Acronyms

ALS	Amyotrophic Lateral Sclerosis
CNS	Central Nervous System
CPG	Central Pattern Generator
CW	Choi Williams
FEES	Fiberoptic Endoscopic Examination of Swallowing
HD sEMG	High-density Surface Electromyography
IED	Interelectrode Distance
IMU	Inertial Measurements Unit
MEACS	Miniaturized EMG ACquisition System
PD	Parkinson's disease
RMS	Root Mean Square
sEMG	Surface EMG
SM	Submental Muscles

UES Upper esophageal sphincter

VFSS Videofluoroscopic Swallowing Study

Chapter 1

Introduction

1.1 Swallowing mechanism

Swallowing is an important human biological function starting at the early stages of pregnancy and continuing throughout life, involving the coordination of more than 30 muscles [1], [2]. It is a neuromuscular process consisting in a very complex sequence of events aimed at moving nutrients from the mouth to the stomach passing trough pharynx and esophagus. The complexity of this sensorimotor behavior is due to the large number of muscles and structures involved to produce a highly coordinated movement. In fact, during a swallow, the musculature around mouth, tongue, larynx, pharynx and esophagus is sequentially activated and inhibited from different levels of the central nervous system (CNS) [3]. These activations are under voluntary or involuntary control. The reflexive portion of a single swallow is under the control of the bilateral centers of the brainstem, involving several cranial and spinal nerves [4]. The right combination of muscles activation is essential for a correct execution of the swallowing process and, as a result, for a good quality of life, being the swallowing event an important part in our daily life. It's conventionally accepted

that swallowing consists of a sequence of biomechanical events clearly distinguishable into three stages: oral, pharyngeal and esophageal [1], [3], [5], [6]. Although oral cavity and pharynx are two separated anatomical structures, they are functionally integrated and interrelated, so that it is still unclear the division between them because of the possible overlapped events over time. For this reason, it is often used the term oropharyngeal swallowing to indicate the first stages of the process. In all the mammals, including humans, oropharyngeal swallowing is a short event, lasting approximately 1 second, while the esophageal phase is less complex and slower [3]. This study is centered on the analysis of the oropharyngeal phase, excluding the esophageal one that was not included in the aim of the project.

1.1.1 Oral phase of swallowing

The oral phase of swallowing is mainly under voluntary control and it lasts differently according to taste, consistency of food and hunger. Mechanoreceptors, chemoreceptors and thermoreoceptors placed in the oral cavity, at the base of the tongue and pharynx, play an important role in the identification of the bolus, being essential for triggering swallows. In normal human subjects, for solid bolus, the oral phase is divided into two steps: a preparatory (*Figure 1 A*) and a propulsive phase (*Figure 1 B*). At the beginning, the tip of the tongue increases the contact with the anterior region of the hard palate, the bolus is pressed against the palate, masticated and manipulated and gradually accumulated against the hard palate surrounded by the upper dental arch [1]. The processing of the food involves circular movements allowing the chewing function in order to reduce food size and obtain an optimal food consistency [1]. During the oral propulsive stage, the posterior tongue drops to open the back of the oral cavity. Being the posterior region of the tongue pressed against the palate, the bolus is pushed posteriorly into the oropharynx triggering the beginning of the pharyngeal phase [3]. The aggregation of the solid bolus takes from fractions of second to 10 seconds in healthy subjects [1]. On the

other hand, for small volumes of liquid boluses, such as saliva, there is no oral preparation [3]. In the latter case the oral phase is short and simple requiring only an initial positioning of the ingested fluid before propulsion [6]. Finally, with large volume liquid bolus it may be possible that the first two phases overlap with each other occurring simultaneously.

1.1.2 Pharyngeal phase of swallowing

The pharyngeal phase (*Figure 1 C*) is considered as a reflex response, so it is an irreversible step. It is made up of a cascade of events triggered from the entry of the bolus in the pharynx itself at the level of the palatoglossal arch. The reflex response is carried out by the Central Pattern Generator (CPG) of the brainstem thanks to a nervous pattern of afferent and efferent fibers. Receptors at the level of oropharynx transmit stimuli to nerves of the brainstem which, through efferent nerve fibers, innervates muscles of larynx, pharynx and esophagus coordinating the reflexive response characterized by a coordinated peristaltic-like wave [3]. Firstly, the velopharyngeal isthmus is closed by the palate, the nasopharynx is sealed through the soft palate in order to prevent pressure escape into the nasal cavity, while the tongue blocks the oral cavity expanding the contact area with the palate posteriorly. The pharyngeal phase plays an important role in airway protection, preventing phenomena like penetration and aspiration during inspiration thanks mainly to the hyoid-laryngeal complex elevation. Penetration occurs if bolus from the mouth or regurgitated from the esophagus enters the larynx above the vocal folds. Aspiration refers to infiltration of materials into the lungs through the vocal folds causing pneumonia and even death [1]. The antero-superior movement of the larynx not only prevents these phenomena, but also helps opening the pharyngeal-esophageal bolus transition. In addition, the closure of the vocal folds and the glottis, and the overlap of the epiglottis on the larynx contribute to a complete airway closure ensuring the safety of airway. Consequently, the normal respiration stops for a while resulting in an apneic period called swallowing apnea and it is restored

right after its interruption with the expiratory phase of the respiratory cycle. As a result, eating, swallowing and breathing are tightly coordinated [1], [7]. In fact, the respiration ceases during the apneic period not only for the airway closure by the soft palate and the closure of epiglottis, but also because of a neural suppression in the brainstem [1]. All swallows take place between late inspiration and late expiration, an interval lasting approximately 0,5 to 1,5 seconds, corresponding to the apneic period [3]. After that, neck and tongue muscles give the propulsive force to the bolus, propelling it with posterior movements, pushing it down throughout the pharynx into the esophagus. At the end of the pharyngeal phase the upper esophageal sphincter (UES), being in tonic contraction until this moment, relaxes in order to let the bolus enter into the esophagus. Finally, the sphincter closes, being contracted, preparing for the next swallow.

1.1.3 Esophageal phase of swallowing

The esophagus is a structure with a tubular shape and it goes from the upper esophageal sphincter (UES) to the lower esophageal sphincter (LES) [1]. The esophageal phase of swallowing (*Figure 1 D*) is governed by a dual control of the somatic and autonomic nervous system. In fact, the esophagus is composed of both striated and smooth muscles [1]. Since the interrelation between laryngeal movements and the opening of the upper esophageal sphincter, it is thought that the mechanism regulating the opening of the sphincter and, consequently, the passage of the bolus, is under neural control for biomechanical causes [3]. During the esophageal phase the bolus propagates thanks to a peristaltic wave until it reaches the lower esophageal sphincter passing into the stomach. Such as the upper esophageal sphincter, at rest the lower esophageal sphincter is tonically contracted in order to avoid reflux, relaxing for the passage of the bolus.

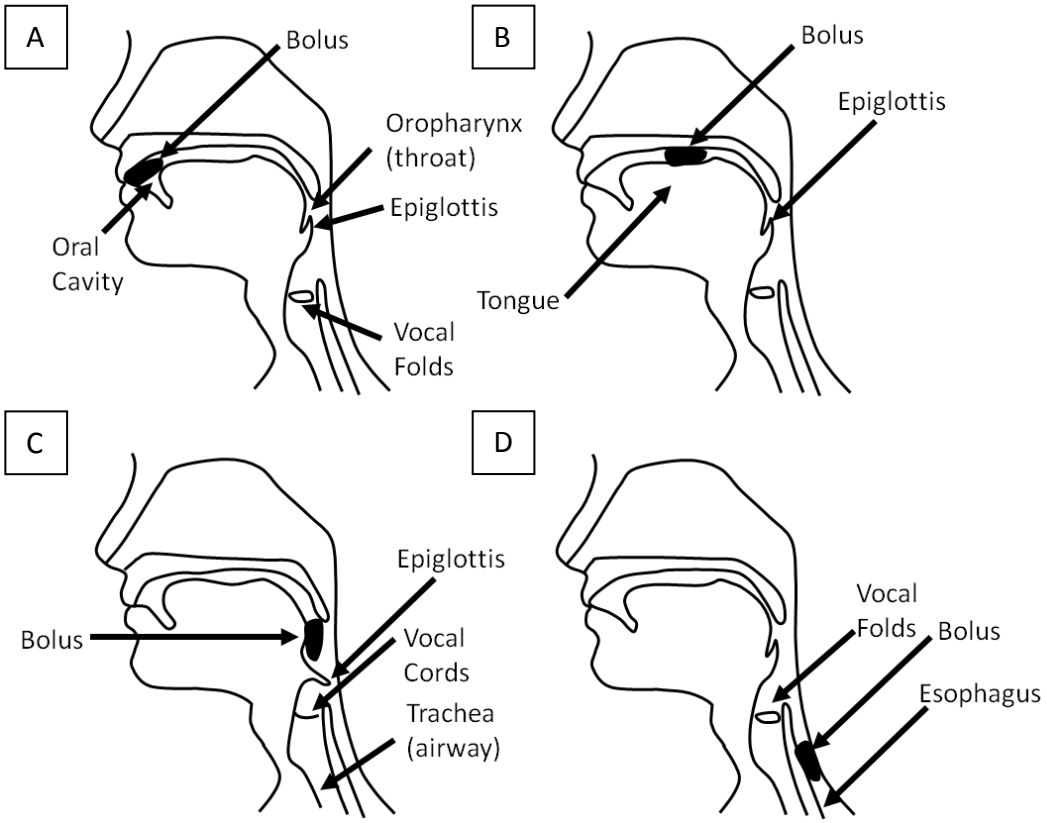

Figure 1 – Swallowing phases: oral preparatory stage (A), oral propulsive stage (B), pharyngeal stage (C), esophageal stage (D).

1.2 Swallowing muscles

During swallowing, the coordinated sequence of event is ensured by a high number of muscles of the floor of the mouth, pharynx and esophagus. There are several groups of swallowing muscles:

- Facial, perioral and tongue muscles
- Submental muscles (SM)
- Infrahyoid muscles
- Cricopharyngeus muscle of the UES.

1.2.1 Facial, perioral and tongue muscles

The first stage of swallowing process highly depends on the type of bolus, resulting in a recruitment of different groups of muscles. The first involved muscles help creating tone necessary for positive pressure in order to promote the bolus propulsion: the orbicularis oris provides the sealing of the lips, while the buccinator helps tensing cheek to maintain food between molars allowing closure of the mouth against food escaping from the oral cavity [3]. For solid bolus, a chewing function is necessary and this is ensured by the activity of the masticatory muscles (temporalis, masseter, medial and lateral pterygoid shown on *Figure 2*) in order to raise and lower mandible for closure and opening of the jaw [1].

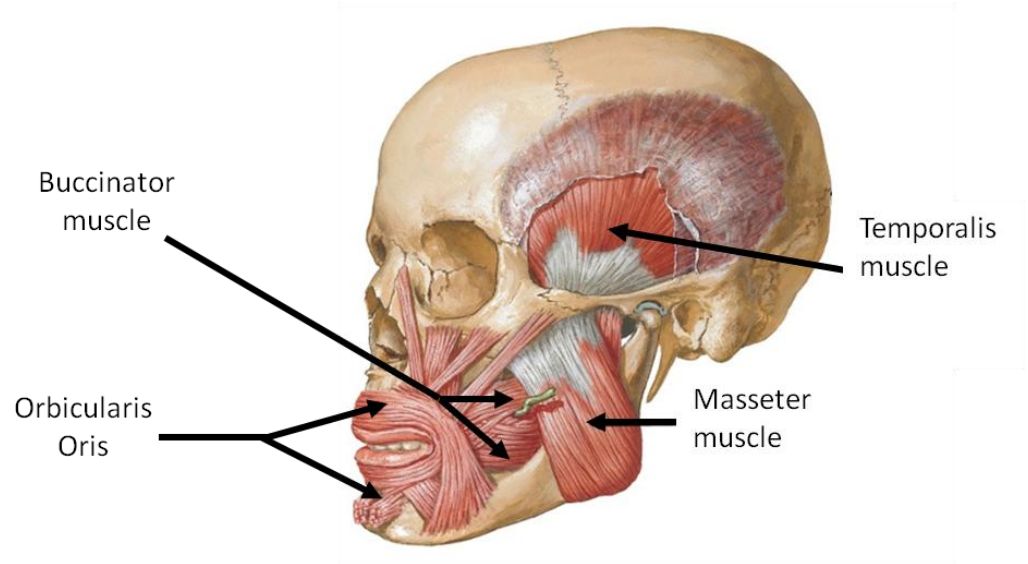

Figure 2 – Main perioral muscles involved in the swallowing process.

Moreover, for bolus preparation, formation, positioning and transport also different tongue muscles are activated in order to move the tongue according to jaw movements. The tongue is responsible of manipulating and pressing the bolus toward the pharynx thanks to a series of movements. The high number of

degrees of freedom of the tongue is due to the fact that it's a highly maneuverable muscular organ composed of intrinsic and extrinsic muscles (*Figure 3*). The former include the superior and inferior longitudinal, vertical and transverse muscles, the latter include hyoglossus, styloglossus, genioglossus and palatoglossus [6].

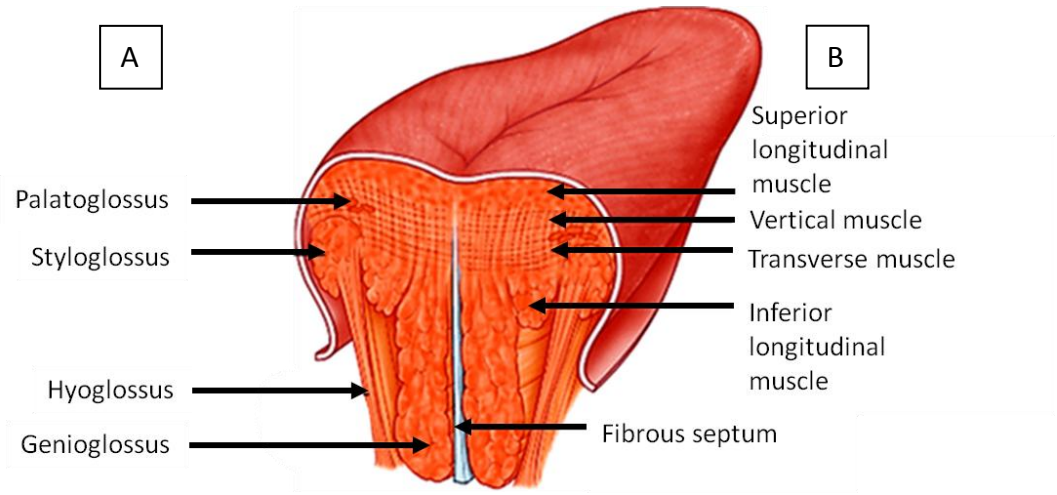

Figure 3 – Transversal section of the tongue. Extrinsic muscles on the left side (A), Intrinsic muscles on the right side (B).

It was found that the end of the activity of perioral muscles triggers the beginning of the pharyngeal phase even though the masseter can activate also during other swallowing phases [3]. Also the type and consistency of bolus could result in a different activation of perioral muscles in terms of onset and duration of the muscular activity. Nevertheless, the maximum occlusion is reached when the bolus is pushed in the posterior region against the palate, before the cascade of reflexive events of the pharyngeal phase [3].

1.2.2 Submental muscles

The submental muscles (SM muscles), known also as submandibular or suprahyoid muscles, refer to a complex of muscles including mylohyoid,

geniohyoid, anterior belly of digastric and stylohyoid muscles (*Figure 4* A). The SM muscles originate on the mandible and attached to the hyoid bone and tongue [1]. This group of muscles allows initiating a swallow thanks to a coordinated series of events and it is activated and controlled by the CPG of the brain stem network [3]. The contraction of the SM complex let a cascade of events start for the safe passage of the bolus toward the esophagus. In fact, the geniohyoid protracts the hyoid bone, while the mylohyoid contributes to raise and stabilize the tongue resulting in a complete control of the hyoid bone itself. Moreover, the anterior belly of digastric helps lowering the mandible to open the jaw and the stylohyoid let the hyoid bone return in a rest condition. For these reasons, the activity of the SM muscles results in elevating the hyoid bone following an antero-superior direction, allowing the hyolaringeal upward movement and triggering the other reflexive events. Since the larynx is pulled up, the apneic period starts, preventing food escaping into other cavities enhancing the relaxation of the upper esophageal sphincter [6]. As a result, monitoring the activity of the SM muscles can provide important information about the swallow onset, the start of the apneic period and the duration of the pharyngeal phase itself.

1.2.3 Infrahyoid muscles

Infrahyoid muscles (*Figure 4 B*) are positioned symmetrically on the left and right sides of the larynx, for this reason these muscles are known as laryngeal muscles. After the contraction of the SM muscles resulting in the elevation of the hyoid-laryngeal complex, the laryngeal adductor activates in order to close the vocal folds [3]. This contributes to a complete airway protection, preventing the passage of the bolus in the larynx. The function of the infrahyoid muscles is to depress the mandible and the hyoid bone (and so the larynx) during swallowing, so that the food bolus could pass the esophagus and reach the stomach [5]. More in detail, the contraction of the thyrohyoid raises the thyroid cartilage and the larynx to the hyoid bone, while the sternohyoid and the sternothyroid lower

the thyroid cartilage and the hyoid bone. As mentioned before, it has been shown that the activity of the laryngeal adductor is a reflexive response induced by the brain stem [3].

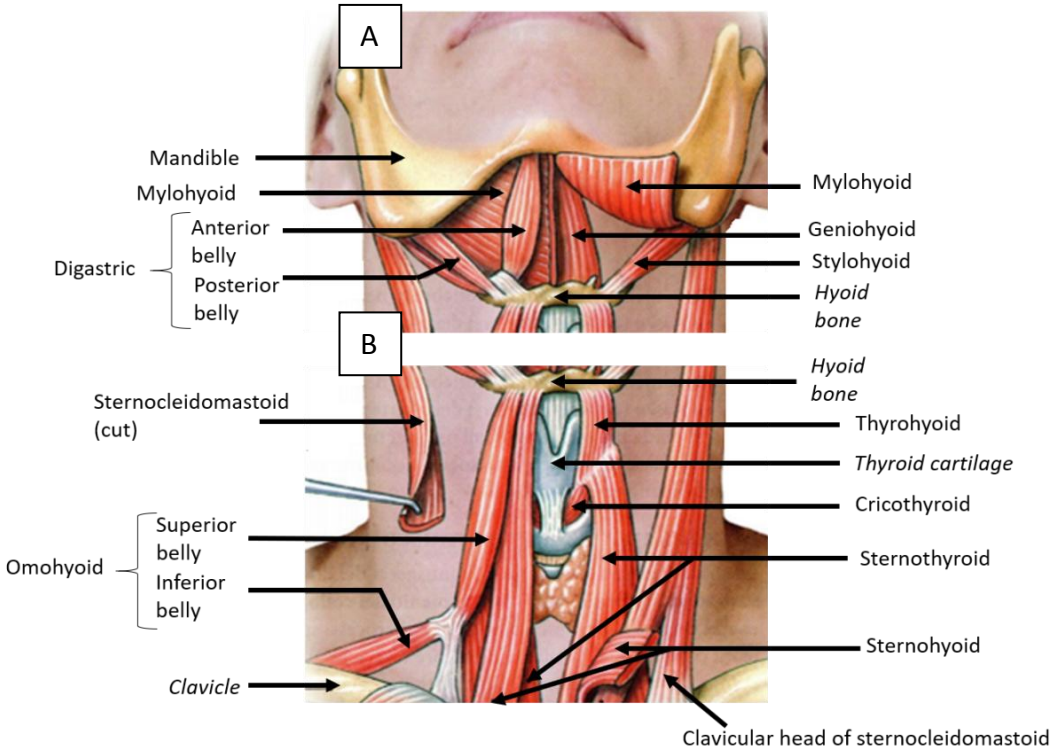

Figure 4 – Submandibular (A) and infrahyoid muscles (B) involved in the swallowing process.

1.2.4 Cricopharyngeus muscle

The upper esophageal sphincter is tonically contracted during the early stages of the swallowing process. During a swallow, when the bolus arrives at the esophageal level, the sphincter relaxes and opens for the bolus passage. The sphincter is controlled by a striated muscle situated at the pharyngoesophageal junction called Cricopharyngeus muscle. The UES opens thanks to three important factors: the relaxation of the CP, the contraction of the SM complex and the pressure of the descending bolus [1]. The activity of the CP muscle

involves the control of both sensory and cortical inputs generating a protective reflex relatively to the oropharyngeal functions [3].

1.3 Swallowing disorders

A difficult or abnormal swallowing resulting from any structural and neurological impairment goes under the name of dysphagia. The American Gastroenterological Association (AGA) distinguishes the causes of dysphagia as: iatrogenic, infectious, metabolic, myopathic, neurological and structural [8]. Dysphagia negatively impacts the health, safety and quality of life of patients, causing serious consequences, potentially taking to death. In fact, complications of the disease could be dehydration, malnourishment penetration and or aspiration of bolus materials and pulmonary complications [5], [10], [9]. Depending on the impaired level affecting the swallowing pathway, functional problems can be divided into oral, pharyngeal and esophageal impairments [6].

1.3.1 Oral problems

Oral problems include mainly muscular weakness (also of the tongue) or dysfunction of the oral receptors resulting in a missed connection with the CNS which triggers the swallows in a wrong way [6]. Results of oral impairments are drooling from the mouth, inability of holding the bolus in the mouth (premature spillage of food), improper bolus formation and transport or wrong positioning of bolus materials, difficulty making the swallow start [6], [8]. Functional problems at the level of muscles of mouth and face can also result in the piecemeal swallowing [8]. This effect is very common among dysphagic patients and consists in multiple successive swallows dividing the bolus into two or more smaller parts [2]. In addition, also structural problems such as loss or misalignment of teeth and cleft lips or palate can alter the masticatory function, reducing the performances because of difficulty in chewing and splitting bolus into smaller portions [1], [6].

1.3.2 Pharyngeal problems

Dysfunctions at the level of the pharynx can produce wrong swallow onsets, ineffective bolus propulsion and maintenance of bolus materials in the pharynx resulting in the need to swallow repeatedly to clear the pharynx [1], [8]. In addition to cleft lips or palate and loss of teeth, other structural abnormalities resulting in pharyngeal impairments could be pharyngeal diverticulum: thickening of the muscular tissue at the level of the inferior pharyngeal constrictors [6]. In this case the bolus can enter the diverticulum and be regurgitated to the pharynx resulting in aspiration [1]. Moreover, since the pharynx is involved in both respiration and swallowing, there could be problems in the bolus transport or in the coordination of breathing and swallowing [6]. Concerning transport problems, since the pharyngeal phase is a reflexive step controlled by the CPG, failure of sensory patterns, weakness or missed coordination of pharyngeal muscles can result in an altered bolus transit. Food material is slowed and maintained in the oropharynx increasing the risk of aspiration [11]. Moreover, pharyngeal problems can derive from impairments of UES opening: an incoordination between the activity of the UES and the suprahyoid muscles can lead to the obstruction of the pharynx without propelling food material [6]. Since UES switches from relaxation to traction thanks to the activity of the suprahyoid and infrahyoid muscles, impaired UES opening can derive both from incorrect traction or missed relaxation [8]. On the other hand, pharyngeal impairments can affect the synergic activity of breathing and swallowing. Being the two functions completely overlapped [12], a co-coordination failure can have critical consequences. As previously described, in healthy subjects there is always an apneic period that ends right after the bolus passage through the pharynx. This is possible thanks to the activity of the SM muscles resulting in the hyolaringeal elevation, the titling of the epiglottis and the closure of vocal folds. A wrong coordination of these events can produce the failure of the airway protection with consequent aspiration and penetration, obstructing bolus propulsion [1], [6].

1.3.3 Esophageal problems

At the esophageal level the bolus passage is ensured by the relaxation of the UES leading to the transfer of the food material from the pharynx to the esophagus. Muscular weakness of the Cricopharyngeus muscle can result in a failure of the opening of the UES with consequent obstruction of bolus passage, more symptomatic with solid boluses [1]. Moreover, since the submental complex activates to maintain the UES open during the swallow, impairments at the level of SM muscles can affect the opening of the sphincter [1], [8]. Also structural abnormalities such as webs or strictures in the esophagus or at the level of the sphincter can cause an obstruction of the normal pathway of the bolus [1]. In addition, there could be other types of esophageal dysfunction affecting the correct peristalsis accompanied with the maintenance of food material in the esophagus after swallowing causing regurgitation through pharynx, increasing the risk of aspiration [1], [6].

1.4 Neurogenic oropharyngeal dysphagia

This disease can include oral impairments, pharyngeal ones, or both [8]. Typically, the causes of oropharyngeal dysphagia are neuromuscular dysfunctions [8]. Mechanical causes include congenital structural abnormalities (e.g. cleft lips or palate, loss of teeth or pharyngeal diverticulae), but also result from pathologies such as tumors, skeletal, dental or muscular pathologies. Neurological causes include cerebrovascular accidents (strokes) as the most common cause of swallowing dysfunction, but also chronic neurodegenerative diseases or motor neuron diseases such as Parkinson or Amyotrophic Lateral Sclerosis.

Stroke Dysphagia is a very common consequence post stroke and the type of dysphagia depends on the location of the stroke itself. In fact, it has been established an incidence of swallowing dysfunction in post stroke patients

ranging from 23% to 50% [4], [13]. Oropharyngeal dysphagia derives from strokes of the cerebral cortex, even though oral impairments are due to the loss of cortical modulation of the oral swallow [6]. On the other hand, if the stroke affects the brainstem there could be effects on the CPG, swallowing interneurons and or efferent fibers altering the reflexive pharyngeal phase of swallowing [14]. Although the bilateral cortical innervations of the swallowing muscles, dysphagia could appear also following a unilateral cortical stroke [7]. In fact, since humans have a dominant hemisphere of the brain for the control of the swallowing functions, a damage at the level of the dominant hemisphere is more exposed to the risk of aspiration [6].

Parkinson's disease Idiopathic Parkinson's disease (PD) affects the CNS being associated to a loss of dopaminergic neurons of the substantia nigra [15]. Among symptoms of the PD there are instability, muscular tremor and rigidity. Studies have reported the presence of dysphagia in parkinsonian patients as high as 52% [6], [8], [16]. Swallowing disorders are related to different symptoms of the PD: bradykinesia, dystonia and dyskinesia [6], [17]. Since bradykinesia results in slowing the reflexive events of the pharyngeal phase, the time for bolus passage increases and consequently the risk of aspiration is higher [15]. Moreover, dystonia affects the activity of the UES: a lack of coordination between the relaxation of the sphincter and the bolus passage can cause the retention of food material into the pharynx causing obstruction [18]. Finally, dyskinesia alters the coordination of the SM complex resulting in a non physiologic muscular activation [6].

Amyotrophic Lateral Sclerosis Amyotrophic Lateral Sclerosis (ALS) is recognized as a motor neuron disease since it consists in a damage of motor neurons of the CNS [6]. ALS patients show major dysfunctions in the first phases of the swallowing process: the pharyngeal stage is prolonged because of the missing inactivity of the laryngeal elevators and the delayed opening of the UES [19]. Magnetoencephalographic studies analyzing cortical processing of swallowing in

ALS Patients demonstrated a reduction in the sensorimotor activation in dysphagic ALS patients [19]. In fact, muscular activation is altered: muscles of jaw and tongue are continuously contracted with upper motor neuron damages, while lower motor neuron impairments result in muscle atrophy [6], [19]. These dysfunctions lead to a non physiological swallowing process affecting bolus formation and transport.

1.5 Assessment of the swallowing function

As mentioned before, swallowing is a physiologically complex and rapid task, involving a precise sequence of events synchronized thanks to the activity of a high number of neuromuscular synergies [3], [5]. As a result, the evaluation of swallowing disorders and its management are difficult because of the intrinsic complexity of the event [8], [9]. A complete evaluation of oropharyngeal dysphagia requires a multidisciplinary team of specialists cooperating together: neurologists, otolaryngologists, speech language pathologists, bioengineers [8]. Swallowing examination can be carried out with clinical examination and or instrumental investigations that generally follow the former [7], [13]. The sequential and ordered phases of the swallowing process can be monitored during deglutition through different approaches (electromyography, accelerometry, videofluoroscopy, videoendoscopy) [3], [17]. Each technique has pros and cons that can be evaluated in order to choose the best one for the assessment of the swallowing function, depending on the questions that are being asked [7]. The choice of the most suitable analysis is important not only for the assessment of the pathology, but also for dysphagia rehabilitation. In fact, during rehabilitation clinicians have to consider the effects of the abnormalities on the bolus passage and airway protection in order to monitor the follow-up of the disease [1].

1.5.1 Electrophysiological evaluation of swallowing function

Only few researchers extensively studied swallowing and its disorders using electrophysiological methods [20]. This is likely due to the anatomical complexity of the body region including several sequentially activated muscles in a limited space. Nevertheless, an electrophysiological evaluation may provide significant insights into the swallowing pathophysiology and the assessment of rehabilitative treatment/process.

Electromyography Electromyography is used to monitor the muscular electric activity. Historically, neurophysiologic studies used intramuscular needle EMG [21]. The technique allows capturing selectively the activity of single motor unit, thanks to its closeness to the needle [21]. On the other hand, conventional sEMG is a non-invasive technique using electrodes placed on the skin above the muscle of interest [21], [22]. The pick-up volume is larger with respect to the needle EMG, covering most of the muscle under the electrodes. The development of traditional sEMG led to the idea of covering muscles with densely spaced electrodes to monitor the distribution of action potential. The result is a multi-channel sEMG known as High Density surface electromyography (HD sEMG). Using multiple electrodes arrays, the selectivity of the system increases and a spatial information is added to the temporal one [23], [24]. The application of the most suitable EMG technique depends on study objectives [25].

Relatively to the purpose of the assessment of swallowing function, outcome measures of HD-sEMG are of greatest interest. The reason is related to the high number of overlapped muscles over a relatively small anatomical region (Figure 4). The use of electrodes array allows the analysis of muscular activation changes through the evaluation of the spatio-temporal distribution of action potentials. In fact, from the direct association between the signal and the level of muscle activation, the local muscular activity could be evaluated [24]. A few studies [5],

[26], [27] have reported the patterns of electromyographic HD-sEMG activity of swallowing muscles analyzing the sequence activation. Zhu et al. [5] described an alternative method for the quantitative assessment of the swallowing function using symmetry indexes computed over HD-sEMG signals (*Figure 5*).

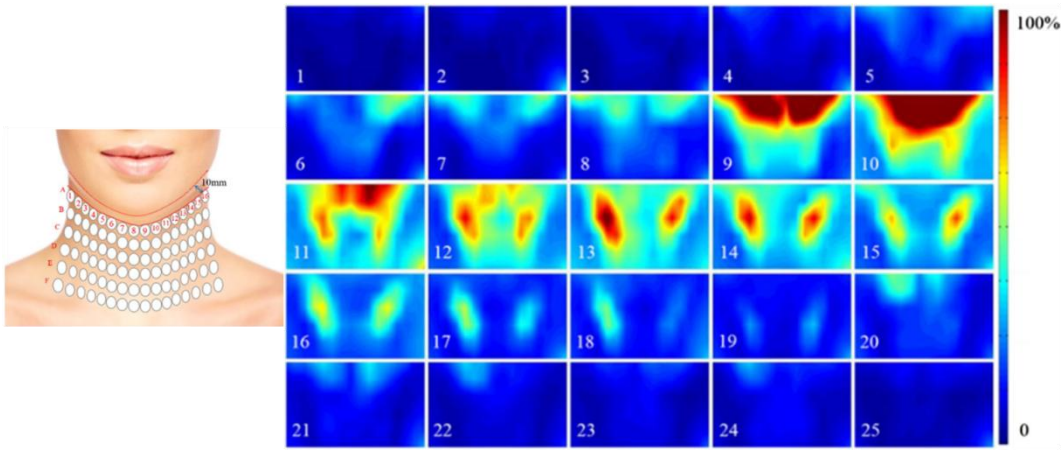

Figure 5 – From left to right: the experimental setup used by Zhu et al. for their study and the dynamic HD-sEMG amplitude maps during a swallow of 5 ml of water [5].

Drawbacks of Zhu's study are the use of 96 electrodes placed one by one, the absence of a mechanical evaluation of the physiological process, the partial investigation of the submental zone, and the use of a global index for the assessment of muscular activation symmetry. In fact, to the best of our knowledge, the only outcome measure is based on the computation of symmetry indexes across the whole recorded signal (few seconds). Since the short duration of the swallowing event, the method could be poorly responsive to high symmetry changes across brief intervals. Consequently, interpretation of results could be misleading. In order to overcome this limitation, it would be more advisable evaluating symmetry indexes on short, consecutive time intervals. Therefore, a swallowing segmentation should be implemented to match symmetry indexes and swallowing phases. In the perspective of performing

quantitative analyses on swallowing phases, the possibility of a mechanical evaluation of swallowing has been investigated.

1.5.2 Mechanical evaluation of swallowing function

As for several other neuromuscular investigations, also the assessment of swallowing function can take advantage of the integration between mechanical and electrophysiological variables. This integration is of paramount importance to provide an electromechanical description the physiological function and to identify the phases of the motor task. As far as swallowing is concerned, videofluoroscopy, nasoendoscopy, mechanical sensors are the most common clinical approaches to study the movement of anatomical structures.

Videofluoroscopy The oldest and reliable procedure for the evaluation of the swallowing physiology is the Videofluoroscopic Swallowing Study (VFSS) [28]. It is an x-ray examination for the imaging of the dynamics of the swallow [29]. The procedure is also known as modified barium swallow because of the mandatory type of bolus used to monitor the swallowing phases [13]. In fact, during the examination, the patient swallows prepared boluses (varying volumes and consistency) made of radio-opaque barium liquid for a visual inspection on the video frames [2], [8], [13]. All the frames are captured in a lateral projection of the subject in order to include upper respiratory tract, oropharynx, palate and the upper esophagus (*Figure 6*) [8]. The main advantage is the clear visualization and quantification of the liquid bolus for all the swallowing phases, so the swallowing specialist can review the swallow events thanks to a slow motion and frame by frame analysis [7], [13]. The VFSS is able to detect early onset of the swallow, misdirection of the bolus into the larynx, trachea or nasopharynx (penetration into airway or aspiration) and also retention of the bolus in the oral cavity [2], [8], [13]. Moreover, being analyzed the lateral view of the subject, the VFSS captures also the hyolaringeal excursion, providing additional information

about the onset of the pharyngeal phase. Nevertheless, there are some weaknesses of the VFSS: high cost, invasiveness, unpleasantness, necessity of a radiographic room and exposure to radiation [29].

Figure 6 – Images of bolus entry into the pharynx from videofluorographic recordings [1]. Arrows on the images indicate the leading edge of the barium.

Nasoendoscopy The fiberoptic endoscopic examination of swallowing (FEES) is the clinical gold standard [28]. A small flexible fiber optic is introduced transnasally and it is used for an endoscopic examination of the hypopharynx and larynx in order to assess the laryngeal and pharyngeal function during a swallow [7], [8], [13]. The output of the procedure is a video providing images of all mucosal surface of nasopharynx, pharynx and larynx (*Figure 7*) [8].

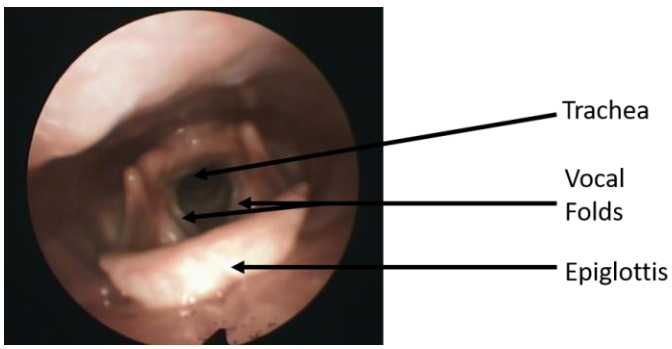

Figure 7 – Selected frame of a video recording during an endoscopic exam of a healthy subject.

As for the VFSS, also the FEES exam requires professional figures like speech-language pathologist or a gastroenterological endoscopist for the examination and the correct technical equipment [13]. Moreover, although it is an easy to

use, cheap and well tolerated technique, possible bedsides can be the discomfort, the possibility of epistaxis, mucosal perforation or allergic reactions [30]. In addition, although the safety of the procedure, the possibility of using normal meals and the absence of radiation, the worst weak spot is the inability to observe the oral stage of swallowing because of the nasoendoscope positioned at the level of the soft palate [13]. In fact, the FEES analyzes the phases right before and after the swallow because of a "video whiteout" produced by the obliteration of the tip of the endoscope at the beginning of the pharyngeal phase [7], [31]. Images can be obscured according to different causes: bolus passage, velopharyngeal closure, epiglottis tilting, displacement of anatomical structures after laryngeal movements [32]. Physiologically, the onset of the swallow is marked by the occurrence of a sequence of events: tongue retraction, velopharyngeal closure, hyolaringeal elevation, vocal folds closure [31]. According to the position of the tip of the endoscope the detected region changes, therefore, in order to evaluate laryngeal functions during a swallow, the suitable position of the endoscope is that with the tip placed at the laryngeal inlet [30]. The probe does visualize the closure of the velopharyngeal isthmus and the retroflexion of the epiglottis only briefly, just before the light of the probe is covered by anatomical structures [31]. For this reason, sometimes the vocal cord closure cannot be captured from the video recordings. Since different studies found out opposing results about the sequence of swallow events during the pharyngeal phase [32]–[34], the combined use of endoscopy and sEMG could help to clarify the correct order of events.

Laryngeal elevation measurements As mentioned before, during the pharyngeal phase the pharynx is elevated and pulled anteriorly resulting in an elevation of the entire hyoid-laryngeal complex (hyolaringeal excursion). The hyolaringeal elevation ensures a cascade of events: adduction of vocal folds, glottis closure and closure of the airway, preventing food escaping into trachea [5]. Structural movement of the larynx is accomplished via the contraction of muscles located in the floor of the mouth (SM complex) and between the larynx and superior

skeletal structures (namely the thyroid cartilage and the hyoid bone). In fact, the contraction of the complex made of mylohyoid-geniohyoid and anterior digastric allows the elevation of the hyoid and larynx, while the contraction of the infrahyoid muscles depresses the two anatomical structures for the transport of the bolus [5]. As a result, tracking the hyolaringeal excursion has been proposed to identify the different phases of the swallowing process [35], [36]. From the extracted profiles of the hyolaringeal accelerometric recordings, further analyses can be carried out to extract features and indices describing the swallowing phases and associated movements (e.g. maximal excursion, swallow onset and offset, duration of the swallow) [37].

Tongue pressure measurements Recently, pressure sensors have been used to objectively describe tongue function during the swallowing process [27]. The propulsive phase is the second step of the oral phase of swallowing that precedes the pharyngeal one. The driving force in propelling boluses from the oral cavity to the pharynx is offered by the tongue pressure produced by the contact of the tongue to the palate [26]. At first, there is an initial close contact of the tongue against the anteromedian part of the hard palate, then also the circumferential and the posteriomedian parts of the tongue get softly in touch with the palate [38]. For this reason, the tongue pressure profile could give additional and useful information not only to evaluate the force of the tongue against the palate, but for the identification of the initial swallowing phase. The main information that can be extracted from tongue pressure measurements are: duration of the tongue-palate contact, maximal magnitude and time to peak pressure.

1.6 Study objectives

Based on the literature analysis reported in this initial chapter, the following considerations emerged: (i) swallowing is a complex sensorimotor event including both voluntary and reflexive activations of several muscles in a limited

body region (ii) an objective assessment of the swallowing process is essential in clinics not only for the diagnosis of the swallowing disorders, but also for their treatment [2], (iii) a quantitative description of this process cannot only rely on either electrophysiological or anatomical variables, but requires a multimodal approach. Therefore, the aim of the present study was to design and validate an integrated measurement framework, including both electrophysiological and mechanical variable detections, for a non-invasive assessment of the swallowing function. The proposed experimental setup includes HD-sEMG for a spatio-temporal evaluation of the electrical muscular activity and accelerometry for the temporal segmentation of swallowing phases based on hyolaringeal excursion. Specific aims are the following: (i) to assess the validity of this innovative setup by comparing the accelerometer-based task segmentation with that obtained with the clinical standard (FEES), (ii) to identify the possible contribution of HD sEMG in the refinement of phase-related symmetry indexes, (iii) to evaluate the sequential muscular activation across swallowing phases. The global long-term goal is to enhance the knowledge of the muscular activations during the swallowing activity and to test the proposed approach for the assessment of rehabilitative treatments.

Chapter 2

Feasibility study

A preliminary study was carried out in order to test the feasibility of EMG and accelerometric recordings during swallowing. The aim was to identify instrumentation, experimental procedures and data analysis for the swallowing phases segmentation and neuromuscular activation assessment. Since the invasiveness of the clinical standard for the evaluation of swallowing function, we were interested in exploring the potential of less invasive methods [36]. For this purpose, HD-sEMG, accelerometric and a pressure measurement systems were tested.

Participants In this preliminary study, the same control group was chosen for all the tested methods. A group of 7 healthy subjects (3 males and 4 females) was recruited, with a mean age of 29,7 years (range: 23-38 years). Participants had normal oral anatomical structures without any swallowing impairments. All the subjects gave their approval for being part of the study, which complied with the guidelines of the declaration of Helsinki.

Procedure All subjects performed the same task: 5 repetitions of a single deglutition of liquid bolus (10 ml of water), standing in upright position with the head in a neutral position. Each recording was stored separately, in order to

assess the repeatability of the technique. Specifically, the water was held in the oral cavity before starting the recording. After the instruction to swallow given by the experimenter, the subject started swallowing normally remaining in the same position. The reason of this sequence of activities was the attempt to avoid any motion and postural artifacts on recorded signals.

2.1 HD-sEMG recordings

High-Density sEMG was used to study the spatiotemporal properties of muscle activation [5].

Instrumentation HD-sEMG signals were acquired using an innovative miniaturized, wireless system (MEACS-Miniaturized EMG ACquisition System, LISiN-Politecnico di Torino, Turin-Italy, shown in *Figure 9*) [39]. The sensor unit was connected to a connector of a grid of Ag electrodes (LISiN-Politecnico di Torino, Turin-Italy). Electrode grids were flexible printed circuits boards (Polyimid, 80 µm thick) with electrodes of the same size and shape, evenly distributed in a grid of 8x4. Specifically, the grids were designed as linear, two-dimensional and flexible arrays with 32 electrodes organized in rows and columns with a fixed interelectrodic distance (IED). The grids of electrodes were taped on the skin using a double-sided adhesive tape and placed above the region of interest. In order to ensure a good skin-electrode contact, the portion under investigation had to be scrubbed through an abrasive paste, before the positioning of the arrays. The layout and design of the electrodes arrays was made taking into account the final purpose of the study: the combination of electrophysiological and biomechanical evaluation of the swallowing function. As a result, in order to identify the best layout, different grids were tested in this preliminary study:

- Electrodes array with an IED of 10 mm (*Figure 8 A*)
- A smaller electrodes array with an IED of 5 mm (*Figure 8 B*)

- A custom-made, cross-shaped array with an IED of 10 mm designed to leave the space for the positioning of an accelerometer between the two central columns, ensuring the same IED between the two medial parts of the array (*Figure 8 C*).

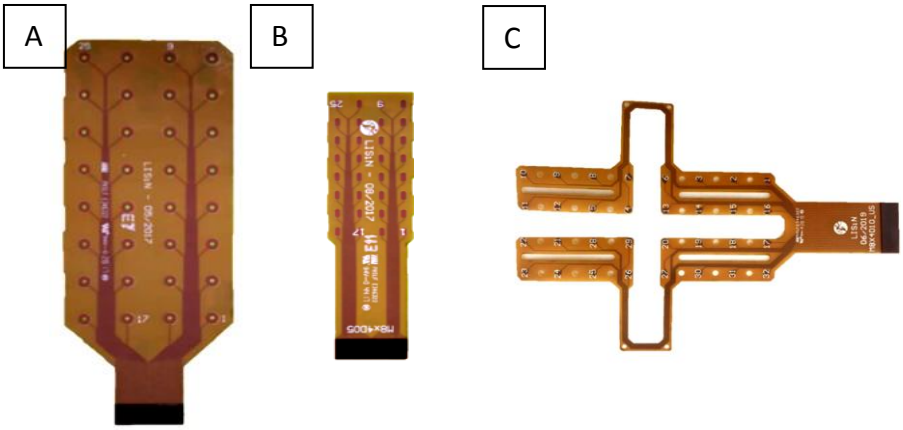

Figure 8 – From left to right: 32 Ag electrodes arrays organized in A) 4 rows and 8 columns with an IED of 10 mm; B) 4 rows and 8 columns with an IED of 5 mm; C) a cross-shaped 4 rows and 8 columns with an IED of 10 mm.

The MEACS system performed the conditioning, sampling, and wireless transmission of the 32 sEMG channels, sampled at 2048 ksps with 16 bit resolution. Data were sent wirelessly to a personal computer for real-time visualization and storage for further analyses. Signals were transmitted to the receiver through an access point acting as a router. The MEACS system (technical specifications in *Table 1*) comes with an acquisition software (Bp, used for the storage of the signals) and a Wi-Fi network Router.

Figure 9 – Sensor Unit module of the Meacs system.

Table 1 – Technical specifications of a sensor unit (MEACS) [39].

Description	***Parameter***	***Value (m.u)***
Number of channels	N	32
EMG Bandwidth	$BWEMG$	10Hz-500Hz
Gain	G	183±1V/V
Common Mode Rejection Ratio	CMRR	82dB
Input Impedance module	$\|ZIn\|$	1,3GΩ (10 Hz) 13 MΩ (1kHz)
Input Range	IR	$10mVpp$
RTI Noise	$NRTI$	<3$\mu VRMS$
A/D Resolution	Res	16bit
Sampling Frequency	fs	2048sps
Communication	-------	Wi-Fi
Receiver Type	-------	PC, Smartphone or Tablet
Max. Synchronization delay	$\Delta tSync$	±500µs
Max. transmission distance	dTX	22m (<0,02% data loss)
Power Supply	-------	600mAh 1-Cell LiPo Battery
Life time (transmitting)	TTX	5h
Dimensions	-------	3,4cm x 3cm x 1,5cm
Weight	-------	16,7g

According to the anatomy of swallowing muscles, three experimental setups were consdered involving different electrodes arrays. The three cases differed in terms of the infrahyoid muscles detection system and the best one was chosen in order to meet two requirements: (i) leave the space in the central region of the neck for a possible use of an accelerometer to track the hyolaringeal excursion, (ii) sample appropriately (in terms of surface covered by the grid) the muscular region of interest. In all the tested setups the same upper grid of 32 electrodes (organized in 4 rows by 8 columns with an IED of 10 mm) was used for

the evaluation of the submental (SM) complex. The upper grid was positioned with the smaller symmetry axis coincident with the sagittal plane, resulting in a complete covering of the region under the chin. As concern the analysis of the infrahyoid muscles of the anterior portion of the neck, three setups were analyzed:

- Two grids of electrodes (organized in 4 rows by 8 columns with an IED of 10 mm, *Figure 10 A*) positioned 10 mm under the upper grid. The three medial electrodes of the lower arrays were symmetric to the correspondent three lateral electrodes of the upper grid. In this way, a space of 20 mm was leaved to the positioning of an accelerometer in the central region of the neck.
- Two grids of electrodes (organized in 8 rows by 4 columns with an IED of 5mm, *Figure 10 B*) positioned 10 mm under the upper grid, such the first lateral electrode of the lower array was symmetric to the first electrode of the lower raw of the upper grid. In this way, a considerable space of 50 mm was leaved to the positioning of an accelerometer in the central region of the neck.
- A custom-made cross shaped grid of electrodes (organized in 4 rows by 8 columns with an IED of 10mm, *Figure 10 C*) positioned symmetrically with respect to the upper grid, leaving 10 mm of distance from the lower raw of the upper grid. A space of 10 mm was available for the positioning of a possible accelerometer thanks to the designated area.

In all the reported cases an adhesive gelled-electrode (Kendall Series, Covidien-MedTronic, Minneapolis, MN USA) with 24 mm diameter and a conductive part in Ag/AgCl was used as a reference electrode. The reference was the same for the different grids of electrodes, in fact the electrode was applied in the scrubbed portion behind the ear, in correspondence of a bone, with no muscles on it (*Figure 11*). Each monopolar signal was computed making the difference between the signal recorded under the single electrode and the reference itself.

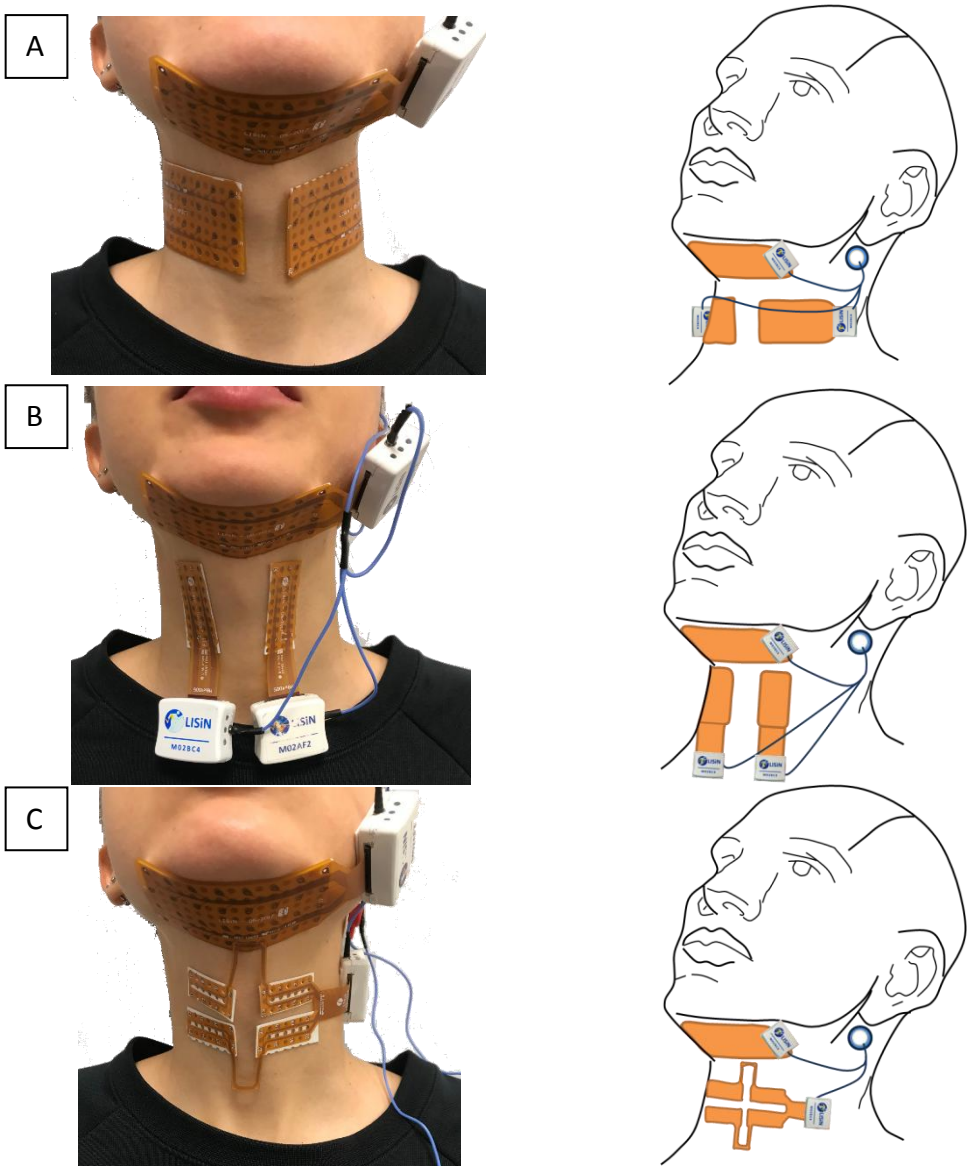

Figure 10 – Different setups considered for the evaluation of swallowing muscles. Analysis of the submental region through a 4x8 electrodes matrix in all the explored cases. Analysis of the anterior region of the neck, from left to right, through: A) two 4x8 electrodes arrays with an IED of 10 mm, B) two 8x4 electrodes arrays with an IED of 5mm, C) a cross-shaped 4x8 electrodes array with an IED of 10 mm. The MEACS systems are connected to the reference electrode positioned behind the ear.

Figure 11 – Reference electrode (Ø 24mm with a conductive part in Ag/AgCl) and its positioning during the trials for the feasibility study.

Signal Processing Recordings of the muscular activity lasted 5 seconds and the obtained monopolar signals were pass-band filtered. Specifically, a 4th order Butterworth filter with a bandwidth of 20-400 Hz was used for this purpose, in line with the frequency band of the electromyographic signal itself [40]. The visual identification of the swallow onset was carried through the envelope of the signal (rectified and low-pass filtered using a 4th order Butterworth filter at 4 Hz). A 2D map of the RMS values (and interpolated with a 6 factor) was generated representing the isolated event corresponding to the act of a swallow. Moreover, the single swallow event (lasting 1,5 seconds) was temporally equally divided into 10 consecutive, non-overlapped epochs in order to look at a sequence of 2D RMS-based maps, representative of approximately 150 ms. Changes of the muscular activity were analyzed frame by frame, for each experimental setup. For a better comparison of the 2D RMS-based maps, the minimum of the color bar was set to a common level computed as the minimum of activity overall the involved arrays, for each analyzed case (case A, B, C). On the contrary, the maximum of the color bar was not common to all the electrodes arrays, relatively to each setup. In fact, it was computed separately as the maximum RMS value of each color map, for the three analyzed case (case A, B, C).

Results and Discussions From the results, with all the different experimental setups, the quality of the signals and, consequently, the Signal to Noise Ratio (SNR), revealed to be adequate for the purpose. In fact, the single swallow is clearly distinguishable with respect to the baseline, enlightened also by the analysis of the envelope of the signals. Specifically, *Figure 12* shows representative examples of 32 monopolar signals superimposing their envelopes. While *Figure 13* is a zoom of the single swallow event lasting 1,5 seconds. Moreover, the simultaneous use of different systems didn't come up with interference.

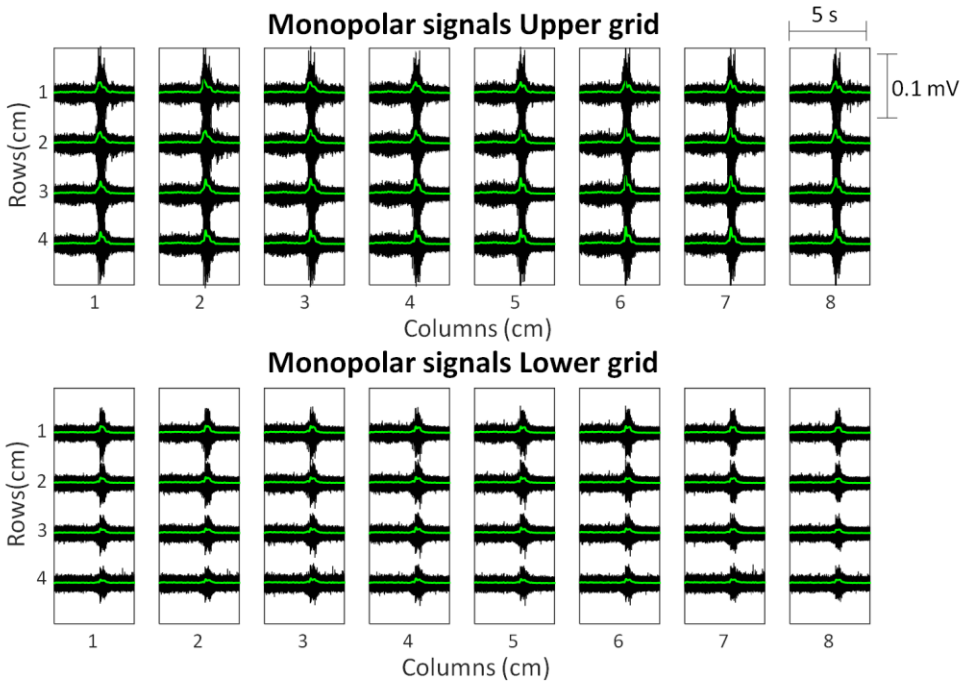

Figure 12 – 5 seconds recordings of a representative subject during swallowing of 10 ml of water. The experimental setup, case C is represented: frontal view of upper grid (4x8 electrodes with IED 10 mm) and lower cross-shaped grid (4x8 electrodes with IED 10 mm). The green traces superimposed on the black signals represent the envelope signals computed through a low-pass filtering at 4 Hz. Signals were normalized by the 98th percentile computed separately, across the grids.

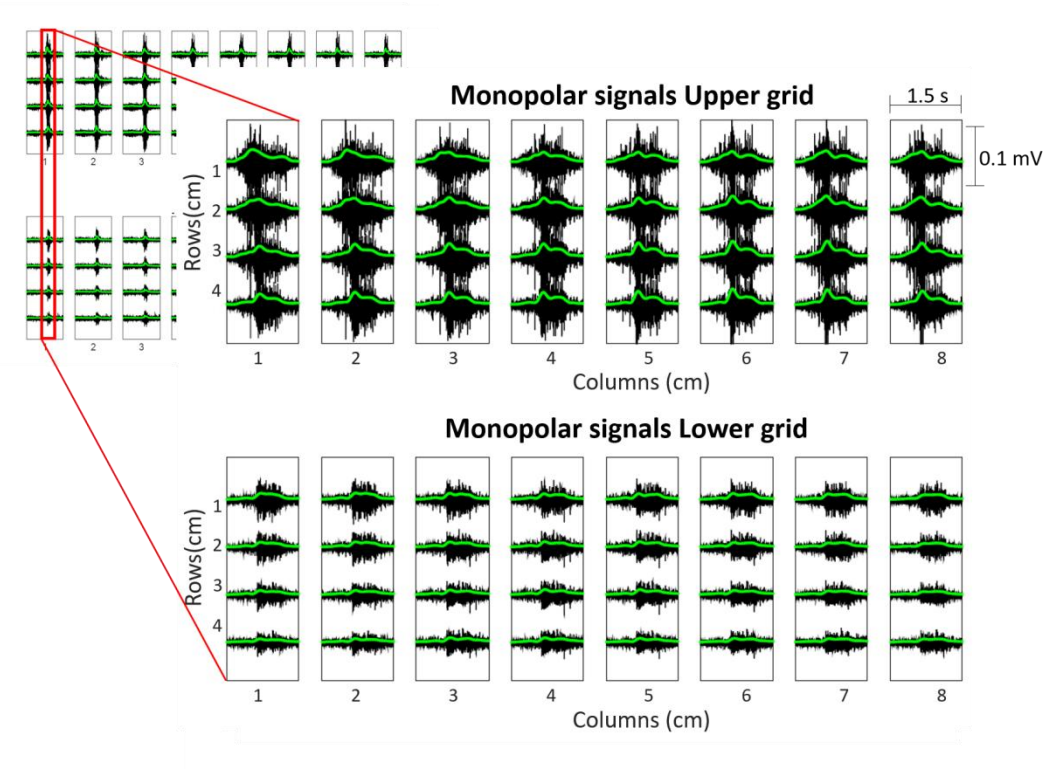

Figure 13 – Zoom of the swallow event (lasting 1.5 seconds) taken from one trial (swallowing of 10 ml of water) of a representative subject with the experimental setup illustrated in the case C. Green traces superimposed on black signals represent the envelope signals computed through a low-pass filtering at 4 Hz. Signals were normalized by the 98th percentile computed across the grids.

The 2D RMS-based maps allowed to visually demonstrate the sequence of the dynamic muscular activities during the swallowing process for qualitative analyses. The distribution of sEMG intensities was achieved using a color bar indicating that hot colors were used for higher intensity. Results were consistent with the swallowing event. In fact, looking at the results obtained from a representative subject relative to the isolated swallowing act, the 2D maps related to the SM complex revealed two symmetric muscular activities. The symmetry was found with respect to the vertical symmetry axis, for all the three explored cases (*Figure 14*). Moreover, the activity of the SM complex was higher than the one of infrahyoid muscles. Nevertheless, at the interface between the

grids of electrodes, intensity values were consistent in all the cases showing a longitudinal continuity of muscle activity. For what concern the differences among the lower grids:

- In the first case, both lower grids of electrodes showed the highest activity in the upper medial corner. In addition, the blue regions on both lateral sides, covering almost half of the color map, indicated a higher sampling volume with respect to the portions of interest. (*Figure 14 A*).
- In the second case, lower color maps showed high muscular intensities in the upper regions of the neck. Nevertheless, the bilateral electrical muscular activities resulted to be broken off in the medial and lateral regions of both lower grids. This suggested a lack of information on both lateral and medial sides. Indeed, the extended leaved empty central region of the neck supports this hypothesis (*Figure 14* B).
- The third case (*Figure 14 C*) presented a good balance between the other two cases: the sampling volume was limited to the regions of interest, ensuring the visual transversal continuity of muscle activity and the IED is the same in both directions. Moreover, the space for the accelerometer was adequate, with no unexplored regions of interest.

A

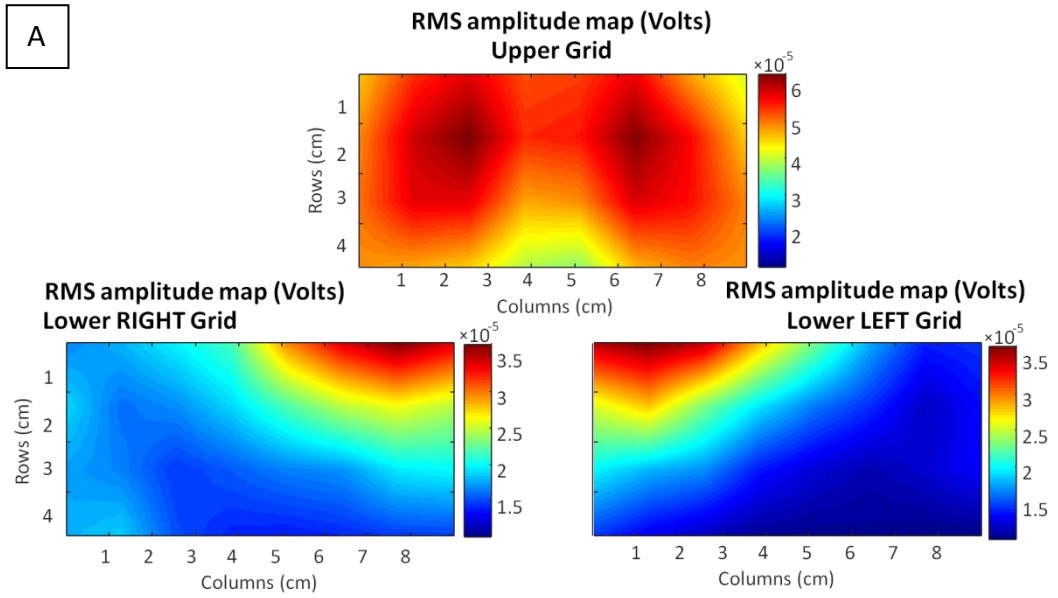
RMS amplitude map (Volts)
Upper Grid
Rows (cm)
Columns (cm)
RMS amplitude map (Volts)
Lower RIGHT Grid
RMS amplitude map (Volts)
Lower LEFT Grid

B

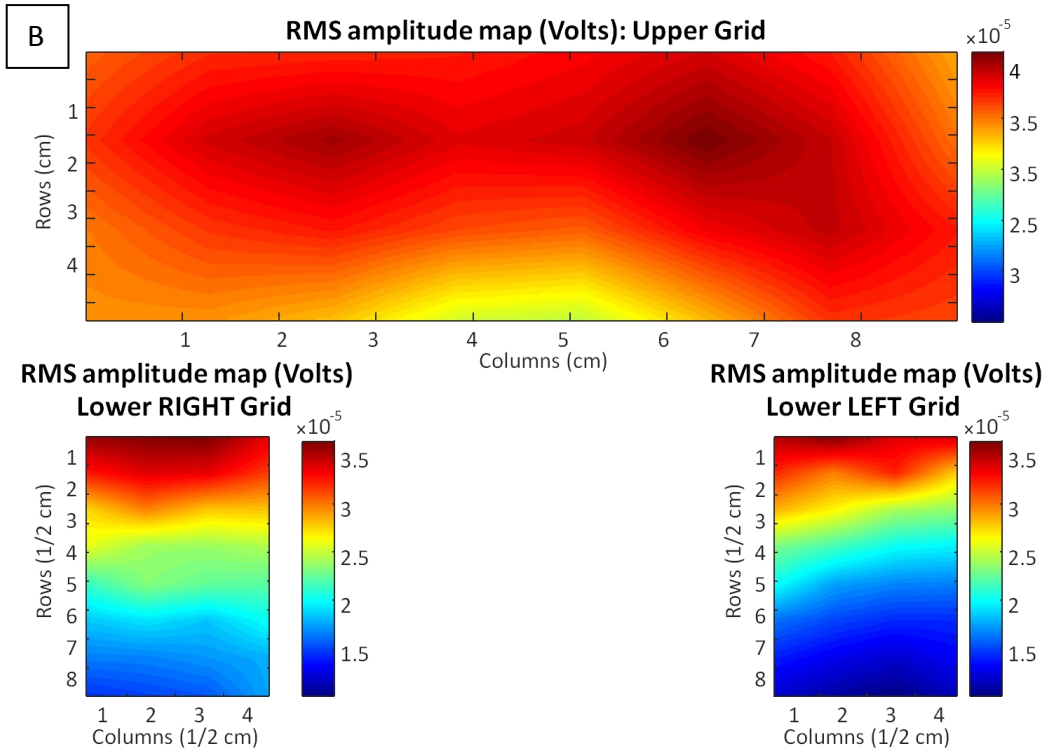
RMS amplitude map (Volts): Upper Grid
Rows (cm)
Columns (cm)
RMS amplitude map (Volts)
Lower RIGHT Grid
Rows (1/2 cm)
Columns (1/2 cm)
RMS amplitude map (Volts)
Lower LEFT Grid

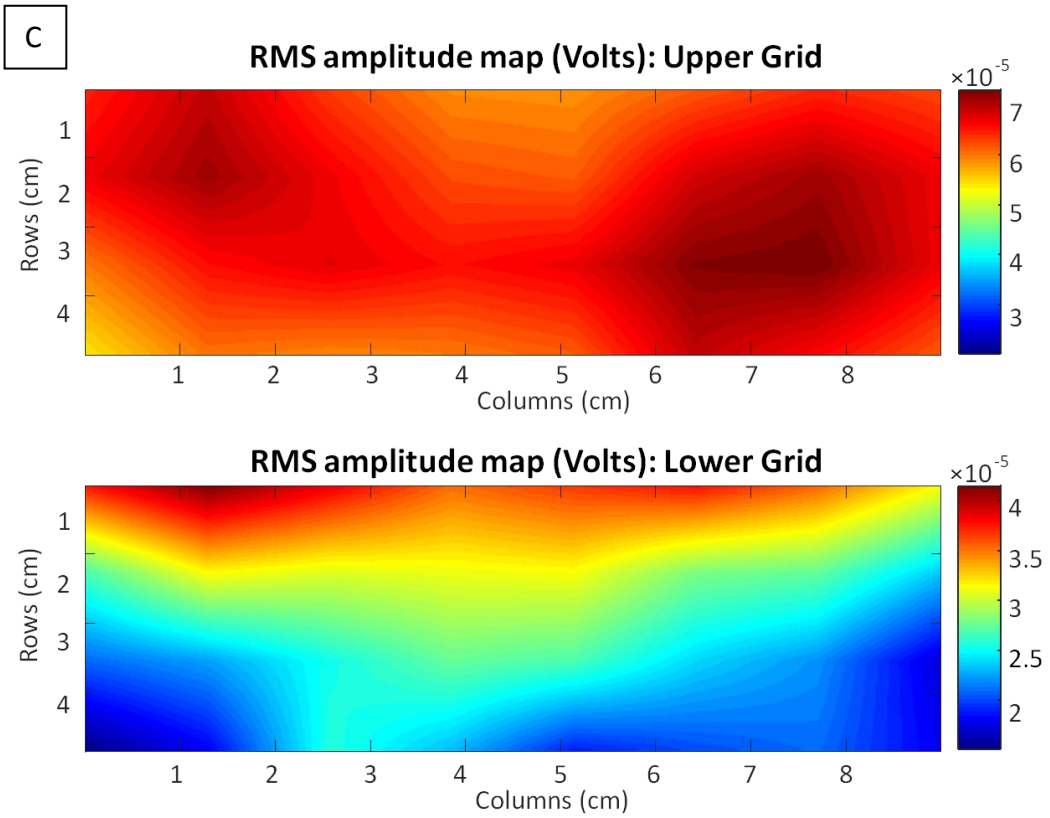

Figure 14 – Dynamic HD sEMG energy maps (RMS-based) during a single swallowing act (10 ml of water) lasting 1.5 seconds. From top to bottom frontal view of the three analyzed cases: a single upper grid of electrodes (4x8 with an IED of 10 mm) for the SM complex and (A) two lower grids of electrodes (8x4 with an IED of 5 mm; (B) two lower grids of electrodes (4x8 with an IED of 10 mm); (C) a lower cross shaped grid of (4x8 with an IED of 10 mm). The minimum of color bar was set at the minimum of activity across the grids, while the maximum was set separately to each matrix.

Looking at the different epochs of approximately 150 ms (*Figure 15*), according to the phases of swallowing, at the beginning of the task there was no activity, being the subject at rest. After the instruction to swallow, the soft palate elevated and the water bolus was pushed posteriorly. For this reason, the activity of the submental muscles increased because of the lifting of the bolus. This is shown by the hot colors in the first epochs of the colormap, representing the

upper matrix of electrodes of the SM region. Moreover, the activity of the SM complex preceeded the acivity of the infrahyoid muscles: the higher intensity of the SM muscular activity was reached earlier (almost 150 ms) than the maximum activity related to the infrahyoid muscles. In fact, only when the bolus was pushed into the pharynx the activated complex of infrahyoid muscles resulted in a higher intensity on sEMG energy maps, while the activity of the SM complex decreased. In the end of swallowing, the EMG activity gradually decreased until the return to its rest level. All these passeges are clearly visible in the example of *Figure 15*.

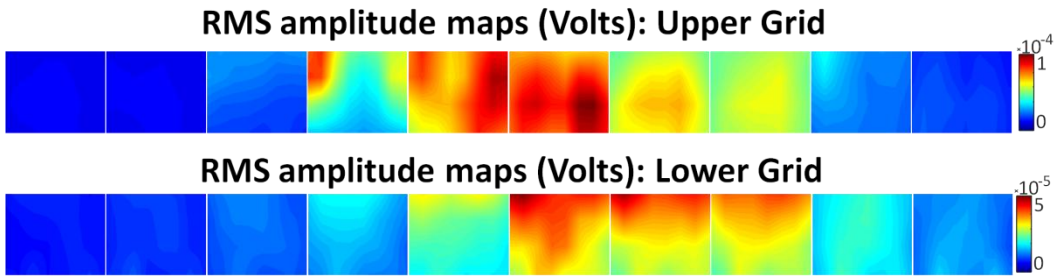

Figure 15 – Consecutive dynamic HD-sEMG energy maps (RMS-based) of 10 non overlapped epochs (each one lasting 150 ms) related to a single swallowing act (10 ml of water). The Experimental setup, case C is represented: a single upper grid of electrodes (4x8 with an IED of 10 mm) and a lower cross shaped grid of electrodes(4x8 with an IED of 10 mm). The minimum of color bar was set at a zero level indicating no activity, while the maximum was set separately to each matrix.

Conclusion The grids of electrodes revealed a good quality of recorded signals. Results suggested the use of HD-sEMG for the assessment of swallowing function as an innovative technique, overcoming the limits related to the other techniques (e.g. invasiveness of the needle EMG, global analysis of conventional bipolar electrodes and other limitations as the positioning of many electrodes one by one of other studies involving the HD-sEMG). Qualitative analyses of dynamic HD-sEMG energy maps (RMS-based) demonstrated a consistency with respect to the performed task. In fact, the muscles activation sequence resulted

in line with the physiology of swallowing. Moreover, among the different setup possibilities, the one involving the use of the cross shaped matrix seemed to be the most suitable for further analyses. Reasons supporting this hypothesis were: the defined space for the placement of an accelerometer, the sampling of portions of interest, the use of only two grids avoiding additional cables (due to the reference electrode), possible interference and eventually problems of synchronism of the systems. This resulted in a simplification of the entire experimental setup, revealing to be a new approach for a continuous visualization of the swallowing process [5].

2.2 Hyolaringeal excursion recordings

Instrumentation A technique developed for non invasive biomechanical assessment of the pharyngeal phase of swallowing is the measure of the acceleration signal recorded over the throat [21], [36]. In fact, since the reflexive activity of swallow starts with the hyoid elevation, the movements of the linked anatomical structures could provide additional input for the segmentation of swallowing event. Therefore, through the recordings of the inertial sensor, a temporal segmentation of swallowing phases based on hyolaringeal excursion can be achieved. An important correlation between laryngeal elevation and the magnitude of an acceleration signal was found by Zoratto et al (2010) using a dual-axis accelerometer placed on the participants' neck recording vibrations in the anterior-posterior and superior-inferior directions [36]. For this reason, in this preliminary study, the movement of the larynx was monitored by an ultra compact linear tri-axis accelerometer (LIS344ALH, STMicroelectronics, Netherland (*Figure 16*) with a selected full scale of ±2g) placed on the skin at the neck level. The sensor gave data about laryngeal elevation over time during a swallow and measured the mechanical upward and downward laryngeal movements [29].

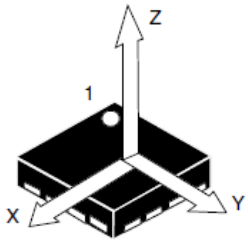

Figure 16 – Inertial sensor LIS344ALH, STMicroelectronics. The directions of the detectable accelerations are shown as X, Y, Z being a tri-axial sensor.

Three different placements of the sensor were tested, as reported in the *Figure 17*, in order to identify the best one among the following locations of the accelerometer:

A) Above the thyroid cartilage
B) On the thyroid cartilage
C) Between the thyroid and cricoids cartilages (cricothyroid space)

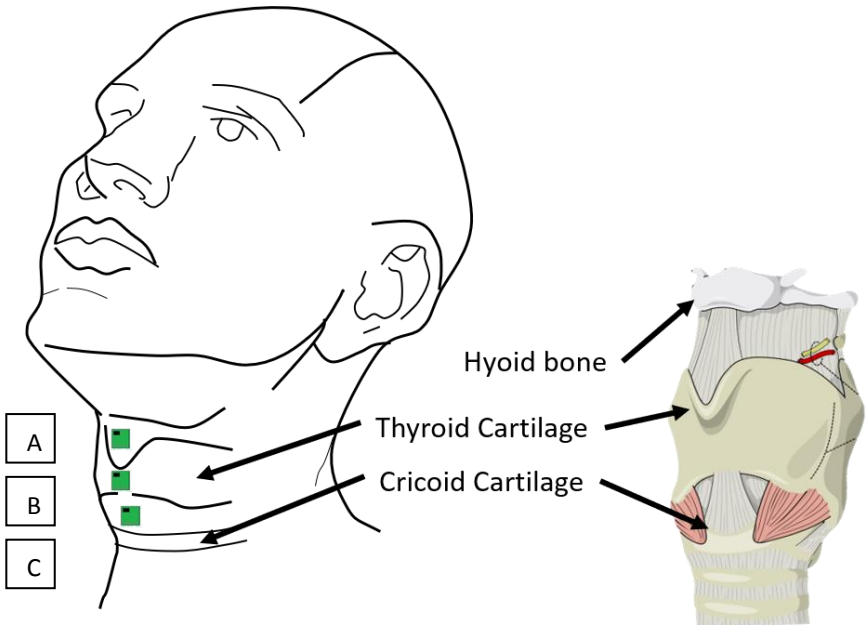

Figure 17 – Different sensor placements with respect to relevant anatomical structures shown on the right. On the neck of the subject, from top to bottom:

accelerometer placed A) above the thyroid cartilage, B) on the thyroid cartilage, C) in the cricothyroid space.

Each location was identified by palpation of the neck of the subject thanks to the physical landmarks recognized in a condition of rest, placing the accelerometer at the midline of the subject's neck. The sensor was fixed in the relative positions via a biocompatible tape (Hypafix, BSN Medical) and oriented in such a way that the Z axis was in the Anterior-Posterior direction and the Y axis was in the Superior-Inferior direction. Moreover, the anterior and superior directions corresponded to positive amplitude as shown in *Figure 18*. The third axis (X-axis) of the accelerometer wasn't taken into account because no remarkable movements have been recorded in the Medio-Lateral direction. This observation was consistent with other studies [37], [36].

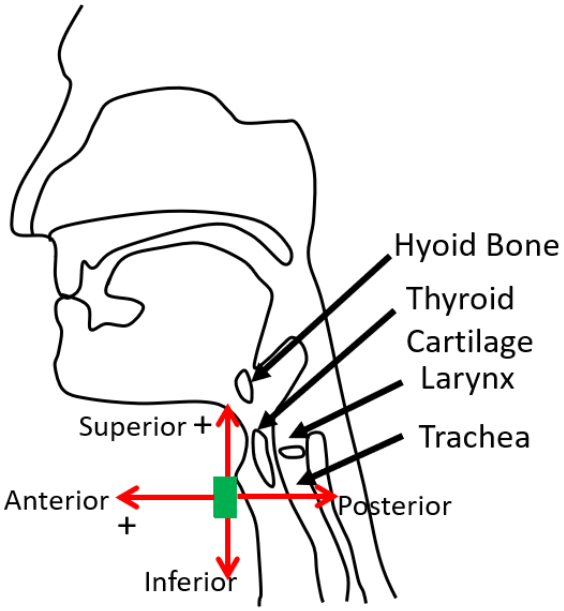

Figure 18 – Sign convention of the axes of the accelerometer on the lateral view of a subject [37].

A modular wireless system (DuePro, OT Bioelettronica, Torino, Italy shown in *Figure 19*) was used for the acquisition of the biomechanical signals coming from the inertial sensor.

Figure 19 – From left to right: top and top with cover view of the DueStation (OT Bioelettronica, Torino, Italy) containing the probes used for the recording of biomechanical signals.

Specifically, a DueBio probe (*Figure 20* with technical specifications reported in the Table 2) was connected to the accelerometer, after being properly configured.

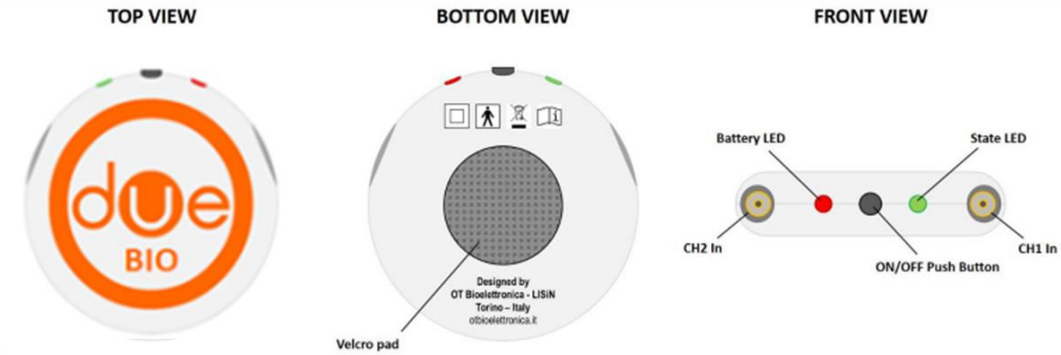

Figure 20 – From left to right: top, bottom and frontal view of the DueBio (OT Bioelettronica, Torino, Italy) probe for the acquisition of two biomechanical or kinematic signals.

Table 2 – Technical specifications of the DueBio probe.

Parameter	***Value (m.u)***
Number of not conditioned signals	2

Number of conditioned signals (Gain 100V/V, Bandwidth 0Hz-100Hz)	2
IMU	3 axes accelerometer (±8g) 3 axes gyroscope 3 axes magnetometer
Input noise (applicable to conditioned signals)	< 2 µVRMS
CMRR (applicable to conditioned signals)	>100dB
Sampling frequency (conditioned and not conditioned signals)	2048Hz
Sampling frequency (IMU)	100Hz
A/D converter resolution	16 bit
Power supply available on the output connectors	0V-3.3V
Receiver	PC(Windows)
Wireless transmission protocol	Bluetooth 4.0
Power supply	3.7V LiPo battery
Charging mode	Inductive
Weight	12g
Size	21mm (Radius) x 1mm (thickness)

The probe served as a power source for the accelerometer itself (with a 3,3V DC power supply without using an external one) and as a receiver of the signal. The connection with the accelerometer was ensured with two jack connectors, one for each direction Y and Z (Figure 21).

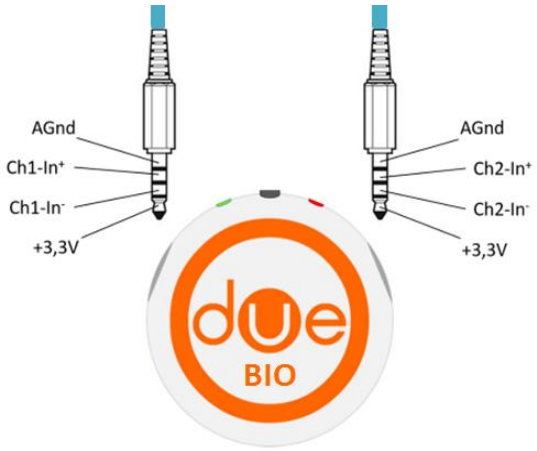

Figure 21 – Connections of the accelerometer and the DueBio probe through jack connectors.

Being two the channels of the probe, as specified in the technical specifications, the sensor was used as a dual-axes accelerometer, also because of the non relevant information from the third axis. Data were transmitted real time, wirelessly from the probe to a PC and stored for further analyses. The entire system was worn through wearable straps belts fixed at the level of the chest to ensure the stability of the system itself.

Signal processing In order to assess the reliability of accelerometric traces a double analysis was performed. Considering the slow dynamics of the laryngeal movements consequently related to low frequencies, a low-pass filter was used. More in detail, a 4^{th} order Butterworth filter with a cutoff frequency of 3 Hz was used, considering that a single swallow lasts more or less 1 second. Each recording lasted 5 seconds and for each subject an alignment was performed between the different trials taking the first recorded signal as a reference for the

assessment of the intra-subject variability. The alignment was carried out searching the maximum of the cross correlation and shifting the signals depending on the delay found. Finally, the aligned signals were averaged in order to obtain a mean behavior. Nevertheless, taking into account that the swallowing mechanism is linked to vibrations (in the range of high frequencies), especially due to the passage of the bolus, the recorded signals were used to extract helpful information for the evaluation of the different stages of the swallowing process. For this reason, a high-pass, 4^{th} order Butterworth filter with a cutoff frequency of 5 Hz was used with the purpose of isolating vibrations related to the movement of the hyolaringeal complex. The high-pass filtered swallowing signals were processed through a segmentation in order to isolate the swallow onset and offset suitable for the identification of different phases. Although being mindful of the possible temporal delay between hyolaringeal elevation and the appearance of a vibratory signal due to the mechanical damping of the soft tissue [36], a method of exceeding a threshold was defined. The threshold was calculated as 5 times the standard deviation of the baseline noise contained in the first 1.5 seconds of each recorded signal (rest condition). Starting from the absolute value of the signal, each point exceeding the empirical threshold was identified. The swallow onset and offset were determined respectively as the first and the last point above the threshold. Nevertheless, an automatic detection of the pharyngeal phase in swallowing could be more advisable. After a qualitative analysis of the results, in order to explore all the spectral bands of the accelerometric signal over time, a time-frequency analysis was carried out. The time frequency distribution of each signal was obtained through the Cohen's transform after being re-sampled at a frequency of 128 Hz for computational reasons. More in detail, a Choi-Williams transform was chosen, passing through the plane of the ambiguity function and using a particular kernel (Eq. 2.1) to attenuate the cross interferential terms.

$$g(\tau, \vartheta) = e^{-\frac{\vartheta^2 \tau^2}{\sigma}} \qquad (2.1)$$

In this case, σ value was set at 0.5. To better understand the importance of information given by the transform on the time-frequency plane, two integrals over time between two values of frequency were computed. The aim was to separate the frequency contributions: higher frequencies linked to the epidermal vibrations and lower frequencies for the slow dynamics movements. The chosen frequency boundaries in the former were 5 Hz and 15 Hz, while in the latter were 1 Hz and 3 Hz. The analysis was carried out for all the recorded signals from the different locations of the inertial sensor.

Results and Discussions The low-pass filtered signals, in according to the literature, showed two visible peaks. In line with the sign convention of the axes of the accelerometer, it was expected a dual behavior of the two channels. In fact, it was expected a first negative peak for the Y-Axis and a positive peak for the Z-Axis due to the anterior-upward movement of the larynx. While the following second peak (positive for the Y-Axis and negative for the Z-Axis) was expected to be linked to the downward movement of the larynx towards its rest condition. In addition, a distance between these two peaks of approximately 500 ms was expected, according to the results reported in literature obtained from measures on healthy subjects [3], [2]. Being the peak distance related to the laryngeal movements, it reflected the apneic period during the pharyngeal phase of swallowing centered between the late inspiration and the late expiration in which the single swallow takes place [3]. Results of *Figure 22* provide a confirmation of the hypothesized behavior of the signals. Moreover, results over the trials, suggested the cricotyroid space as the most suitable for the accelerometric recordings, focusing on Z axis of the inertial sensor.

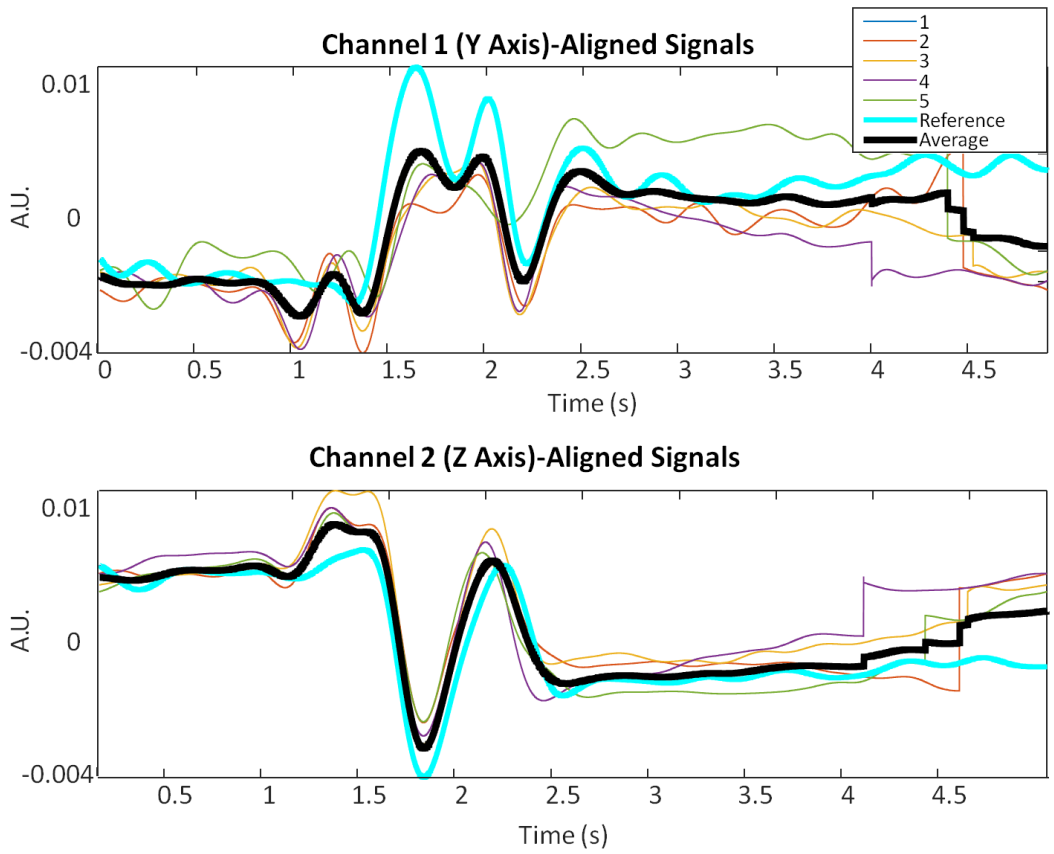

Figure 22 – Examples of trends of 5 seconds laryngeal movements recordings during swallowing of 10 ml of water. Recordings from the accelerometer in the cricothyroid space are represented. Signals were low-pass filtered at 4 Hz and recordings from different trials (of the same representative subject) were aligned using the method of the maximum of the cross-correlation. The bold black signal represents the average from all the trials after the alignment. The bold cyan signal represents the signal taken as the reference with respect to all the trials.

Nevertheless, the analysis on other trials showed that this type of processing was not so reliable for an automatic detection of swallowing segmentation, although the acceptable intra-subject variability. In fact, measures showed a very high inter-subject variability. Moreover, some of the unexpected trends (*Figure 23*) revealed many oscillations instead of two smooth peaks, making the

identification of the instants of interest difficult for the evaluation of the swallowing phases.

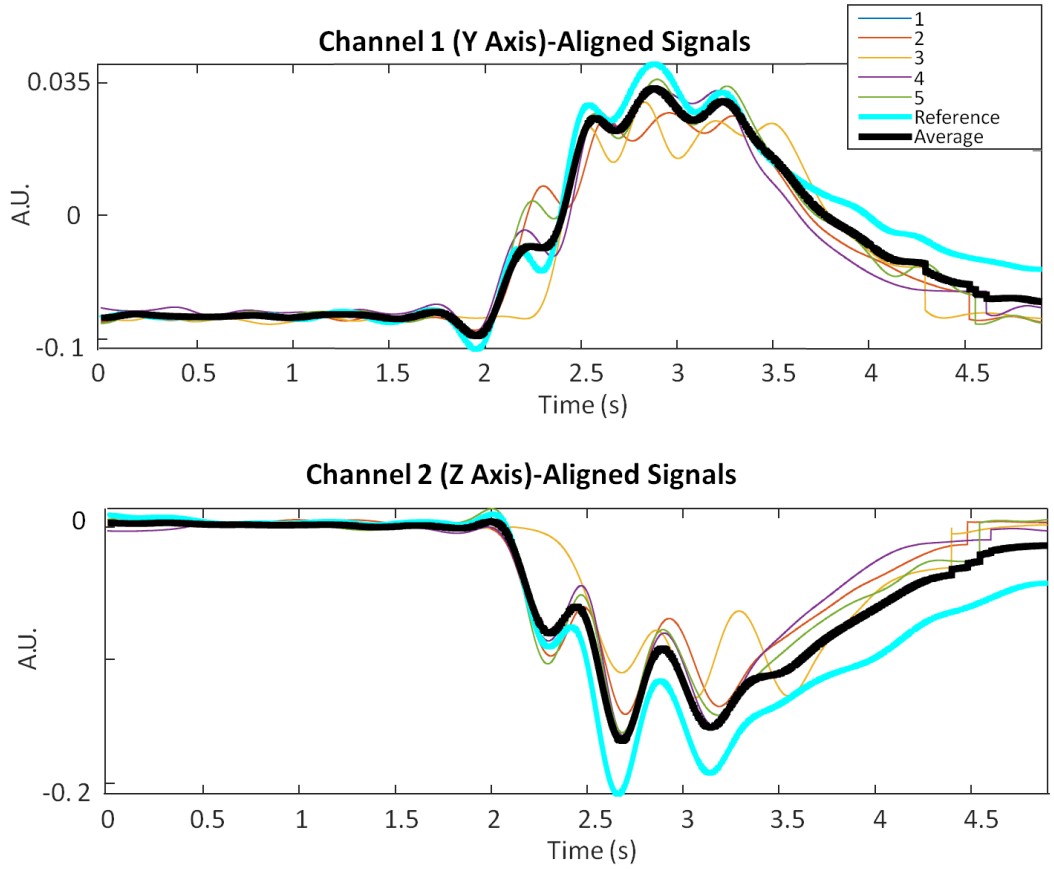

Figure 23 – Examples of unexpected trends of 5 seconds laryngeal movement recordings during swallowing of 10 ml of water. Recordings from the accelerometer in the cricothyroid space are represented. Signals were low-pass filtered at 4 Hz and recordings from different trials were aligned using the method of the maximum of the cross-correlation. The bold black signal represents the average from all the trials after the alignment. The bold cyan signal represents the signal taken as the reference with respect to all the trials.

On the other hand, the results of the high-pass filtering, used in order to overcome the disadvantages related to the low-pass filtering, are shown in the *Figure 24*. The peaks above the threshold were superimposed on the signals, the

first and the last one were identified with two green vertical lines ideally corresponding respectively to the swallowing onset and offset:

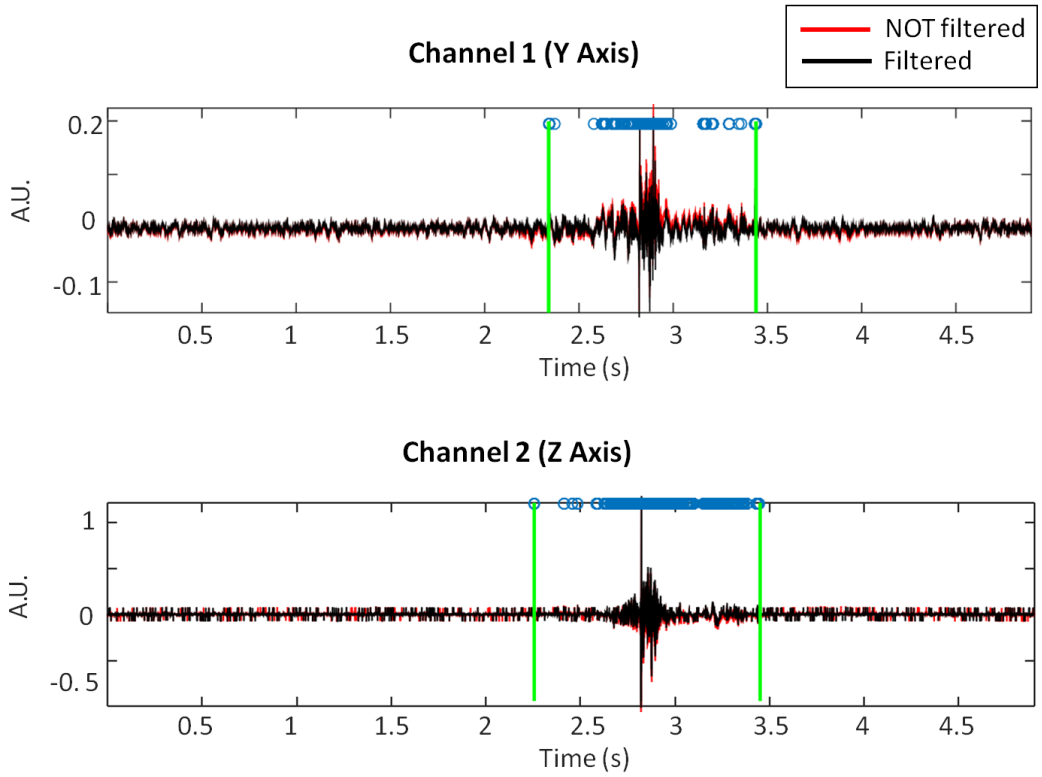

Figure 24 – Examples of 5 seconds laryngeal movements recordings during swallowing of 10 ml of water from three different placements of the inertial sensor. Signals were high-pass filtered at 5 Hz and recordings are represented superimposing the peaks exceeding a threshold (computed as 5 times the standard deviation of the baseline noise of the first 1.5 seconds). Recordings from the accelerometer in the cricothyroid space are represented.

Regarding the positions of the inertial sensor, results revealed a higher SNR for the Z-Axis recordings (*Figure 24*). Results of the threshold-method revealed to be unreliable. Some trials revealed further problems in finding the expected peaks, underlining the lack of repeatability of the technique. In fact, since the threshold method found peaks also outside the interval of the single swallow, a visual inspection was necessary to ensure the reliability of the found peaks. For this

reason, this method was prone to error and could be subjective. Consequently, working on a time-frequency plane potentially reveal more significant information in finding instants of interest (swallow onset and offset). In the end, examples of the CW transforms signals recorded from both Y and Z directions are shown in the figures below (*Figure 25*).

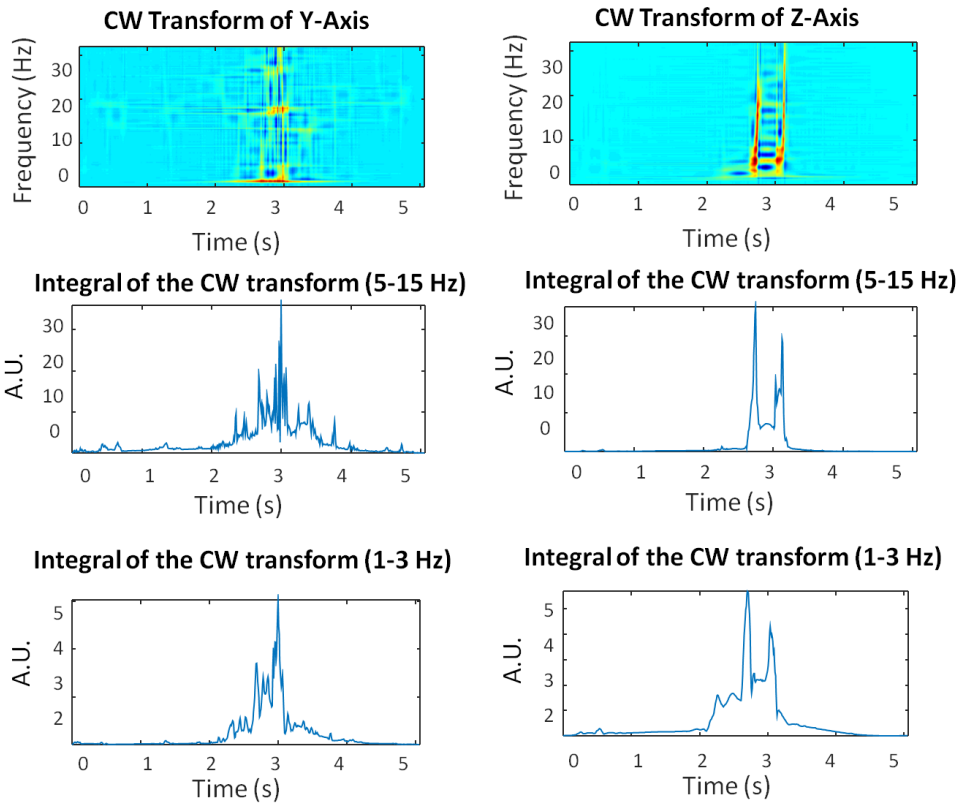

Figure 25 – Examples of 5 seconds laryngeal movements recordings during swallowing of 10 ml of water from three different placements of the inertial sensor. Not filtered signals related to both Y and Z directions were used for the computation of the CW t-f transform. Two integrals over time (between 5 and 15 Hz and between 1 and 3 Hz) were computed in order to identify the instants of onset and offset of a single swallow. Recordings from the accelerometer in the cricothyroid space are represented.

The integrals of the CW transform showed two components: at higher and lower frequencies. The integral computed between 5 and 15 Hz demonstrated the presence of peaks with respect to the baseline. Since these peaks were related to the epidermal vibrations due to the hyolaringeal excursion, they could be attributable to the swallow onset and offset. Indeed, the peak distance revealed to be in line with the distance over time expected from the previous researches (approximately 500 ms). Moreover, the distinctness of these peaks is more noticeable on Z-Axis traces than the Y-Axis ones. On the other hand, the integral of the CW transform computed between 1 and 3 Hz was related to the slow dynamics of the swallowing task. As a result, it included any baseline raisings, also those due to postural variations. It was suggested that lower frequency components take into account anatomical displacements related to the preparation to the reflexive pharyngeal phase. Whereas, higher frequency components could be attributable to the vibrations due to passage of the bolus.

Conclusion The analysis led to the conclusion that the most advantageous condition for the purpose was related to the sensor placed in the cricothyroid space. The reasons were: (i) the highest signal to noise ratio, (ii) the easiest identification of the peaks of interest, (iii) the smallest inter-subject and intra-subject variability and the highest repeatability of the technique observed in signals of the channel 2 (Z direction). Moreover, the analysis on the t-f plane revealed an immediate visualization of the moments of interest potentially usable for the swallowing segmentation.

2.3 Combined recordings of hyolaringeal excursion and HD- sEMG

Once demonstrated the usability of the HD-sEMG and the accelerometer for both electrophysiological and mechanical swallowing analysis, with the present feasibility study, we carried out also simultaneous recordings of muscular activities and hyolaringeal excursion.

Instrumentation HD-sEMG was acquired using two MEACS systems (*Figure 9*): one for the upper matrix (4x8 electrodes-IED 10 mm) positioned on the SM complex and one for the cross shaped matrix for infrahyoid muscles (4x8 electrodes-IED 10 mm). The placement of the electrodes arrays was in line with the one illustrated in case C (*Figure 10*). The hyolaringeal excursions were recorded using the inertial sensor illustrated in the *Figure 16*, placed on the midline at the level of the cricothyroid space. The entire experimental setup is reported in *Figure 26*.

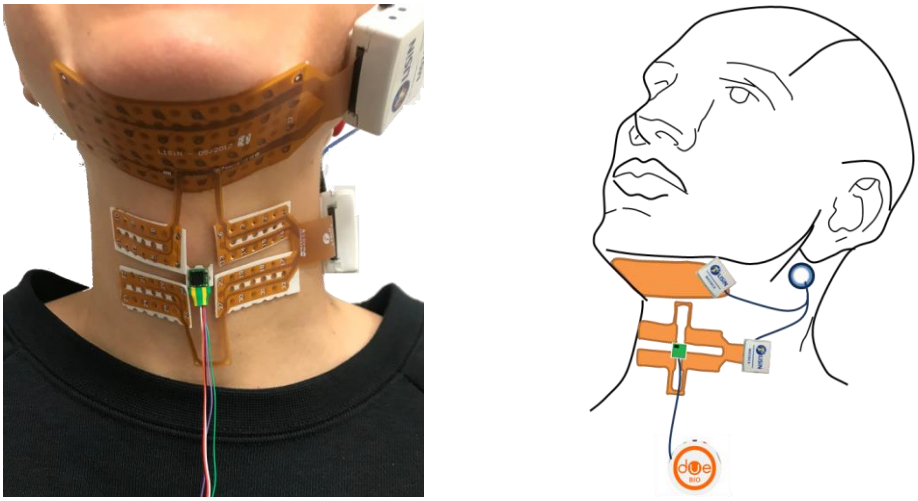

Figure 26 – Complete setup for the combined recordings of the acceleration of the throat and muscular activities through the HD-sEMG system.

Signal Processing Recordings were performed as described previously, following the same tasks. Accelerometric signals were analyzed in a t-f plane and processed analogously to paragraph 2.2. As concern HD-sEMG, monopolar signals were processed as explained in paragraph 2.1, and also 2D RMS-based color maps were computed. In this case, the consecutive non-overlapped epochs were chosen with a different temporal support. In fact, a manual segmentation based on visual inspection through the recorded frame analysis provided temporal boundaries for epoch division, adequately superimposed on the signals.

Results and Discussions Recorded signals demonstrated a satisfying SNR and negligible power line interference. The global trend of the accelerometer signal followed the one of the EMG envelopes. Moreover, looking at the RMS-based color maps, the sequence of muscular activity showed the pattern of muscular activation during the swallowing event and a good consistency was found between color maps and accelerometric traces. In fact, at first, there was no active region and the inertial sensor showed a period of baseline rest. After the instruction to swallow, the subject of the *Figure 27* activated at first the SM region. As the complex activity increased, an increase of the integral of the CW between 1 and 3 Hz was observed, reflecting the preparation to the swallowing event. The following activation of infrahyoid muscles was confirmed by the appearance of hot colors also in the lower color map, until the overall intensities reached a maximum. In correspondence of this epoch the processed accelerometric signal (integral between 5-15 Hz of CW transform) showed the highest oscillations. Both upper and lower EMG activities decreased in the last epochs because of the onset of the esophageal phase. During the last epoch, although the absence of activity read from the color bar, the processed accelerometric signal was not at the baseline. This was probably due to the return of the anatomical structures toward the rest condition, being a passive activity without involving any muscle activity. Nevertheless, it may be enlightened that the selected temporal boundaries could be shifted of hundreds of ms because of the effect of mechanical damper offered by soft tissues. Indeed, this effect could result in a temporal delay between the beginning of the muscle activity and the appearance of a corresponding accelerometric signal [36].

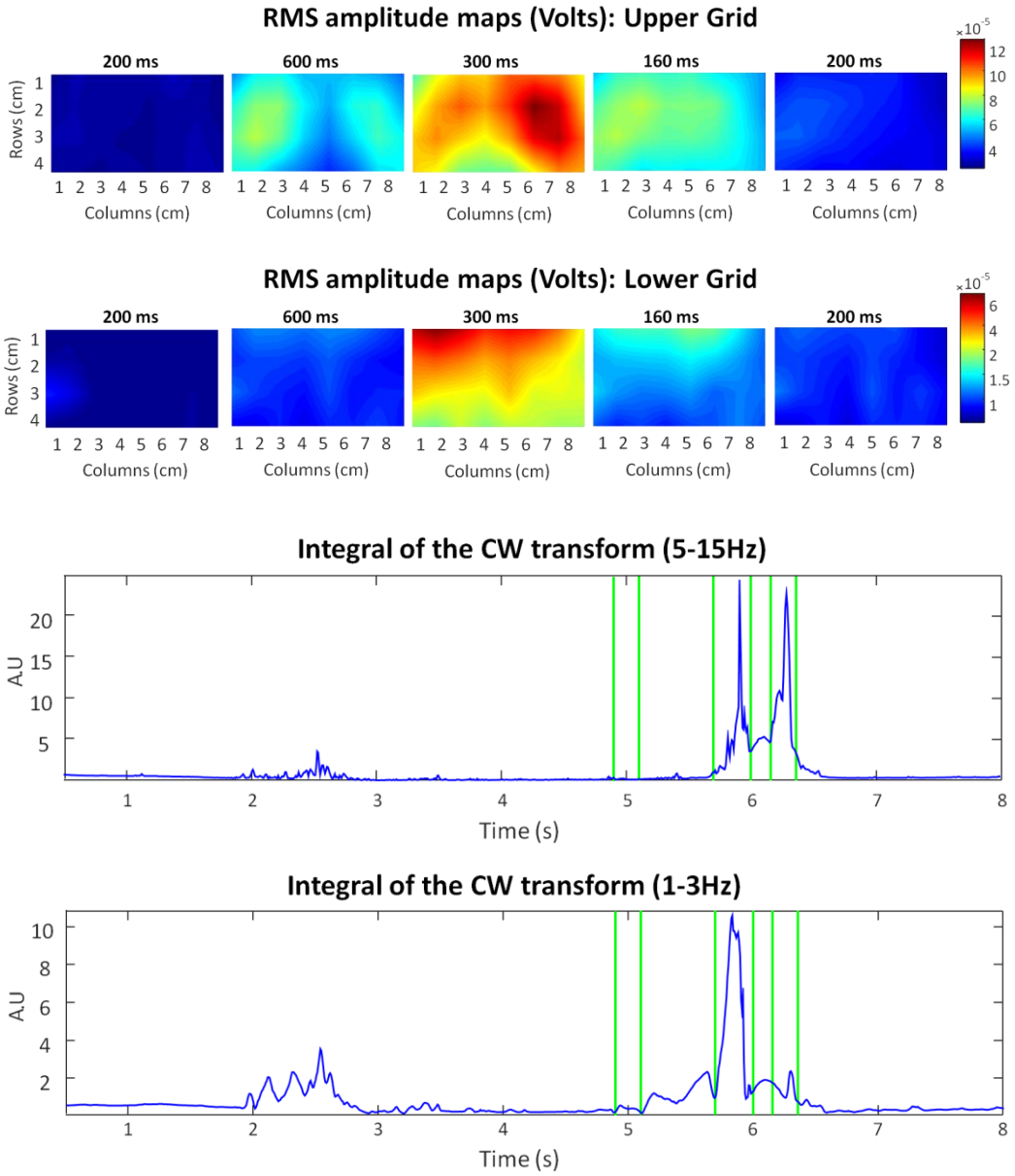

Figure 27 – From top to bottom: frontal view of consecutive dynamic HD-sEMG energy maps (RMS-based), processed accelerometric signals (integral of CW 5-15 Hz and 1-3 Hz) related to a single swallowing act (10 ml of water) of a subject. The minimum of color bars was set at the minimum of activity across the two grids, while the maximum was set separately to each matrix. Vertical green lines

on the accelerometric signals refer to temporal boundaries of epoch division obtained from manual segmentation.

The same pattern was not found analyzing the sequence of muscular activities of another subject. In fact, in the second representative subject the first SM complex activation was preceded by a previous infrahyoid muscles activation (*Figure 27*). The reason was the high inter-subject variability as concern the pattern activation of swallowing muscles. Nevertheless, the same intra-subject consistency between RMS-based and accelerometric signal was found. Specifically, the representative subject of *Figure 28*, at first, weakly activated the infrahyoid complex. A correspondence of this activation was found analyzing the processed hyolaringeal excursion signal (integral of the CW between 1 and 3 Hz) showing a preparation to the event. Then the SM complex activated on both left and right sides. This activation was accompanied by a slow increase of the integral computed between 1 and 3 Hz from the CW transform. Also in this case, the activation of infrahyoid muscles followed the SM activity up to a maximum. This epoch is traced by highest oscillations of the processed accelerometric signal (integral between 5-15 Hz of CW transform). After a decrease of the activity of both muscular regions, a peak associated to no muscular activity was identified underling a common aspect among different subjects although the variability in the sequence of muscular activation.

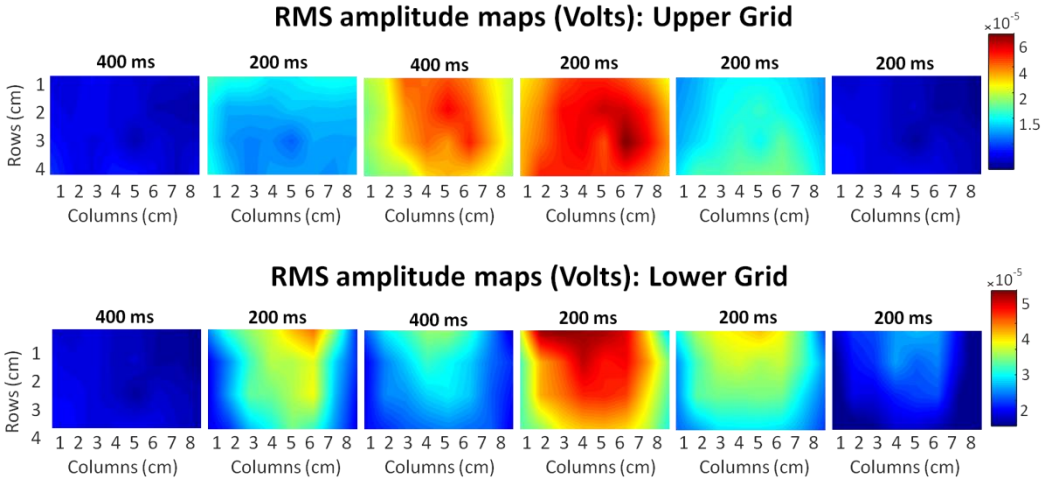

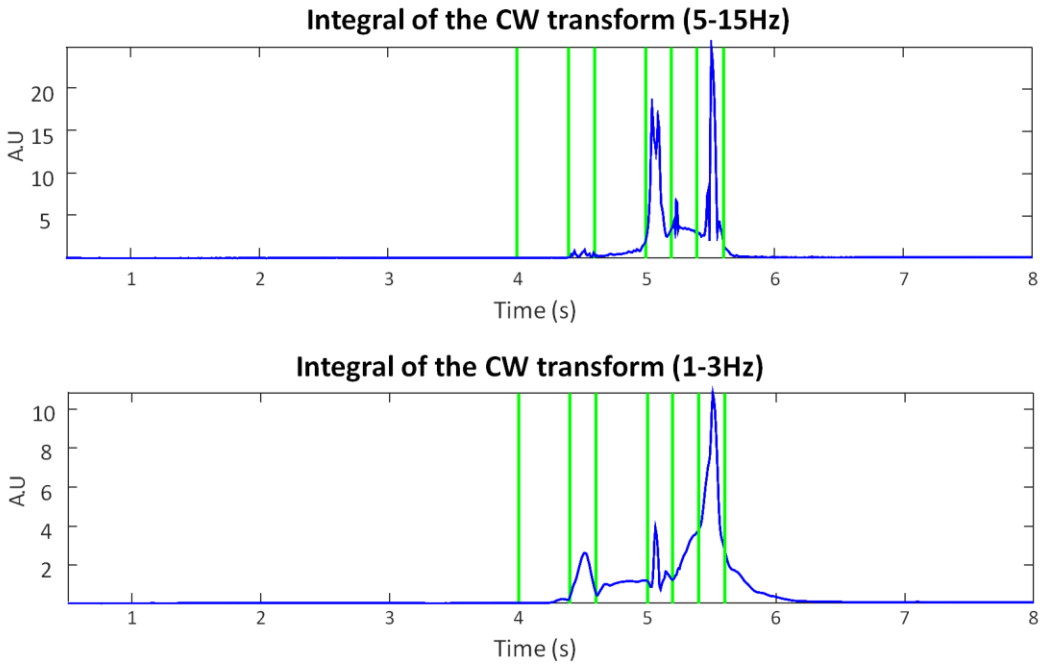

Figure 28 – From top to bottom: frontal view of consecutive dynamic HD-sEMG energy maps (RMS-based), processed accelerometric signals (integral of CW 5-15 Hz and 1-3 Hz) related to a single swallowing act (10 ml of water) of a subject. The minimum of color bars was set at the minimum of activity across the two grids, while the maximum was set separately to each matrix. Vertical green lines on the accelerometric signals refer to temporal boundaries of epoch division obtained from manual segmentation.

Conclusion Results suggested the good agreement between both electrophysiological and mechanical evaluation of the swallowing process. Specifically, two frequency components emerged: lower frequencies were in line with the first preparatory phases of swallowing, while higher frequencies were involved in the reflexive activities of swallowing relative to the passage of the bolus. Moreover, visual inspection led to a coherent swallowing phases segmentation. 2D RMS-based maps allowed to visually demonstrate the spatiotemporal activation of muscles, increasing local information over time. The weak spots are the intra-subject variability of the swallowing itself and the

subjectivity of the segmentation, due to the arbitrary choice of temporal boundaries for epoch division.

2.4 Tongue Pressure recordings

The profile of tongue pressure can be achieved using a pressure sensor held in the mouth in direct contact with the tongue and the palate. In fact, Fukoka et al. showed how the use of a super-thin sensor sheet could be helpful in order to extract tongue pressure patterns during swallowing in healthy people [26].

Instrumentation The tongue pressure was recorded through a thin disk-shaped force sensor (FlexiForce Sensor model Standard A201, Tekscan) (*Figure 29*) fixed to the palate through an adhesive paste for orthodontic devices. Technical specifications of the sensor are reported in the *Table 3*.

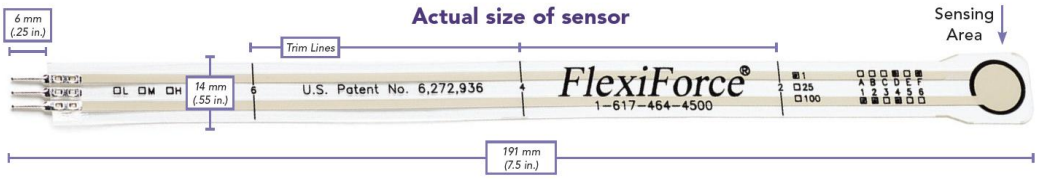

Figure 29 – Sensor for measurements of the tongue pressure.

Table 3 – Technical specifications of the FlexiForce, sensor used for the measure of tongue pressure against the palate.

Parameter	***Typical Performance***
Linearity (Error)	< ±3%
Repeatability	< ±2.5% of full scale
Hysteresis	< 4.5 % of full scale
Drift	< 5% per logarithmic time scale
Response Time	< 5µsec
Operating Temperature	-40°C – 60°C

The positions of the sensor were determined in according to previous researches [38] and are reported in the following *Figure 30*.

- Anterior Position (A): 5 mm posterior to the incisive papillae.
- Posterior position (P): one-third posterior between incisive papillae and posterior edge of the palate.

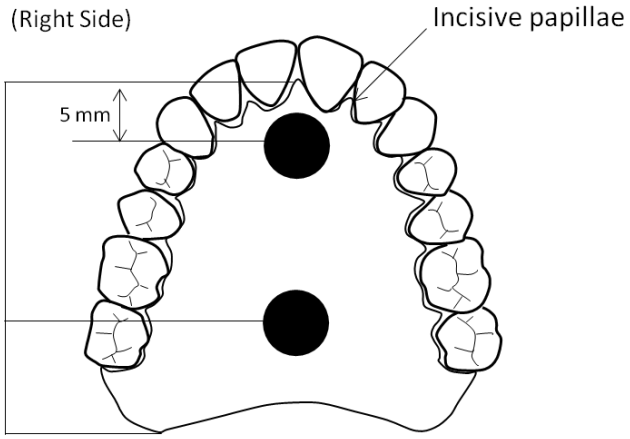

Figure 30 – Locations of pressure sensors on the palate. A) Anterior position (5 mm posterior to the incisive papillae); P) posterior position (one-third posterior between incisive papillae and posterior edge of the palate).

Also in this case, the output of the conditioning circuit of the pressure sensor was connected to the input of a DueBio probe (*Figure 20*) through a single jack connector, sent real-time, wirelessly to a PC and stored for further analyses. Two sensors were used simultaneously, recorded from the two channels of the probe in order to avoid any delay between the two signals. The long cables covered by a vinyl tube of the sensors came out from the oral cavity and were connected to the correctly configured probe inserted in a wearable straps belt ensuring the stability of the system.

Signal processing Recordings of the tongue pressure lasted 5 seconds and the obtained signals were smoothed using a low-pass filter. More in detail, a 4^{th}

order Butterworth filter with a cutoff frequency of 5 Hz was used for this purpose.

Results and Discussions From the analysis of the pressure traces, the signal to noise ratio was adequate for the purpose (an example is reported in *Figure 31*). It can be noticed a correlation with the swallowing event: the pressure increased over time reaching a maximum, after the instruction to swallow and then it returned to its rest condition. Comparing the trends deriving from the two different locations of the sensor, the sensor in the anteromedian position reached the maximum earlier than the one in the posterior position, in line with the propulsive wave pushing the bolus toward the oropharynx.

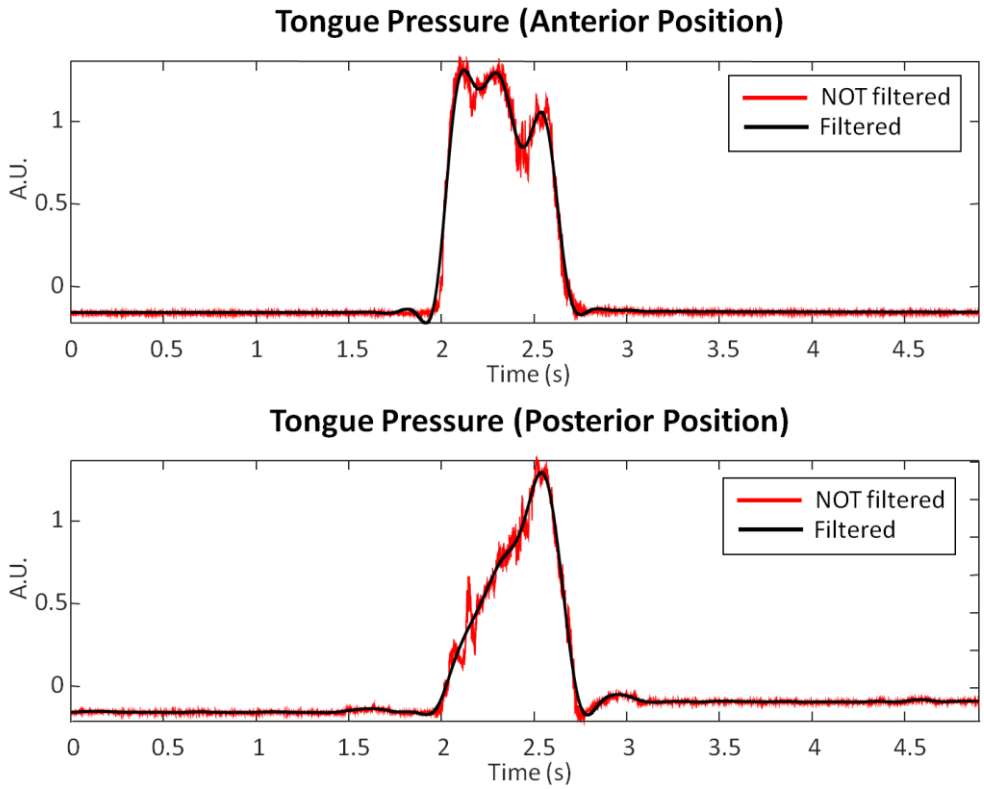

Figure 31 – Simultaneous 5 seconds recordings of the tongue pressure measured by two sensors during swallowing of 10 ml of water. From top to bottom:

anteromedian and posteromedian position. Signals were low-pass filtered at 5 Hz.

Conclusion The pressure sensor revealed to be adequate for the measurements of tongue pressure, although there could be problems when evaluating tongue pressure during mastication and the possible interference of the long cables of the sensor may affect the measures during swallowing. Moreover, the anatomical differences among participants (e.g. a narrow curvature of the palate) could make the sensor positioning difficult and the adhesive paste could be uncomfortable for the patient. Pressure sensors could, however, provide information about the strength of the contact that can be measured over time, changing in response to the functional movements of the tongue during swallowing [38]. Consequently, the use of the sensor couldn't be excluded for the evaluation of the tongue force against the palate as an additional, useful index for the assessment of the pathology of the swallowing function.

2.5 Conclusions

The aim of the studies described in this chapter was to verify the feasibility of detection and integration of three different assessment techniques: HD-sEMG, accelerometry, dynamometry. In order to achieve the purpose, an electrophysiological study was carried out involving different types of electrodes arrays. Results led to the choice of two types of grids of electrodes allowing to cover the SM and the infrahyoid muscles. Specifically, a 4x8 electrodes array was chosen for the upper muscles complex, while a custom-made cross-shaped matrix (4x8 electrodes) was chosen for the lower muscular region. Color maps computed from recorded signals provided a spatiotemporal pattern of muscle activation consistent with the expected timing and sequence of swallowing muscles, as described in literature. These findings suggested the possibility of further quantitative analyses. Moreover, for what concerns the mechanical measurement of swallowing activity through an accelerometer, the analyses suggested that the best position of the inertial sensor is the cricothyroid space

instead of other anatomical landmarks. The present study demonstrated also the possibility to merge these two macro analyses (electrophysiological and mechanical) by proposing a complete setup comprehensive of both technologies. Consequently, it was proved the feasibility of the proposed experimental setup as a new approach for the assessment of swallowing process. Finally, the dynamometric study revealed the possible use of a pressure sensor for the measurements of tongue pressure against the palate. Although tongue force profile can be achieved easily, this method was leaved in favor of the use of the accelerometry for the temporal segmentation of swallowing phases, because of potential discomfort for the subject.

Chapter 3

Comparison with standard clinical assessment: a validation study

3.1 Introduction

In the previous chapter we defined the experimental setup including HD sEMG and biomechanical variable detection and we proved the feasibility the proposed experimental approach. The following step is the validation of the proposed experimental setup. In clinical settings the objective analysis of the swallowing event is performed through the Fiberoptic Endoscopic Evaluation of Swallowing. FEES is a reliable technique used in clinics for the assessment of swallowing disorders and it was considered as ground truth to validate the swallowing onset estimation based on accelerometry. This validation may be relevant as the accelerometer-based segmentation has the potential to overcome the weak spots of the clinical standard (invasiveness, complication of setup, need of a visual, frame by frame analysis). For this purpose, simultaneous recordings of video FEES, hyolaringeal excursion, masseter, SM and infrahyoid muscles activity were performed. In this chapter we report the description of the experimental study aimed at (i) validate the swallowing onset estimations based on

accelerometer, (ii) identify the possible contribution of HD sEMG in the refinement of symmetry indexes, (iii) evaluate the spatiotemporal variation of EMG activity

3.2 Participants

Ten healthy subjects (4 male and 6 female) were recruited. None had oral problems or swallowing impairments, according to clinical evaluations of a specialized laryngologist. The mean age of the participants was 37 years, ranging from 28 to 50 years. The present study was carried out at the Casa di Cura Privata of Policlinico, Milan, Italy. The study was approved by the ethical committee of the Casa di Cura Privata del Policlinico di Milano (Ref number: 754628). Participants received detailed explanations about the protocol, the aims of the study, the involved risks and techniques of investigations before signing the consensus. All the stored information were and will be handled respecting the Italian norm about the protection of personal data (D.lgs. 196/2003). Recruited subjects gave the written informed consent and their approval for the divulgation of photographs with scientific purposes.

3.3 Materials

Mechanical evaluation A mechanical evaluation of the swallowing function was carried out using an accelerometer placed in the cricothyroid space, according to anatomical landmarks. The characteristic of the inertial sensor and the used acquiring system were described in paragraph 2.2.

Electromyographic evaluation In order to sample from all superficial muscles involved in the swallowing oropharyngeal phase, according to preliminary studies in literature [41], two EMG techniques were used:

- *HD-sEMG*: the setup included Ag electrodes arrays for SM and infrahyoid muscles investigation as described in paragraph 2.1 (case

C). Outcome measures were 32 monopolar signals recorded with respect to a reference electrode positioned in the region above the ear.

- *Conventional sEMG*: bipolar signals were obtained using two methods according to the muscular region under investigation. For SM and infrahyoid regions, bipolar signals were extracted from the monopolar recordings of the electrodes arrays by differentiating pairs of monopolar signals 2 cm apart (see the details in the following *Figure 36*). For masseter muscles, pairs of surface electrodes (one for each side, left and right) were attached to the skin above the masseter (adhesive electrodes, Ø 24 mm, 15 cm cables long, SpesMedica, Genova, Italy). Electrodes were positioned with an IED of 2 cm, for each side. Muscle activity was recorded using a Due system (OT Bioelettronica, Turin, Italy - *Figure 32*). Technical specifications are indicated in *Table 4*. The outcome measures were two bipolar signals one for the left and one for the right side. The electrical activity of masseter is relevant to segment the swallowing phases as the end of the oral phase of swallowing is characterized by a propulsive force given by muscles around the mouth. As a result, the masseter activity may be used to identify the passage from the oral to the pharyngeal phase, although it could be activated also in the earlier stages.

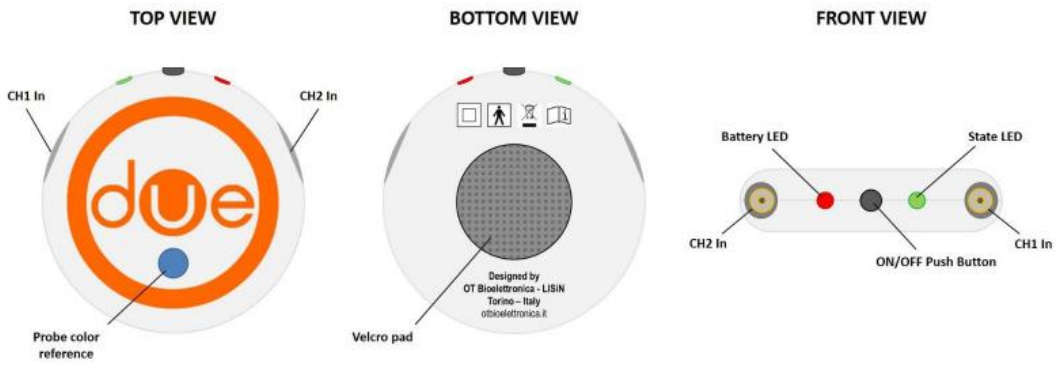

Figure 32 – From left to right: top, bottom and frontal view of the Due (OT Bioelettronica, Torino, Italy) probe for the acquisition of two sEMG signals.

Table 4 – Technical specifications of the Due probe.

Parameter	***Value (m.u)***
Number of sEMG signals	2
Gain	200 V/V
Bandwidth	10÷500 Hz
Input noise	< 2 μV_{RMS}
CMRR	>100dB
Sampling frequency	2048Hz
Input range	±8 mV RTI (Referred To Input)
A/D converter resolution	16 bit
Receiver	PC(Windows)
Wireless transmission protocol	Bluetooth 4.0
Power supply	3.7V LiPo battery
Charging mode	Inductive
Battery lifetime during continuous transmission	13 hours
Weight	12g
Size	21mm (Radius) x 1mm (thickness)

Clinical standard evaluation Video-FEES recordings were performed using a flexible endoscope (Optomic, Madrid, Spain) introduced transnasally. Technical specifications are illustrated in *Table 5*.

Table 5 – Technical specifications of the flexible endoscope used for video FEES.

Parameter	***Value (m.u)***
Image guide system	18000 pixels
Outer diameter	3,4 mm
Flexible part diameter	3,2 mm
Depth of field	2,5-50mm
Deflection angle	130° up/down
Direction of view	0°
Working length	300mm

Video were acquired using a stroboscope allowing the user to carry out the recordings thanks to a continuous light examination synchronized with the Optomic HD camera, whose technical specifications are included in *Table 6*. Video FEES were acquired with a frame rate of 25 fps and stored in a personal computer for further analyses.

Table 6 – Technical specifications of the integrated system strobolux III LED +HD (Optomic, Madrid, Spain).

	Parameter	***Value (m.u)***
HD camera	Shutter speed	1/100000 s
Stroboscope	Analysis frequency	60-1000 Hz
	Phase range variation	0° - 400 °
LED cold light source	Life of LED lamp	60000 h

A synchronization among the used systems was necessary for a correct comparison with the aim of the swallowing segmentation. More in detail, since the EMG data and the accelerometric signals were recorded with the same software (Bp, Politecnico di Torino, Turin, Italy), a hardware synchronization was performed. Therefore, an external trigger was used to carry out the synchronization between the video-FEES and the other recording systems. Since the starting of the video FEES was controlled by a pedal, an inertial sensor (DueBio, OT Bioelettronica, Torino, Italy properly configured as Inertial

Measurements Unit-IMU) was placed on it, in order to track acceleration changes according to the direction of gravitational acceleration.

The complete setup is shown in the *Figure 33*.

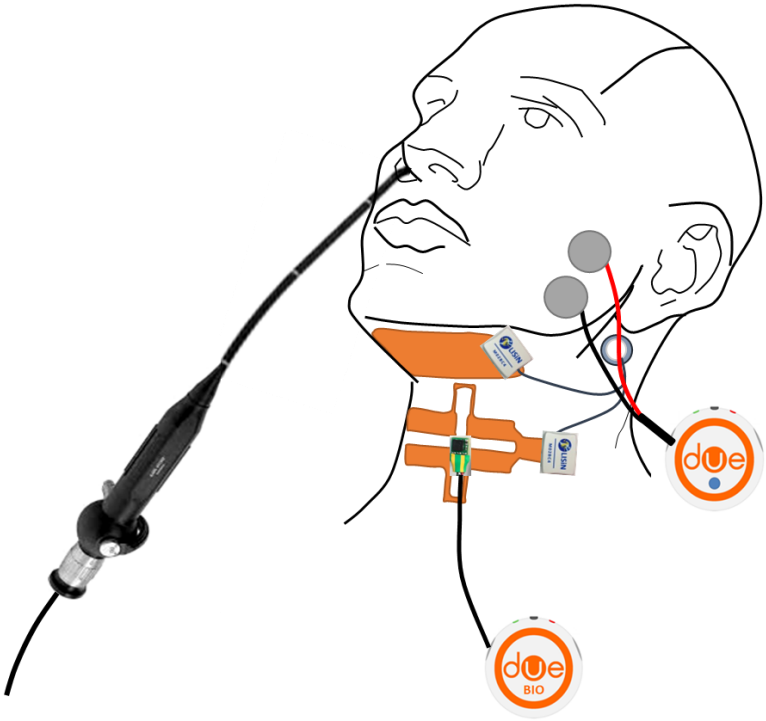

Figure 33 – Experimental setup involving: HD-sEMG systems for the SM and infrahyoid muscles, conventional bipolar recordings for the evaluation of masseter activity (bilaterally), accelerometry for the mechanical evaluation of swallowing and a nasoendoscope for the FEES. The accelerometer placed on FEES pedal to trigger the FEES acquisition beginning and the other signals is not shown.

3.4 Procedure

During each acquisition, simultaneous recordings of video FEES, accelerometry, conventional and HD sEMG signals were performed. The subject was seated on a chair ready to complete the swallowing tasks. The protocol consisted of five different tasks, according to the type of bolus analyzed: saliva (dry swallow), 3 ml

of water, 10 ml of water, 3 ml of gelled water, 10 ml of gelled water. Each task was repeated three times in order to assess the intra-subject repeatability. After the positioning of electrodes arrays and accelerometer, the speech pathologist introduced the endoscope transnasally. Once reached the correct position of the probe to achieve a detailed view of the oropharynx, the recordings started and the subject received the instruction to swallow. The bolus was held in the oral cavity before starting the recording and the subject started swallowing normally, remaining in the same position. The video recordings started by hitting a pedal. Acceleration changes provided by the IMU placed above the pedal were synchronously recorded on the Bp software with physiological signals (EMG and accelerometer) to guarantee the temporal alignment. At the end of the 15 trials the nasoendoscope was carefully removed by the speech pathologist.

3.5 Data Processing

3.5.1 Preliminary analysis

Video analysis Video recordings from FEES were analyzed frame by frame, through visual inspection. The aim was to identify characteristic instants in order to analyze the correspondence with electromyographic and accelerometric traces and extract a new method for swallowing segmentation. Four moments of interest were detected, for the trials of all subjects *Figure 34*:

- Retraction of the tongue, just before the hyolaringeal excursion ($t_{Retraction}$);
- Epiglottis tilting;
- Swallowing whiteout referred to the first white frame due to the covering of the tip of the nasoendoscope (t_{Wo});
- The first again visible moment after the swallow signing the end of the event (t_{End});

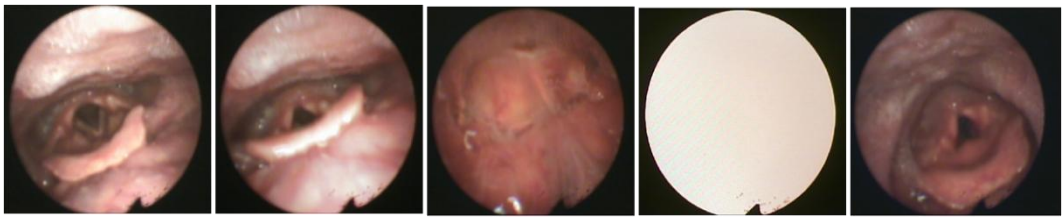

Figure 34 – FEES frames relative to the extracted moments of interest of a representative subject during a single task (3 ml of water). From left to right: rest condition, retraction of the tongue, epiglottis tilting, whiteout, end of the swallow.

The conventional reference point is the video whiteout because of its correspondence to the pharyngeal restriction as the swallowing reflex starts [30]. White frames could be due to different causes: the oncoming bolus, the dislocation of the nasoendoscope tip, the epiglottis tilting [32]. All of these events are related to the swallowing reflex. Moreover, since the oral cavity view from the nasoendoscope changes with respect to the position of the endoscope, t_{Wo} resulted to be generally accepted as the most reliable reference frame since the high inter-subject variability. In addition, because of the lack of synchronization between video recordings and other signals, the IMU signal was used to identify the time delay. A representative outcome recording of the IMU is shown in *Figure 35*. For each trial the first point of baseline after acceleration changes was manually identified and added to the corresponding instants extracted from the video analysis. The second spike was taken into account to consider the release of the pedal.

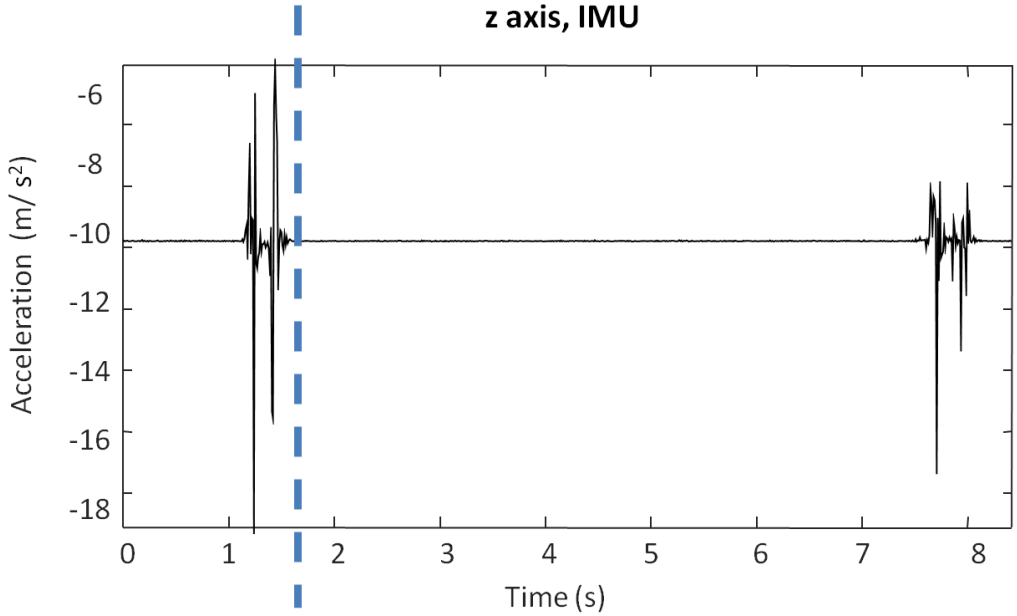

Figure 35 – Example of IMU signal obtained during a recording of a representative subject performing a single trial. Variations from the baseline are referred to acceleration changes due to the hitting of the pedal. Deviations at the beginning and at the end of the IMU signal are referred respectively to the start and the end of the video recording. The blue dashed line identifies the reference time used to temporal align signals.

Accelerometry In order to compare the swallowing onset estimation based on accelerometer and FEES, preliminary analyses were carried out on the recorded signals. The feasibility study suggested the presence of two main frequency contents: lower frequency (< 5 Hz) associated with the preparation of the swallow, higher frequency (> 5 Hz) for the evaluation of the final phases of swallowing. For this reason, a low-pass filter was used as a processing method of the accelerometer aimed at the swallowing onset identification. More in detail, a 4^{th} order Butterworth filter with a cutoff frequency of 4 Hz was used. A correspondence between time references from FEES frames and accelerometric traces was inspected. Therefore, an evaluation of the signal amplitude before, during and after the FEES-onset was carried out. Three intervals were isolated:

from 500 ms before to the $t_{Retraction}$, from $t_{Retraction}$ to t_{Wo}, from t_{Wo} to 500 ms after t_{Wo}. For each interval the RMS value was calculated results were averaged among all trials, separately for each subject. Statistical analyses were performed using the software STATISTICA 7. Data of all subjects were averaged in order to carry out a matched-pair analysis. Specifically, a Willcoxon matched pairs test was used to test whether the RMS value relative to the third interval was statistically significant different ($p > 0.05$) from the RMS value of first one, indicating a higher amplitude of accelerometric signal in the portion after the t_{Wo}.

sEMG A 4^{th} order Butterworth filter with a bandwidth of 20-400 Hz was used both for conventional and HD sEMG. Envelopes of the signals were obtained with a low-pass filter (a 4^{th} order Butterworth at 4 Hz). Moreover, for HD-sEMG signals, a preliminary visual inspection was carried out. Data were processed as follows:

- A Notch filter centered at 50, 100 and 150 Hz was applied to attenuate power line interference.
- Linear interpolation of single channels was carried out for low quality EMG signals (with high background noise or baseline instability). The interpolation was computed as the average of neighboring electrodes with respect to the channel to interpolate. On average, not more of 2 electrodes per subject were interpolated.
- Further misleading channels were not considered for the following analyses.

In order to compare conventional and HD-sEMG techniques for the swallowing assessment, bipolar signals were estimated from the HD-sEMG recordings for SM and infrahyoid muscles. Moreover, in order to extract one signal separately for left and right side, the electrodes array was ideally divided into two parts. Bipolar signals for left and right sides were computed as the difference between one electrode signal of the third row and the correspondent of the first row of the electrodes array resulting in a IED of 2 cm (*Figure 36*).

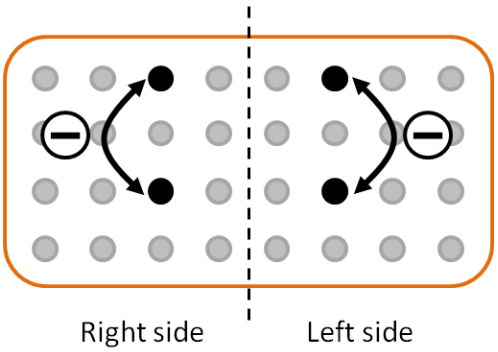

Figure 36 – Frontal view of electrodes array showing how to extract bipolar signals from a 32 electrodes matrix (4x8 with an IED of 1 cm). Signals were computed as the difference between a signal of the third row and the correspondent of the first row represented in black. Right and left sides are referred to the subject.

3.5.2 Swallowing onset identification

A threshold method was used to automatically identify the swallowing onset based on the accelerometric signal. Working on low-pass filtered signals, a visual inspection was performed to identify a rest condition in the first seconds of recordings: the subject was relaxed with no postural changes. Acceleration changes within the rest period were averaged and the relative standard deviation was computed. A threshold was set at the mean value of the baseline ± 3 times the standard deviation of that interval. The accelerometer-based swallowing onset (t_{Acc}) was identified as the first point of the signal overcoming the threshold (*Figure 37*). A visual inspection was necessary in order to cross-check the method and exclude the outlier cases. Nevertheless, across the trials, only 10% of cases was deleted and not included for the analysis.

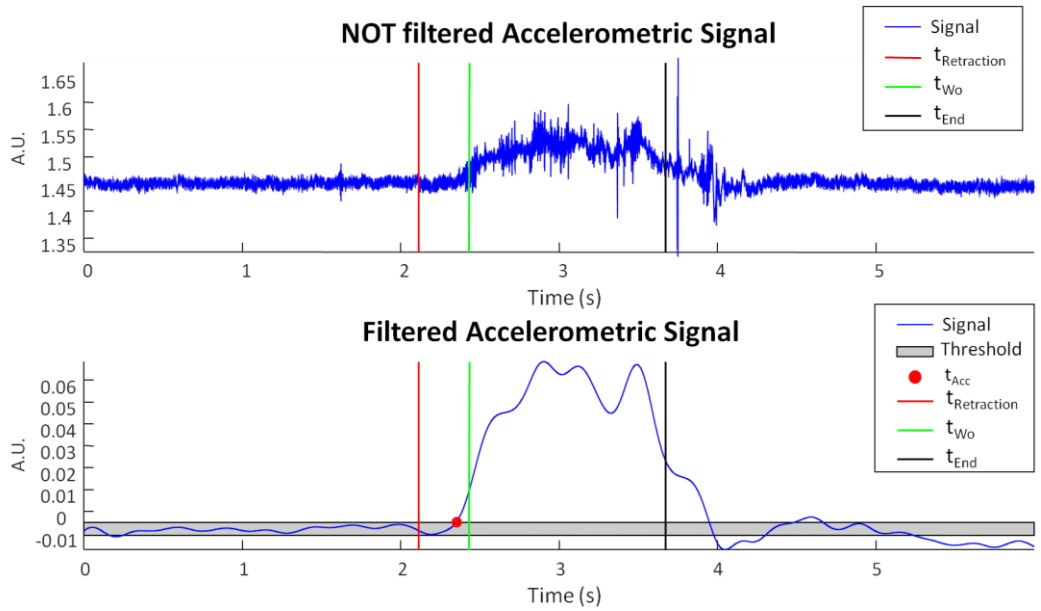

Figure 37 – Example of accelerometric signal of a subject performing a single task (swallowing of 3 ml of water). The red spot is the point identified as swallowing onset using the threshold method: the first point above the mean of a rest period ± 3 times the standard deviation (grey area).From left to right reference FEES-base instants: retraction of the tongue, epiglottis tilting, whiteout, end of the swallow.

Once identified the accelerometer-based swallowing onset, a validation of the detected instants was carried out. For each subject, a comparison between the swallowing onset identified with the two methodologies (t_{Wo} and t_{Acc}) was performed. More in detail, the analysis was centered on the difference between the two methods-based instants ($t_{Acc} - t_{Wo}$). Positive values were referred to identified delayed t_{Acc} with respect the clinical standard onset, vice versa for the negative values. Results were evaluated to compare the identification of the swallowing onsets based on accelerometer and FEES. Statistical analyses were performed organizing data into boxplots and using the software STATISTICA 7 for further analyses. Boxplots visualization was used in order to identify the interquartile range of the deviation of accelerometer-based swallowing onset with respect to the whiteout, considering the average of the trials across the

population. A Shapiro-Wilk test was used to assess the normal distribution of data of all trials of the subjects. A Two-Way repeated measures analysis of variance (ANOVA) was used to inspect effects on the swallowing onsets of the factors “type of swallowing onset estimation” and “type of bolus” were evaluated. The three trials of each bolus were averaged, given the low inter-trial variability for each subject.

3.5.3 Swallowing segmentation

Symmetry Indexes An index called Left/Right Index (LRI) was proposed with a triple aim: (i) validate the use of the accelerometer for the swallowing segmentation, (ii) compare the conventional sEMG and HD-sEMG techniques, (iii) assess the symmetry of the muscle activity with respect to the left/right sides. Three signals for conventional sEMG were considered for each side (left and right): bipolar EMG signals from the masseter, expected bipolar signals from HD-sEMG recordings of SM and infrahyoid muscles as explained in *Figure 36*. The LRI was defined as:

$$LRI = \left(1 - \frac{\sum\left|RMS_{left} - flip(RMS_{right})\right|}{\sum\left(RMS_{left} + RMS_{right}\right)}\right) * 100$$

where RMS_{left} and RMS_{right} were the RMS values of the portion of interest, obtained respectively from left and right sections. When evaluating conventional sEMG signals, RMS values derived from a single electrode, while evaluating HD-sEMG signals, RMS values derived from a 4x4 electrodes section. For this reason, dealing with HD-sEMG signals, the RMS values of one side had to be flipped for a correct check of the symmetry between the two opposite parts. Taking into account the swallowing onset identification through both methodologies (clinical standard and accelerometry), a symmetry analysis was performed. Since the duration of the swallowing act, electromyographic signals were divided into three sections, each one lasting 1.5 seconds, relative to the before, during and after moments of the swallow (*Figure 38*). Indexes were computed separately for

each section. Moreover, indexes were extracted considering t_{Wo} and t_{Acc} as reference for the segmentation, in order to assess the validity of the accelerometer-based segmentation compared to the clinical standard.

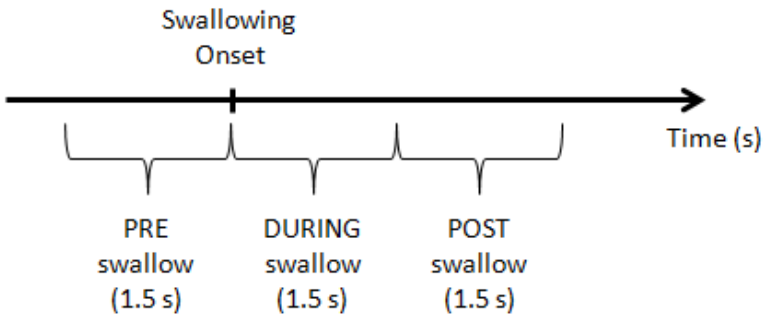

Figure 38 – Identification of the three sections of interest, taking into account the swallowing onset. The LRI was computed separately for each portion of interest for both the two methodologies used for the swallowing onset identification (t_{Wo} and t_{Acc}).

LRI values of the three sections were averaged for all trials, separately for all the subjects in order to evaluate the inter subject variability as concern the use of the two identified swallowing onsets. Mean values with respective standard errors of LRI were also computed separately for the three muscular regions of interest and for the three swallowing periods. In addition, a common average among all the subjects, separately for the swallowing segment and muscular regions, was performed in order to carry out a statistical test. A Two-Way repeated measures analysis of variance (ANOVA) was used. The effects on the symmetry indexes of the factors "type of swallowing segmentation" and "type of bolus" were evaluated. The aim was to test the effect of the segmentation method *(*FEES- and accelerometric-based*)* and the type of bolus on LRI estimation. Analogously, the same analysis of the LRI among the three hypothesized swallowing phases was carried out on HD-sEMG signals. Specifically, only LRI derived from the accelerometer-based segmentation (t_{Acc}) were computed. The comparison between LRI indexes of conventional and HD sEMG was performed taking into account the average of the trials across the

subjects, separately for the three swallowing segments for SM and infrahyoid muscles. To the best of our knowledge, quantitative analyses on the swallowing event were not so extensively covered in literature. Nevertheless, Zhu and colleagues [5] proposed a quantitative index (Left/Right Energy Difference LRED) for an electrophysiological evaluation of swallowing. Using the setup shown in *Figure 5*, the symmetry analysis was performed evaluating the difference between left and right muscular activation:

$$LRED = \frac{\sum RMS_{left} - \sum RMS_{right}}{\frac{1}{2}\sum(RMS_{left} + RMS_{right})} * 100$$

Since their study was applied on healthy subjects, we tried to compute the LRED on our recorded data, using their results as a benchmark. For the three accelerometer-segmented phases, LRED values were calculated separately for the two regions of interest. Results were displayed in a scatter plot in order to make a direct comparison with Zhu's results. In order to avoid any bias, the same task was compared: the swallow of 10 ml of water.

Barycenter Since the dynamic topographic analysis offered by the HD-sEMG technique, the symmetry of the muscular activity for HD-sEMG was evaluated by introducing a new methodology. The barycenter of muscular activity was computed on different epochs. Starting from the swallowing segmentation achieved through the accelerometric traces, monopolar signals from both muscular regions of interest (SM and infrahyoid muscles) were divided into three phases, according to *Figure 38*. For each swallowing phase a further division into 100 ms epochs was performed, totaling 15 epochs for each section. For each epoch, monopolar signals were referenced to the spatial average (the average of all the 32 electrodes signals) [42]. Each epoch went to the computation of a 2D RMS-based color map. The position of the barycenter was estimated by implementing the geometric definition and weighing points of the electrodes array by the intensity of RMS values. Considering X and Y coordinates

respectively as the medio-lateral and infero-superior axis of the electrodes array, the coordinates of the barycenter were computed as:

$$G_x = \frac{\sum_{i=1}^{N}(x_i * a_i)}{\sum_{i=1}^{N} a_i} \qquad G_y = \frac{\sum_{i=1}^{N}(y_i * a_i)}{\sum_{i=1}^{N} a_i}$$

where x_i, y_i and a_i were respectively the coordinates of each point with respect to the lower left corner of electrodes array and the intensities of RMS values. An example of barycenter calculation was proposed in the following *Figure 39*:

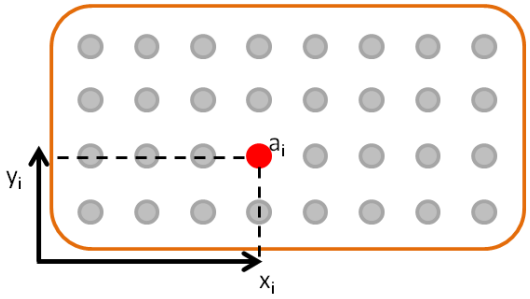

Figure 39 – Example of barycenter computing. The displayed 4x8 electrodes array represents the RMS values computed for all the 32 recorded signals. Coefficient a_i refers to the RMS intensity of the red point, while x_i and y_i refer to the coordinates of that point with respect to the lower left corner of the array.

X and Y coordinates were normalized according to a reference system centered at the center of the electrodes array. As a result, positive deviations above the zero level were referred to upward-left displacement, negative deviations were referred to downward-right considering right and left with respect to the subject. For each segmented phase a scatter plot comprising of the barycenter coordinates of all trials across subjects for the two muscular regions was computed. A Shapiro-Wilk test was used to assess the normal distribution of the recorded data in order to verify the rejection of the null hypothesis. The ellipse comprising the 90% of the data was searched in order to enclose the displayed points. More in detail, an ellipse centered in the median of the points cloud was computed. The carried out analyses involved different steps: the extraction of

the eigenvalues from the co-variance matrix of the scattered data, the computation of the rotation matrix according to the angle between the eigenvalues and the cloud points, the evaluation of the ellipsoidal trajectory able to enclose the 90% of data and the rotation of the ellipse according to the rotation matrix previously calculated. Moreover, a measure of correlation was carried out between LRI coefficients and barycenters in order to assess the reliability of the LRI. Since the LRI was developed taking into account symmetry changes not only in the medio-lateral direction, but also along the infero-superior direction, the magnitude of the barycenter was considered (Eq 3.1) for correlations analyses.

$$|G| = \sqrt{G_X^2 + G_y^2} \qquad (3.1)$$

Specifically, for each swallowing phase the Pearson correlation coefficient was extracted considering all the epochs of the trials, for each subject.

Amplitude maps HD-sEMG recordings were segmented according to the accelerometer-based swallowing phases. As a result, monopolar signals were divided into three consecutive non-overlapped intervals: pre, during and post swallow as described in *Figure 38*. For each portion of interest, the RMS values were calculated on all the 32 monopolar signals. RMS-based color maps were obtained scaling all values between intensity minimum and maximum of the whole RMS signal for visualization purposes, separately for the regions of interest. Respectively, minimum and maximum were represented with cold and hot colors, reading the information from the color bar. In order to assess the coherence between the RMS-based color maps and the mechanical behavior of swallowing, the three portions of monopolar signals were visually inspected and for each phase, the barycenter of the color map was superimposed. In the end, the central swallowing phase was further divided into different 100 ms epochs for the evaluation of the detailed spatiotemporal information about the muscular activity.

3.6 Results and Discussions

3.6.1 Preliminary analysis

Video Analysis and Accelerometry Results from Willcoxon test showed a statistically significant difference between the amplitude (RMS value) of accelerometric signals to 1.5 s intervals after and before FEES-based onset (*p<0.05*). The matched paired analysis showed the common trend of all subjects: an increase of amplitude value with respect to the portion before the swallowing whiteout. Single subject behavior is represented in *Figure 40*: for each subject mean and standard error represent the amplitude distribution of the 15 trials (5 bolus x 3 repetitions).

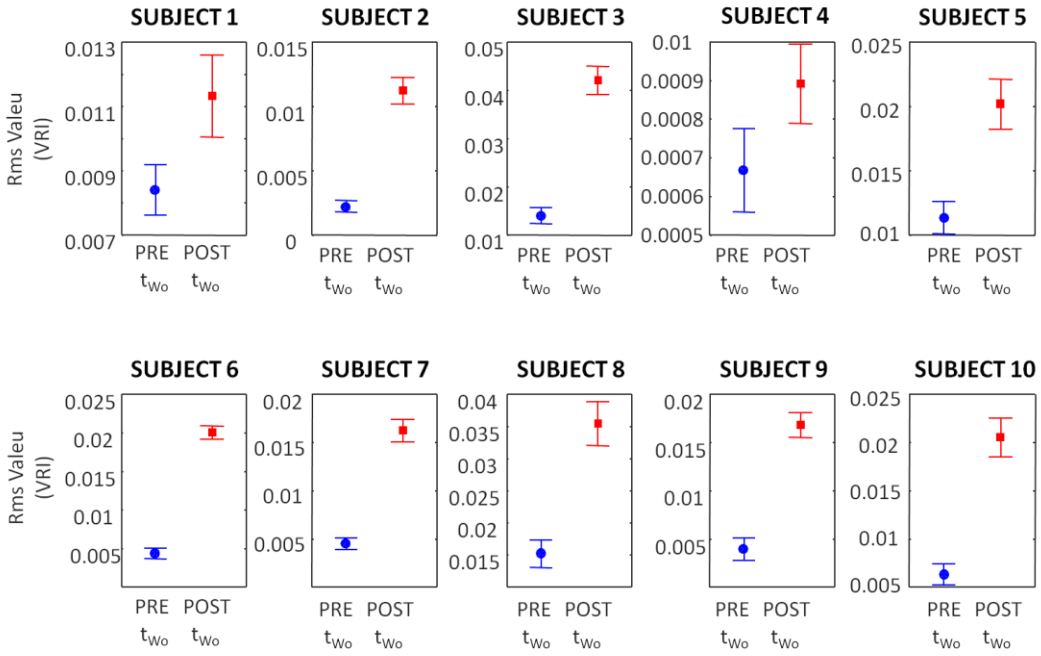

Figure 40 – Mean and standard errors between trials for each subject of RMS values computed in the portion after and before the FEES onset (PRE t_{Wo} and POST t_{Wo}).

Since the portion after the swallowing whiteout corresponded to an increasing of the accelerometric signal amplitude value, results suggested setting an amplitude threshold as a reasonable automatic method for the swallowing onset identification from accelerometric traces (t_{Acc}).

sEMG The visual inspection of conventional and HD-sEMG led to the conclusion that the experimental setup was adequate for the purpose, as suggested by the feasibility study. In fact, the experimental setup revealed good quality signals, showing an increasing muscular activity in correspondence of the swallowing onset. The presence of a time delay among the activity onsets of the three regions of interest (masseter, submental and infrahyoid muscles) confirmed the pattern of swallowing muscular activation described in literature [3], [5]. In fact, looking at the results reported in *Figure 41*, synchronized masseter and SM muscles onsets tracked the starting of the swallowing activity. On the contrary, the increasing activity of infrahyoid muscles was delayed with respect to the other investigated muscles. This was in line with other results taken from literature and with the swallowing physiology itself [3], [43]. In fact, at the beginning, the bolus is prepared and pushed towards the upper digestive ways by contracting the tongue and submental muscles, while the reflexive part of the swallowing event related to the passage of the bolus resulted from the activation of muscles of the neck.

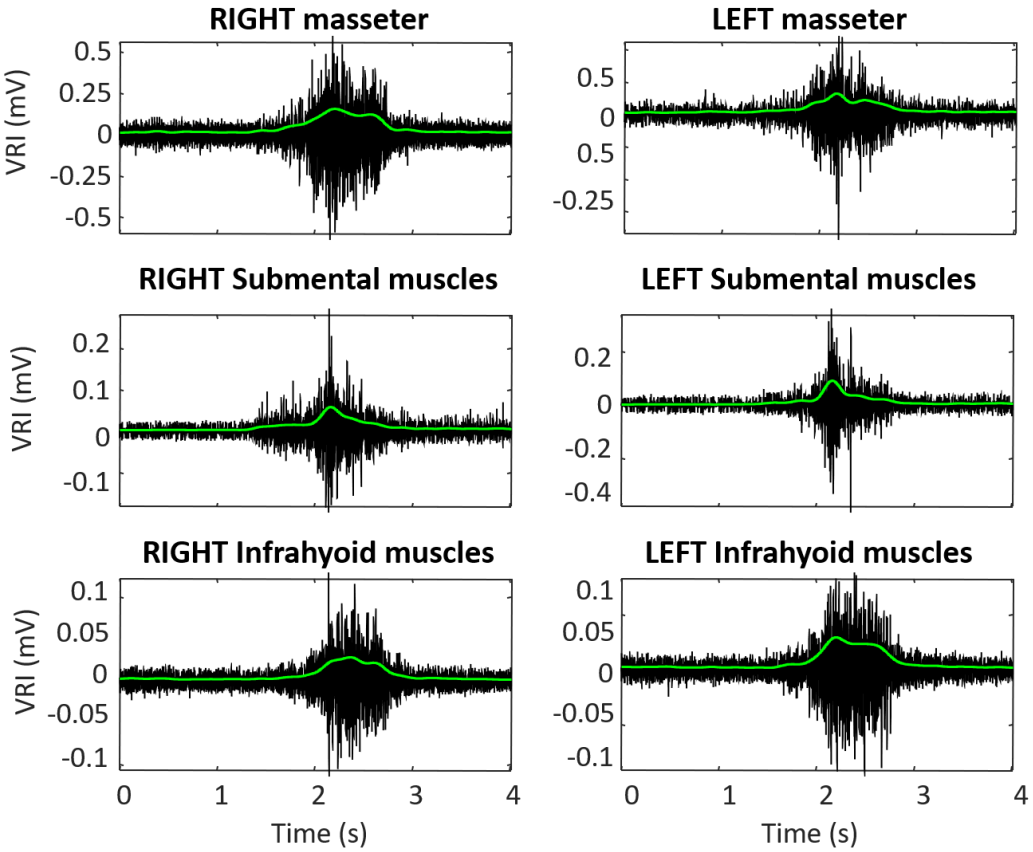

Figure 41 – Bipolar sEMG signals recorded from the proposed setup during a single swallow of 10 ml of water from a representative subject. Columns are referred to right and left side with respect to the subject, while rows show the activity of the three muscular groups under investigation: masseter, submental and infrahyoid muscles. Specifically for SM and infrahyoid muscles expected bipolar sEMG signals were computed starting from the HD-sEMG recordings according to paragraph 3.5.3, Figure 36. The green traces superimposed on the black signals represent the envelope signals computed through a low-pass filtering at 4 Hz of the rectified signals.

These results were supported also by the HD-sEMG signals showing a detailed view of muscular active regions (*Figure 42*).

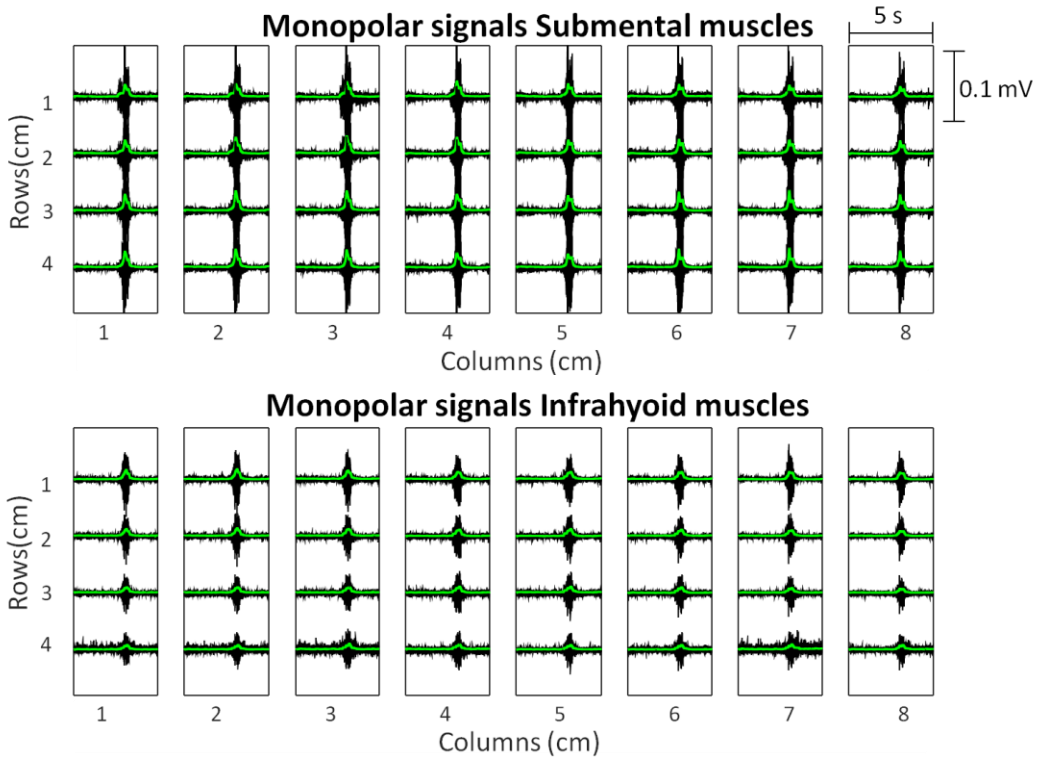

Figure 42 – HD-sEMG recorded from the proposed setup during a single swallow of 10 ml of water from the same representative subject of Figure 41. The green traces superimposed on the black signals represent the envelope signals computed through a low-pass filtering at 4 Hz of the rectified signals. Signals were normalized by the 98th percentile computed across the electrodes arrays.

3.6.2 Swallowing onset identification

In order to validate the use of accelerometer as a method to identify the swallowing onset, we compared the accelerometer-based swallowing onset (t_{Acc}) to that obtained with clinical standard (t_{Wo}). The average of all the trials across the participants showed that the accelerometer consistently underestimated to swallowing onset of 250 ms (interquartile range: 300 ms - *Figure 43*).

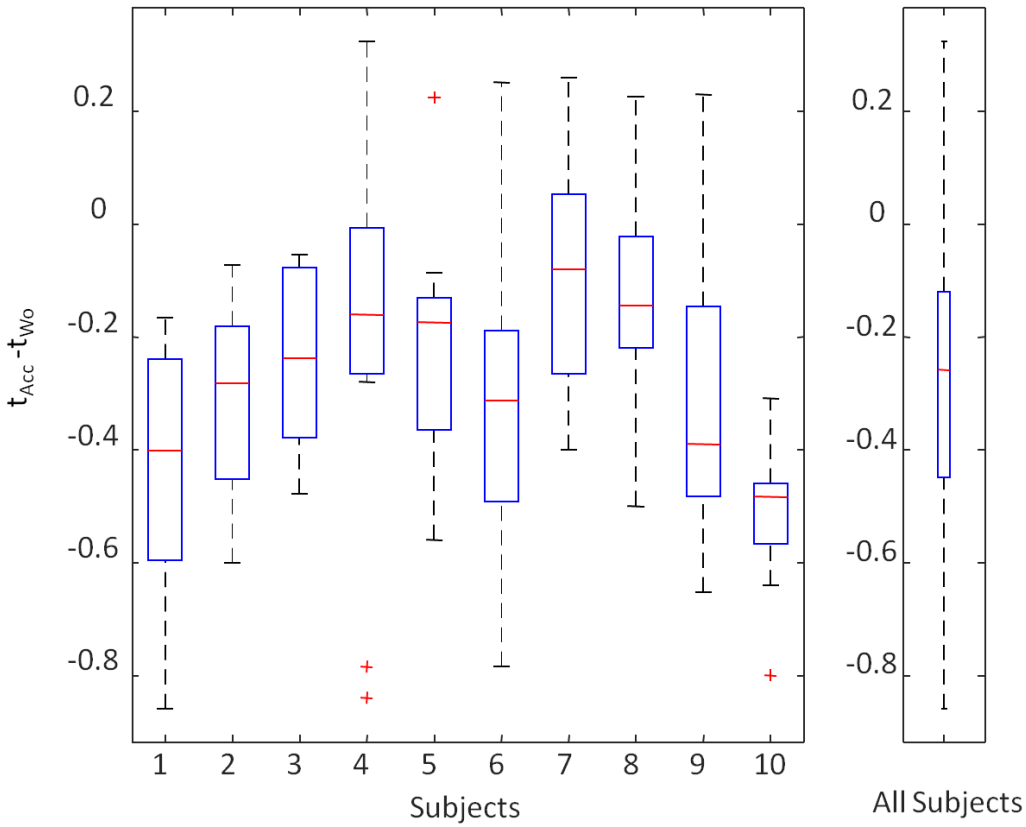

Figure 43 – Differences between the accelerometer-based and the FEES-based swallowing onset. Positive and negative values refer respectively to late and beforehand t_{Acc} with respect to t_{Wo}. On the left: boxplot analysis of the average of the 15 trials separately for the 10 subjects. On the right: boxplot obtained averaging all trials of all the subjects.

Results from the repeated measures Two-Way ANOVA statistical test (factors: bolus, onset estimation method) showed a statistically significant difference ($p<0.05$) between the two swallowing onset identification methods (accelerometer and FEES) (*Figure 44*).

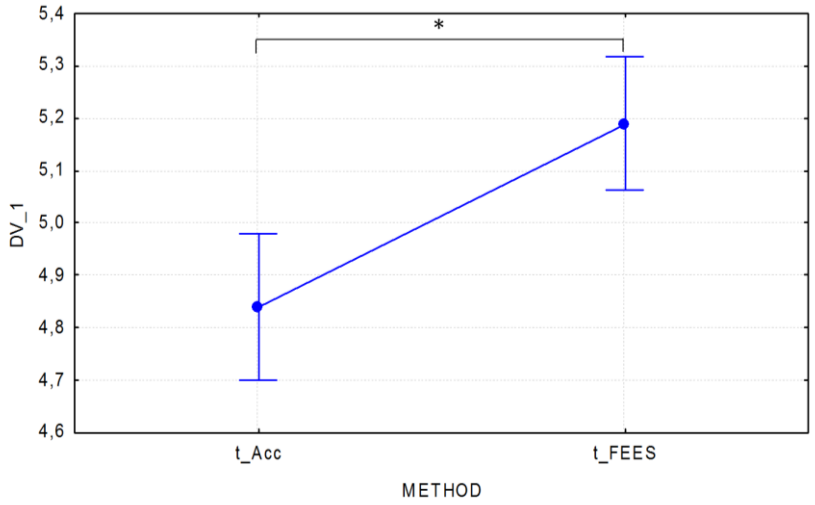

Figure 44 – Two-Way ANOVA results on effects of the factor "type of swallowing onset estimation". Statistically significant difference was represented through a (*) indicating a p-value<0.05.

On the contrary, results obtained from the ANOVA test on the effect of the type of bolus on onset estimation showed no statistically significant differences, meaning that neither volume nor type of bolus affect the swallowing onset estimation (*Figure 45*).

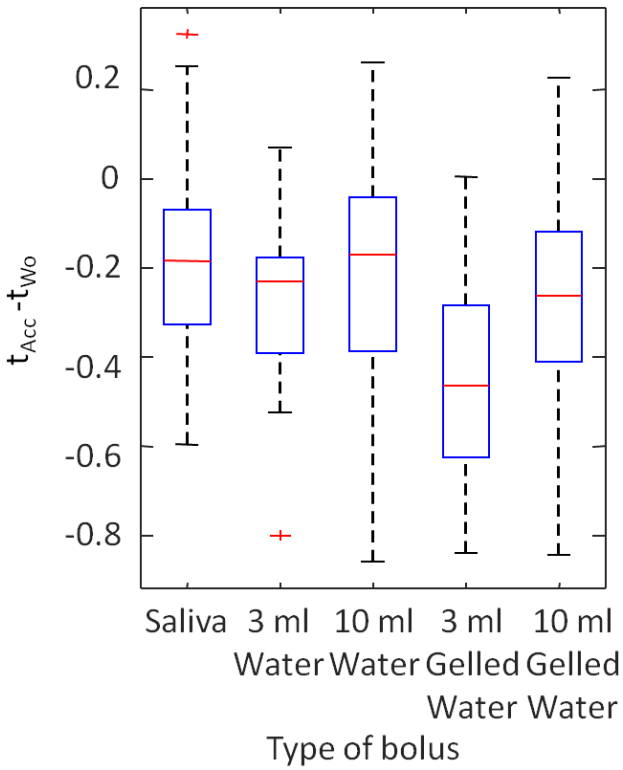

Figure 45 – Boxplot representation of the average of the trials of the same type of bolus, for all the subjects. Data are referred to the differences between the accelerometer-based and the FEES-based swallowing onset. Positive and negative values refer respectively to late and beforehand t_{Acc} with respect to t_{Wo}.

In the end, it could be advisable to remind that the budget of time uncertainty is about dozens of ms, considering the possible delay among recording systems, the video frame rate and the electromechanical delay of anatomical structure movements. As a result, the identified instants could be shifted of this quantity on time axis. Nevertheless, considering that the swallowing act lasts at least 1.5 seconds, the accelerometer-based swallowing onset could be considered for swallowing segmentation analysis.

3.6.3 Swallowing segmentation

Symmetry index Statistical results on LRI analysis showed no statistically significant differences ($p<0.05$) between LRI values computed with the two methodologies: FEES- or accelerometer-based (*Figure 46*).

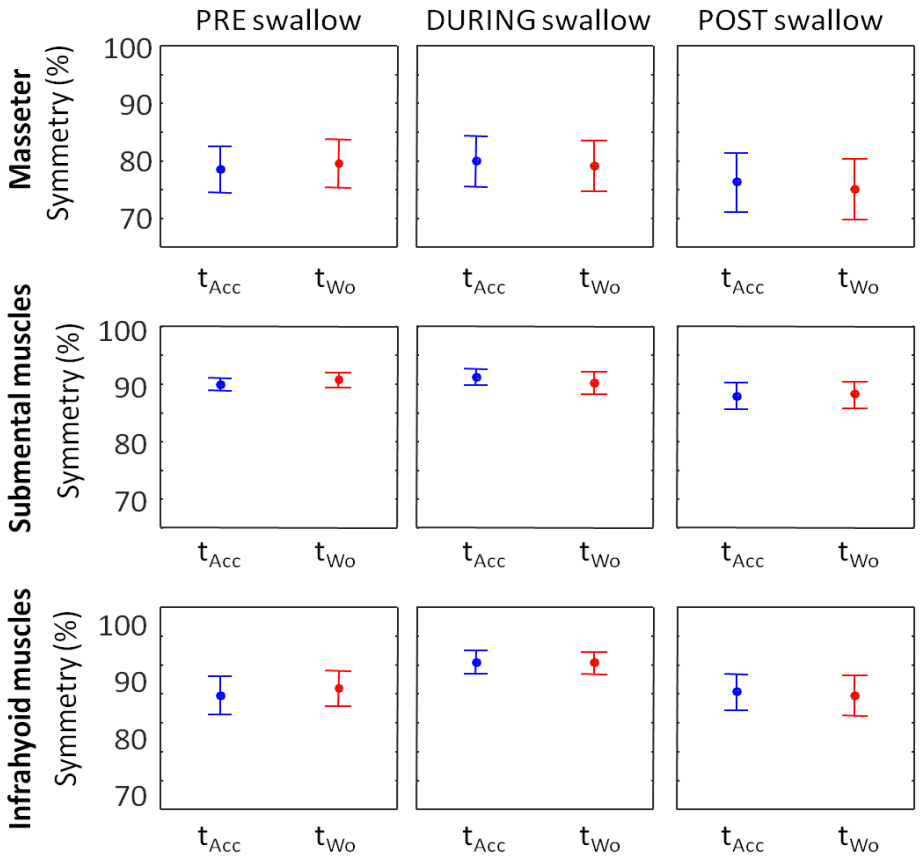

Figure 46 – Left/Right Indexes computed on conventional sEMG signals taking into account FEES- (red) and accelerometry-based (blue) swallowing onset. Each column represents a swallowing phase: before, during and after the swallow identified with the two methodologies. While, each row represents the muscular region of interest. LRI of all trials of all subject were averaged and the standard error was superimposed. Statistically significant differences were found using a Two-Way ANOVA results.

Specifically, a detailed analysis of LRI among single subjects was performed. Results suggested that the two methodologies for the swallowing onset identification led to the same results since the two traces resulted overlapped (*Figure 47*). However, the higher symmetry differences between LRI computed on t_{Acc}- and t_{Wo}-segmentations were found in the first swallowing phase. These findings could be due to the fact that the early stages before the pharyngeal phase are very subjective since they include the preparation of the bolus and tongue movements that are detectable with the proposed setup. The high variability of recorded signals reflected in a higher deviation from the results obtained with the clinical standard. Nevertheless, difference values were very small (at least, a 10% symmetry difference).

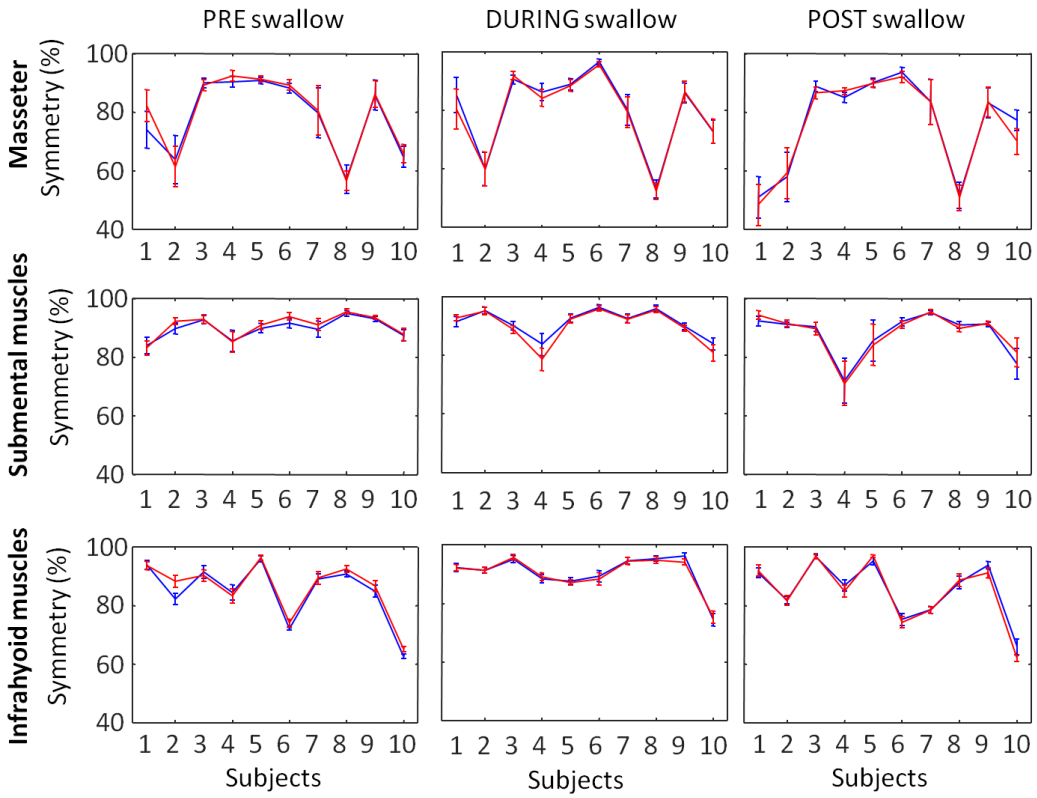

Figure 47 – Left/Right Indexes computed on conventional sEMG signals taking into account FEES- (red traces) and accelerometry-based (blue traces) swallowing onset. Each column represents a swallowing phase: before, during and after the

swallow identified with the two methodologies. While, each row represents the muscular region of interest. LRI of all trials were averaged and displayed superimposing the standard error, separately for each subject in all the three swallowing phases.

Since the LRI values were not statistically different when estimated with the two methodologies (accelerometer- and FEES-based), the validity of the accelerometer is confirmed as far as measures are aimed at finding symmetry differences in swallowing muscular activation.

As a result, taking the accelerometer-based swallowing onset (t_{Acc}) as a reference for the swallowing segmentation, the comparison between the LRI on HD_sEMG and conventional sEMG signals was analyzed (*Figure 48*). Masseter was not taken into account because no HD-sEMG was performed on it.

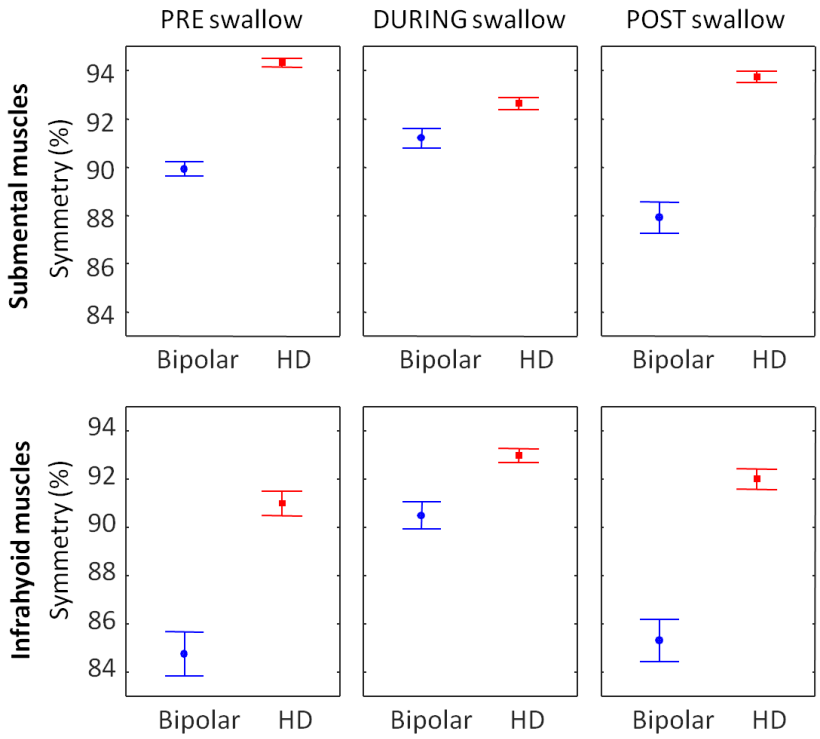

Figure 48 – Averaged Left/Right Indexes computed on conventional (blue) and HD sEMG (red) signals among all the trials of all the subjects. LRI are displayed superimposing the standard errors. The accelerometer-based swallowing onset

was considered for the segmentation. Each column represents a swallowing phase: before, during and after the swallow. While, each row represents the muscular region of interest.

Since the participants were clinically evaluated as healthy subjects, without any swallowing impairments, the basic hypothesis of the expected results was a complete symmetry of muscular activity, for both regions of interest (SM and infrahyoid muscles). In this perspective, results from the comparison of LRI computed on conventional and HD sEMG signals suggested a higher suitability of HD-sEMG technique for the assessment of the muscular activation symmetry during swallowing. In fact, in all the swallowing phases and for both the muscular complexes, symmetry values relative to LRI computed on HD-sEMG signals were higher. Moreover, looking at the standard errors, the variability among trials and subjects shown by the LRI of HD-sEMG signals resulted to be lower with respect to the one referred to conventional sEMG signals. These findings were attributed to the accurate symmetry analysis carried out by the electrodes arrays. In fact, the proposed method is able to track the spatial variation of potentials thanks to many recording electrodes above the regions of interest. In order to assess the reliability of the present symmetry investigation, results coming from the comparison between existing works in literature are reported in *Figure 49*. Results suggested to be in line with a symmetry index based on HD sEMG described in literature [5]. In fact, the variation of muscular activation ranges from -20% to 20%, as expected from previous researches, using LRED index. However, the use of the existing symmetry indexes (LRED [5]) could reveal some limitations: the lack of tracking the symmetry on infero-superior axis, the absence of advantages from the sophisticated experimental setup, the global analysis of symmetry changes in muscular activation and the inclination to find false positive symmetry cases. As a result, our findings demonstrated that with a simpler and easy-to-use setup, the same trends could be achieved. Therefore, the LRI could be considered as a refining of the LRED since it includes the symmetry on y-axis, stressing the mirror effect between left and right sides of

the subject, being more selective and increasing the relevance of true positive symmetry cases.

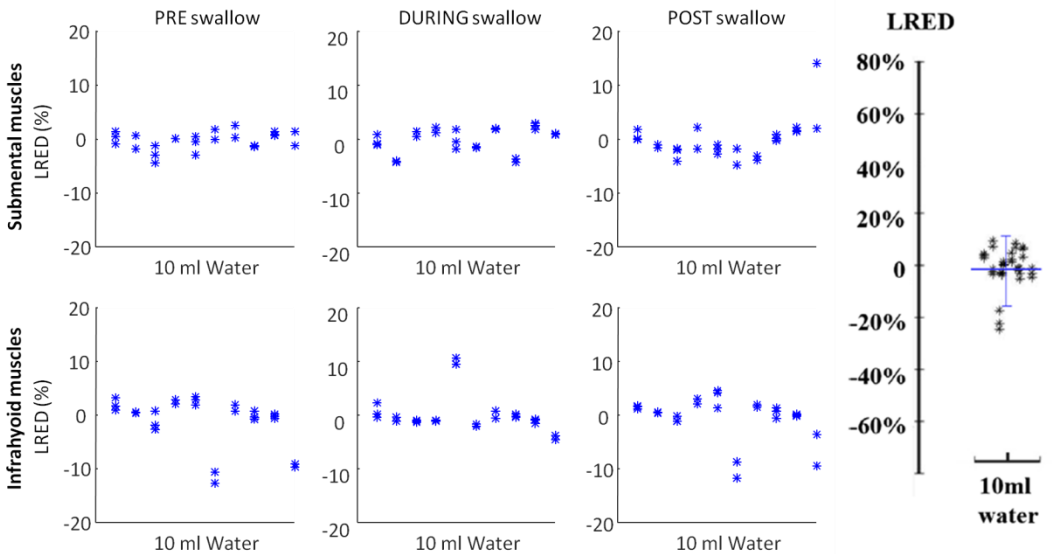

Figure 49 – Left/Right Energy Difference index computed on HD-sEMG signals of a group of healthy subjects during swallowing of 10 ml of water. On the right results obtained by Zhu et al [5]. On the left LRED indexes computed on our recorded data. LRED of different epochs were averaged among trials and subjects and represented respectively for the three swallowing phases.

Barycenter Points cloud referred to the position of barycenters in different swallowing phases, is less condensed for the electrodes array covering the SM complex (*Figure 50*). Nevertheless, in all the analyzed cases, the maximum displacement of the coordinates of the barycenter is approximately of 0.5 cm. Moreover, displacements on medio-lateral direction were higher than those on infero-superior direction, especially for the infrahyoid muscles.

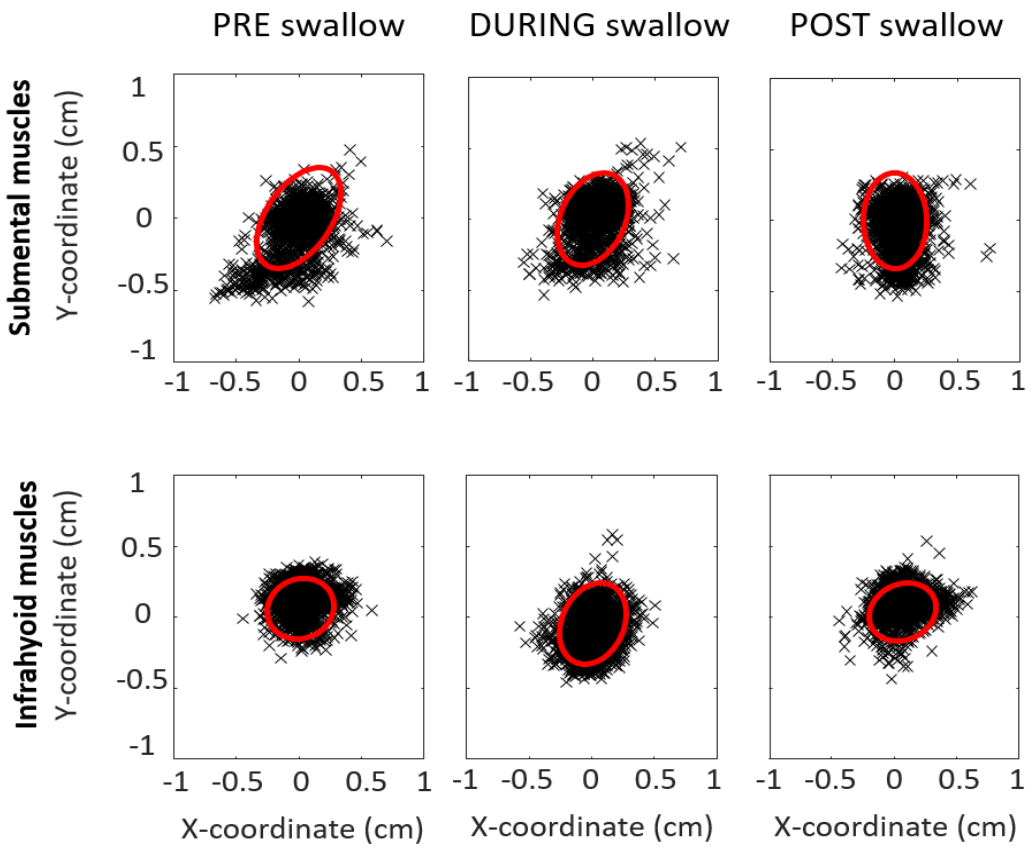

Figure 50 – Scatter plot of the coordinates of barycenters in different epochs. X axis traces medio-lateral displacements, while Y axis traces infero-superior displacements. Positive values identify an upward-left displacement, otherwise, negative values are referred to downward-right displacement. Columns are referred to the swallowing phases identified through the accelerometer. Rows are referred to muscular regions of interest. The red ellipse encloses the 90% of the points distribution and is centered in the median of the distribution itself.

At the end, results obtained from the correlation measures showed a high correlation between the magnitude value of the barycenter and the LRI coefficients (*Figure 51*). Statistical analyses led to the result of $p<0.001$, with R values very close to the unity. Results suggested that the LRI could provide reliable information about the symmetry of the muscular activation. The difference between the two methods for the evaluation of the symmetry

muscular activity is the fact that the barycenter shows the direction of the unbalance of its position (left and right referred to the subject). On the contrary, although the LRI indicates with high precision the presence of muscular activity symmetry, it doesn't keep memory of the unbalance side.

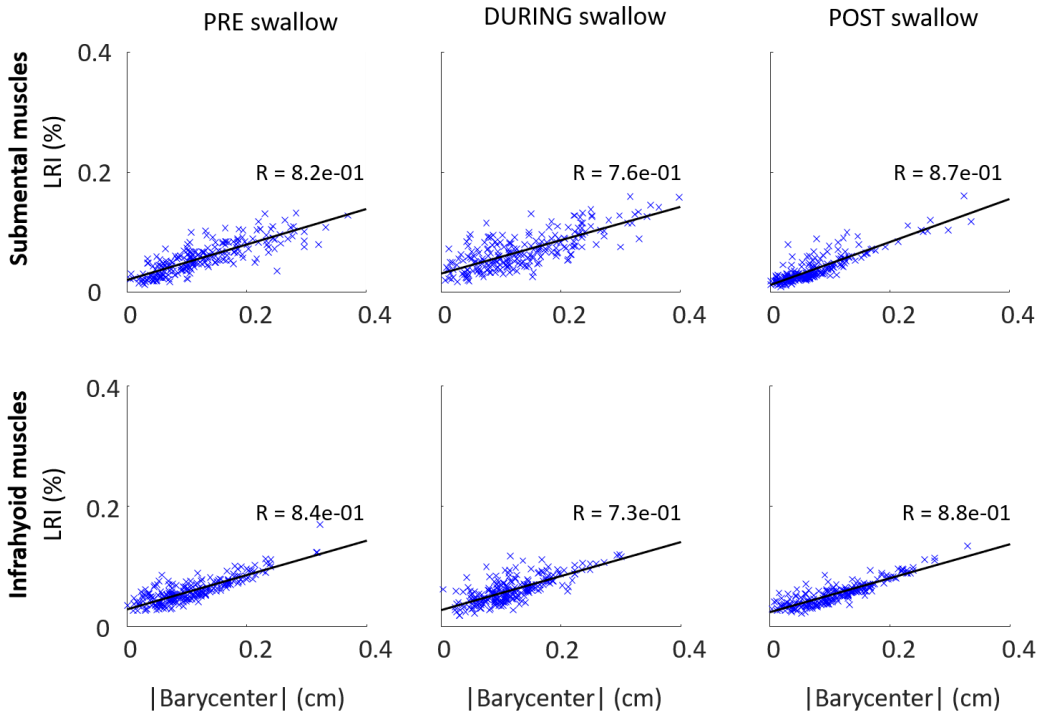

Figure 51 – Pearson correlation measures between the magnitude of the barycenter and the LRI. A representative subject was taken as example. Columns are referred to the segmented swallowing phases, while rows are referred to the muscular regions of interest. Each phase was divided into 15 epochs and barycenters were displayed for one of each. All cases reported p-value less than 0.001.

Amplitude maps The muscular activation patterns derived from the accelerometer-based segmentation were in line not only with physiological, but also with biomechanical events associated to the swallowing activity. In fact, looking at the surface EMG amplitude distributions of a representative subjects (*Figure 52*), the first swallowing phase refers to a period of rest (baseline for the

accelerometric trace) and corresponded to a low amplitude distribution (cold colors). The highest acceleration changes were included in the central swallowing phase relative to the pharyngeal phase of swallowing. During this phase both submental and infrahyoid muscles reached the maximum of their activity and the superimposed barycenters revealed a symmetrical muscular activation between left and right sides. Finally, the last swallowing phase represented the return to the rest condition. Results suggested also the coherence between EMG amplitude distribution and identification of the position of the barycenter of muscular activity.

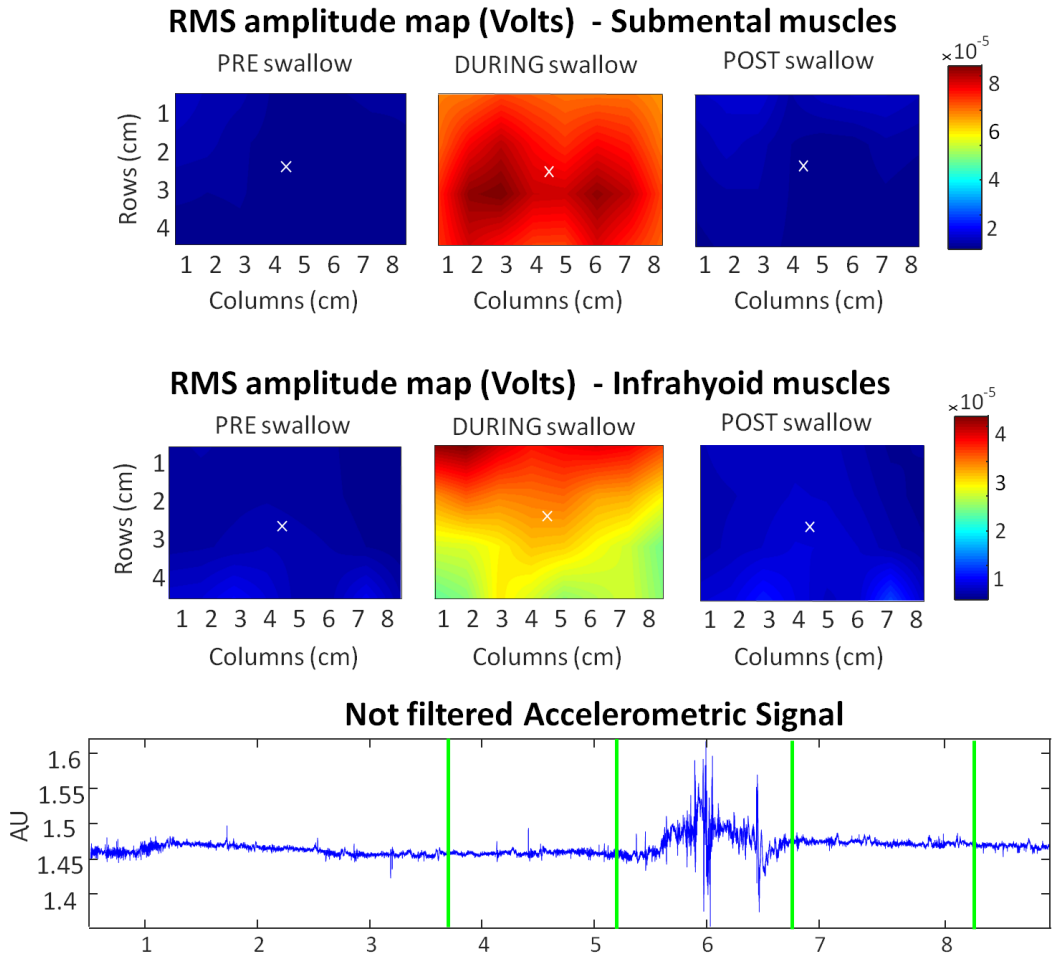

Figure 52 – Surface EMG amplitude distribution (RMS) over the skin on submental and infrahyoid muscles during a swallow of 10 ml of water of a representative subject. Columns are referred to the three different swallowing phases relative to the accelerometer-based segmentation. Common minimum and maximum were considered separately for the two muscular regions. The blue trace represents the not filtered accelerometric signal superimposing green lines referred to time boundaries identified through the swallowing segmentation.

Epochs of interest of the central swallowing phase were reported on *Figure 53* analyzing the sequence of muscular activities. Results suggested that SM muscles activate at the early stages of the swallowing process. On the contrary, infrahyoid muscles activity later extinguishes because of their late activation, since they are involved in the reflexive portion of the swallowing act. Moreover, SM muscles activate with higher intensity with respect to infrahyoid muscles intensity.

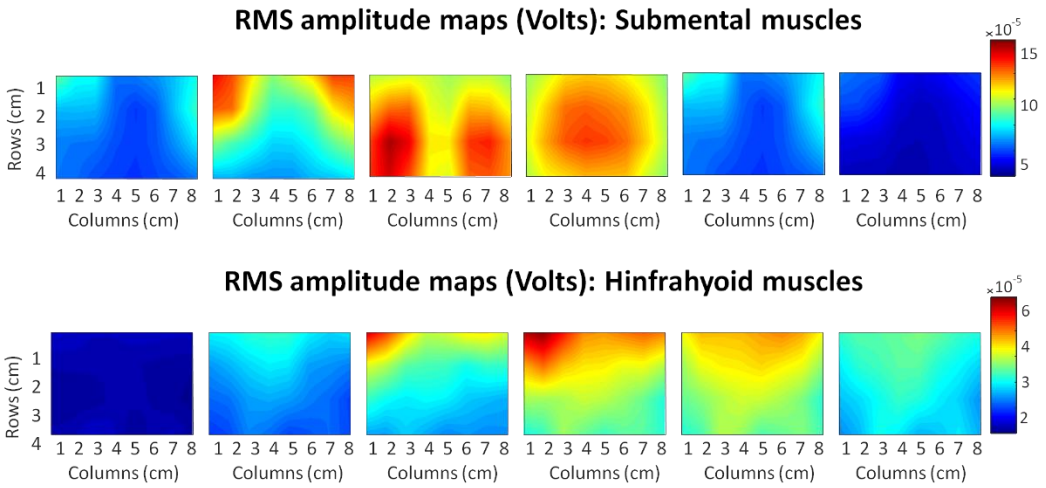

Figure 53 – Surface EMG amplitude distribution (RMS) of 100 ms epochs obtained from the central swallowing phase of the same representative subject of Figure 52.

Chapter 4

Dysphagic patient: a preliminary evaluation

4.1 Inclusion/Exclusion criteria

In order to perform a preliminary evaluation of the proposed experimental setup in patients, a single neurogenic dysphagic patient was recruited. The patient was chosen according to inclusion criteria, as specified in the protocol for the ethic committee:

- Confirmed diagnosis of neurologic impairments by neurologists evaluating clinical and instrumental data relative to the patient;
- Dysphagia diagnosis by speech pathologist by evaluating clinical and instrumental data relatively to the patient;
- 18 years old at least.

Exclusion criteria were:

- Cognitive impairments;

- Positive anamnesis about swallowing impairments due to other diseases with respect to the neurologic pathology;
- Clinical instability;
- Absence of the written consensus.

The recruited subject (male subject, 78 years old), suffered from Parkinson's disease, diagnosed in 2011. Dysphagia resulted from the neurogenic disease. The level of dysphagia was assigned using the DOSS (Dysphagia Outcome and Severity Scale) [44] and it was estimated at the fifth level of the scale (ranging from 1-normal swallowing to 7-severe dysphagia).

4.2 Materials and Methods

The experimental setup is described in paragraph 3.3, without including the FEES. The task, similarly to the validation study, involved: 3 trials with 5 different types of bolus (saliva, 3 ml of water, 10 ml of water, 3 ml of gelled water, 10 ml of gelled water). Mechanical and electrophysiological variables described in paragraph Data Processing3.5 were computed and compared with those of healthy subjects.

Accelerometry Accelerometric traces were processed to provide the swallowing segmentation. The swallowing onset was extracted adopting the threshold method explained in paragraph 3.5.2. Three swallowing macro-phases were extracted, following passages of paragraph 3.5.3. The central region was further divided into 100 ms epochs, for a total of 15 epochs (in 1.5 s).

sEMG Recordings from masseter, SM and infrahyoid muscles were analyzed through: filtering, envelope calculation, bipolar extraction from HD-sEMG recordings – paragraph 3.5.1. Muscular activation patterns were inspected through RMS-based amplitude maps over time.

Barycenter The evaluation of the barycenter of amplitude maps was carried out over time. Coordinates X and Y were computed across different epochs of HD

sEMG signals as mentioned in paragraph 3.5.3. The distribution of the barycenters computed on amplitude maps was superimposed on the points cloud relative to the barycenters distribution of healthy subjects. Moreover, histograms of X and Y coordinates of the barycenter on both muscular regions were analyzed for healthy and dysphagic subjects.

4.3 Results and Discussions

Accelerometry and sEMG Results showed that the pathologic swallowing was not performed through a single muscular activation. In fact, it is divided into two or more events (*Figure 54*). This effect is known as piecemeal deglutition and it consists of consecutive swallows by dividing the bolus into smaller portions [15].

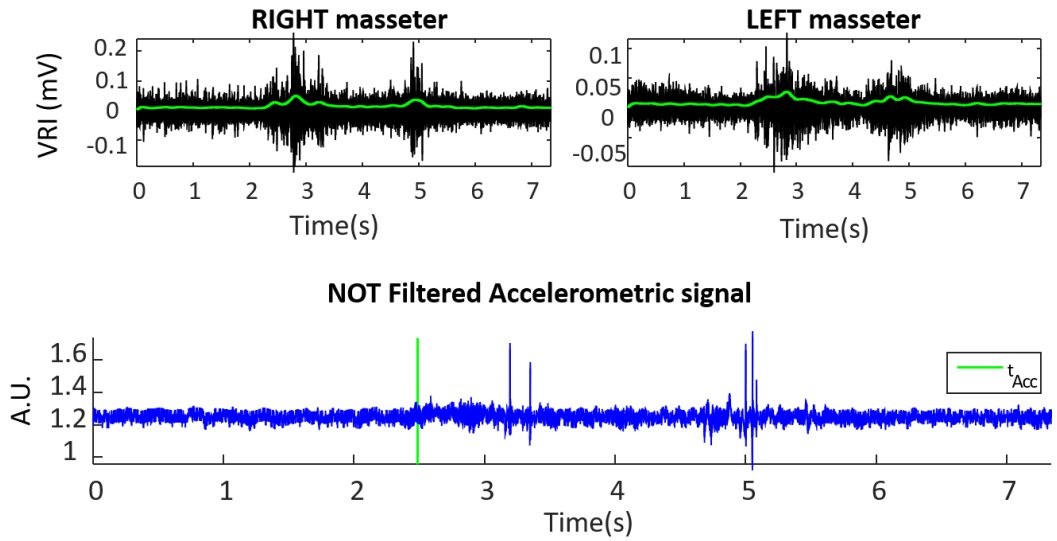

Figure 54 – EMG and accelerometric signals from 7 seconds recordings of a dysphagic subject during swallowing of 3 ml of water. From top to bottom: right and left masseter sEMG signals, not filtered accelerometric signal. Green traces on sEMG signals are the envelopes, while the green line on accelerometric signal refers to the swallowing onset, identified as described in paragraph 3.5.2.

In addition, increasing volumes of bolus resulted in a prolonged muscular activation with multiple swallows, as shown in *Figure 55*.

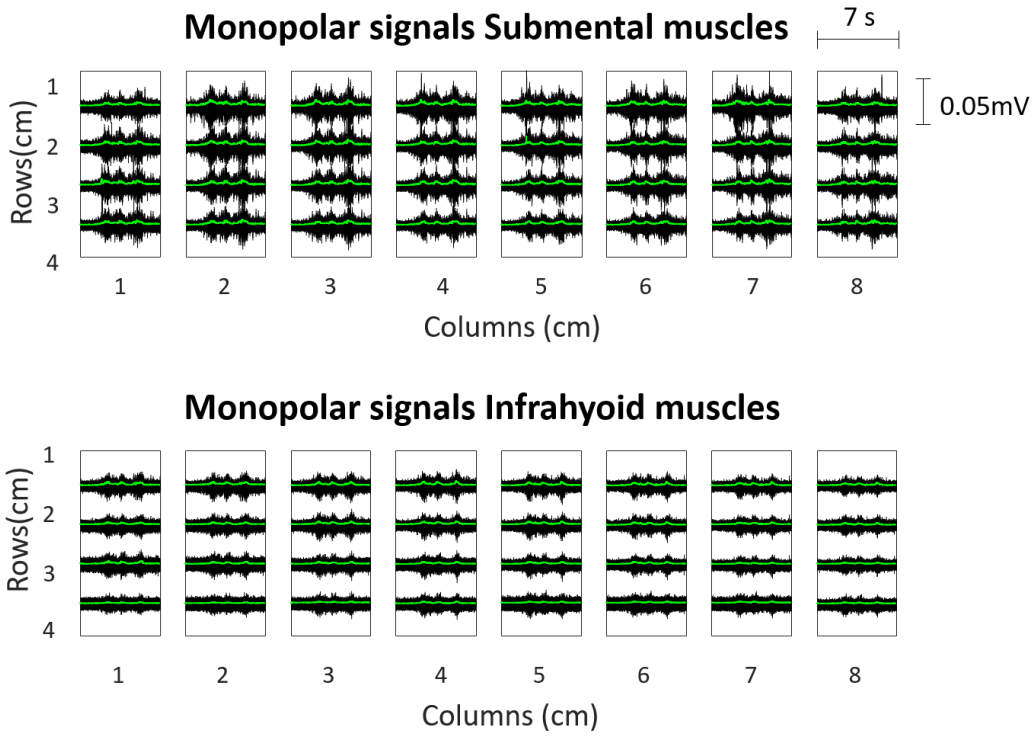

Figure 55 – Monopolar signals recorded from SM and infrahyoid muscles during 7-s recordings of a dysphagic subject during swallowing of 10 ml of water. Green traces are the envelopes computed on single channels.

Barycenter Results from the dysphagic patient suggested the presence of asymmetric muscular activation with respect to healthy subjects. Nevertheless, barycenter displacements were limited to 0.5 cm. Specifically, barycenters of infrahyoid muscles of the dysphagic patient was not enclosed in the ellipse comprising the 90% of the physiologic barycenters. In fact, the dysphagic points cloud is consistently (across epochs) dislocated in the medio-lateral direction (X-axis) with respect to the distribution of healthy subjects' barycenters *(Figure 56)*. On the other hand, the barycenter distribution obtained from the EMG of SM muscles was comparable (although not tested statistically) to that of healthy

group (both infero-superior and medio-lateral directions) The apparent difference between the symmetry of the two muscular regions may be explained by the effects of Parkinsonian symptoms (e.g. bradykinesia, tremor, and dystonia). These factors could result in variable asymmetric muscular activation limited only to a group of muscles. In fact, there is no reason to suppose the same symmetry impairments on both muscular regions, since Parkinson disease doesn't entail the presence of an entire pathologic half-side, differently to other disorders (e.g. stroke).

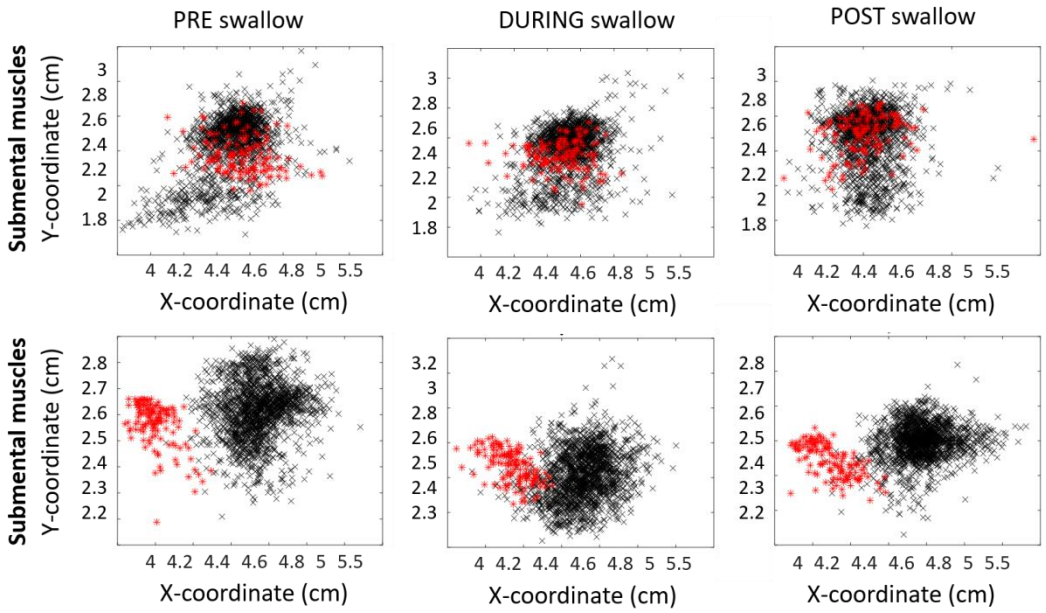

Figure 56 – Barycenters distribution of the patient (red) and the healthy group (black). Columns are referred to the swallowing phases (pre, during and post swallow), while rows are referred to the muscular region (submental and infrahyoid muscles). Positive values identify an upward-left displacement, otherwise, negative values are referred to downward-right displacement.

The analysis of the bar histograms of X coordinate of barycenters of infrahyoid muscles further confirmed the above-described observations for the three swallowing phases. As shown in *Figure 57*, a clear separation between the barycenter x-coordinate distributions of the individual pathological subject and

that of the population of healthy subjects. On the contrary, bar histograms of X coordinate of barycenters showed two overlapped distributions of healthy subjects and dysphagic patient, meaning no difference in terms of barycenters displacements between the two populations (*Figure 57*). In conclusion, this single case study suggests that our experimental approach has the potentiality to highlight or detect deviations of muscular activation from physiologic trends. Nevertheless, a larger pathologic sample size should be taken into account for further analyses for dysphagia assessment and treatment.

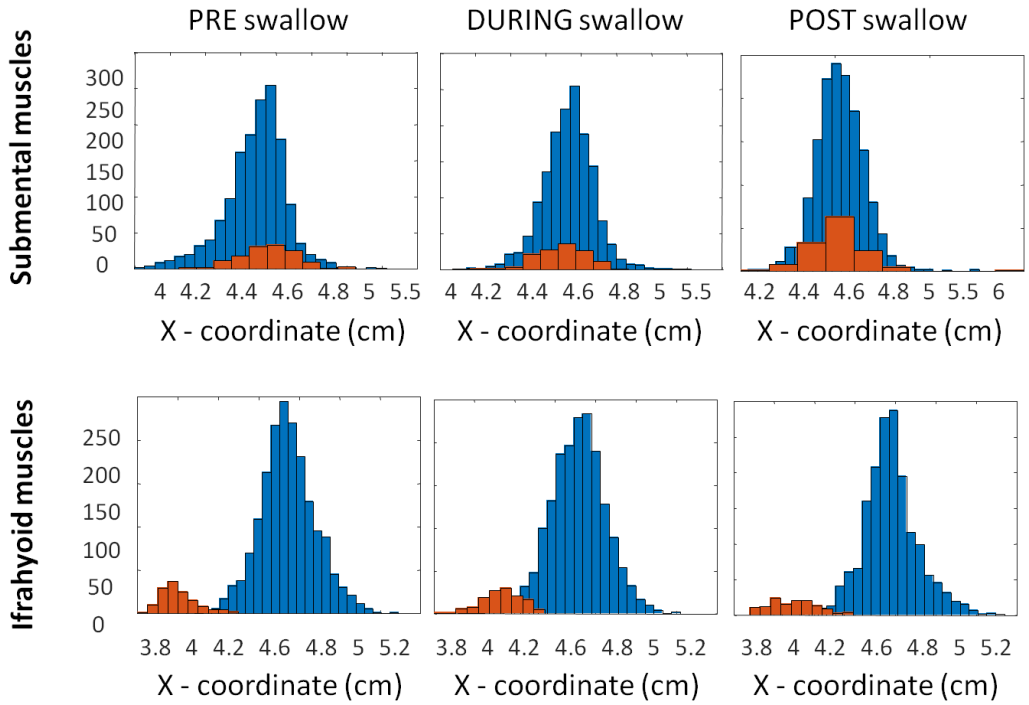

Figure 57 – Bar histograms representation of X coordinate of barycenters of healthy subjects (blue) and a dysphagic patient (orange). Columns are referred to the swallowing phases (pre, during and post swallow), while rows are referred to the muscular region (submental and infrahyoid muscles).

Chapter 5

Conclusions

Swallowing is a complex sensorimotor behavior, involving a large number of muscles and anatomical structures. It consists of a sequence of biomechanical events clearly distinguishable into three stages: oral, pharyngeal and esophageal [1], [3], [5], [6]. Any impairment of the swallowing pathway is referred to as dysphagia. An objective analysis of swallowing structures could be used to understand the physiopathology of swallowing impairment, to target its treatment and quantitatively following its evolution. For a correct understanding of the swallowing process, a complete evaluation of the physiologic swallowing function is necessary.

Currently, conventional bipolar sEMG is used for an electrophysiological evaluation of the swallowing function. The main outcome variable of EMG studies is the left-right muscle activation symmetry, an index based on EMG amplitude of left and right submental and neck muscles. Symmetry index is usually computed without performing any temporal segmentation of the swallowing into the constituent phases, i.e. considering the whole signal. This provide a global symmetry indication that may not reflect local asymmetries in one of the short swallowing phases. The swallowing phases identification is clinically performed through the gold standard of Fiberoptic Endoscopic

Evaluation of Swallowing, a technique that, due to its invasiveness, is rarely used for standard evaluations of swallowing function. It is therefore relevant to identify a method to non-invasively achieve the swallowing segmentation. Another area of possible improvement of the standard clinical approach is the EMG detection. For instance high-density EMG (HD sEMG) has been recently suggested as a method to identify the complex evolution of muscular activation during swallowing [5] and provide more reliable symmetry indexes. The main goal of the project was to define an experimental setup integrating biomechanical and electrophysiological measures in order to (i) non-invasively segment swallowing phases, and (ii) describe the spatiotemporal evolution of muscle activation.

A preliminary feasibility study was performed to explore the possibility to merge the two macro analyses (electrophysiological and mechanical) by combining different measuring systems. An integrated measurement framework comprising accelerometry and surface electromyography (HD sEMG) was developed. The best configuration of electrodes arrays and positioning of the accelerometer were investigated. The most suitable experimental setup was composed by an accelerometer placed on the cricothyroid space and two electrodes arrays for the evaluation of swallowing muscles. Specifically, a grid of 32 electrodes (organized in 4 rows and 8 columns - IED of 10 mm) was used for the submental region, while a custom-made cross shaped grid of 32 electrodes (organized in 4 rows and 8 columns - IED of 10 mm) was used for infrahyoid muscles.

Afterwards, a validation study aimed at the definition of an accelerometer-based swallowing segmentation was performed for the refinement of specific phase-related indexes. Purposes were: (i) to evaluate the estimation of the clinical standard onset using accelerometric traces, (ii) to identify the possible contribution of HD sEMG in the refinement of symmetry indexes, (iii) to evaluate the sequential muscular activation across swallowing phases.

The swallowing onset estimations based on accelerometer were compared to those obtained from the clinical standard FEES. Accelerometry revealed a systematic bias towards an underestimation of the clinical standard swallowing

onset, regardless to the bolus type or volume. Nevertheless, the symmetry index estimation based on the segmentation techniques was not statistically different, suggesting that, in healthy subjects, the observed underestimation is not clinically relevant.

Two alternative methods for the evaluation of muscular activation symmetry based on HD sEMG were proposed: one is a modified version of the symmetry index proposed by Zhu, and the other one is based on the barycenter of the amplitude maps. With respect to previous researches in literature [5], the proposed symmetry analysis takes advantage of the spatial variation of the potential within the swallowing phases.

Finally, the topographical evaluation of muscle activity through HD-sEMG amplitude maps revealed the possibility to track the spatiotemporal activation of muscles of interest with a high degree of detail.

The potentiality of the proposed methods in describing different behaviors between dysphagic patients and healthy subjects was confirmed by a preliminary application of the experimental setup on a patient with swallowing impairments. Clinical studies on a large population of dysphagic subjects are required to ascertain whether these initial and very preliminary results can be generalized to dysphagic patients with different pathologies.

The present study proposed an innovative experimental setup that revealed to be: non-invasive, easy to use, able to provide qualitative and quantitative data for further analyses. Although the complexity of the proposed protocol, implying a high number of electrodes, it improved a similar multichannel approach described in literature [5], where individual electrodes were positioned on the skin surface.

In conclusion, the proposed measurement framework allowed (i) to provide an alternative non invasive approach to identify the swallowing phases, currently performed invasively in clinical settings, (ii) to compute event-related symmetry indexes, improving the global symmetry analysis used in literature, (iii) to identify spatiotemporal evolution of muscular activation with a punctual description of

the swallowing process over time, (iv) to detect deviations from the physiological trends.

Considering the positive methodological improvements on the assessment of the swallowing function on healthy subjects, the integrated experimental framework proposed in this study is ready for a validation on a population of patients with swallowing impairments should be carried out.

Bibliography

[1] K. Matsuo and J. B. Palmer, “Anatomy and Physiology of Feeding and Swallowing : Normal and Abnormal,” *Phys. Med. Rehabil. Clin. NA*, vol. 19, no. 4, pp. 691–707, 2008.

[2] C. Ertekin and J. B. Palmerb, *Physiology and electromyography of swallowing and its disorders*, vol. 53, no. l. Elsevier B.V., 2000.

[3] C. Ertekin and I. Aydogdu, “Neurophysiology of swallowing,” vol. 114, pp. 2226–2244, 2003.

[4] M. Paciaroni, G. Mazzotta, F. Corea, and V. Caso, “Dysphagia following Stroke,” pp. 162–167, 2004.

[5] M. Zhu *et al.*, “Evaluation of normal swallowing functions by using dynamic high‐density surface electromyography maps,” *Biomed. Eng. Online*, 2017.

[6] S. Hamdy, “The anatomy and physiology of normal and abnormal swallowing in oropharyngeal dysphagia,” no. April, pp. 1–15, 2017.

[7] A. L. Perlman and D. Ph, “Dysphagia in Stroke Patients,” vol. 16, no. 4, 1996.

[8] A. G. A. T. Review and O. Dysphagia, “AGA Technical Review on

Management of Oropharyngeal Dysphagia," pp. 455–478, 1999.

[9] R. Martino, N. Foley, S. Bhogal, N. Diamant, M. Speechley, and R. Teasell, "Incidence , Diagnosis , and Pulmonary Complications," pp. 2756–2763, 2005.

[10] F. Movahedi, A. Kurosu, J. L. Coyle, S. Perera, and E. Sejdi, "Anatomical Directional Dissimilarities in Tri-axial Swallowing Accelerometry Signals," vol. 25, no. 5, pp. 447–458, 2017.

[11] K. A. Kendall, S. Mckenzie, R. J. Leonard, M. Ine, and A. Walker, "Timing of Events in Normal Swallowing : A Videofluoroscopic Study," vol. 83, pp. 74–83, 2000.

[12] S. B. Y. Hukuhara, "THE ACTIVITY OF BRAIN-STEM RESPIRATORY NEURONS AND SPINAL RESPIRATORY," 2019.

[13] S. Singh and S. Hamdy, "Dysphagia in stroke patients," pp. 383–392, 2006.

[14] D. Han, Y. Chang, C. Lu, and T. Wang, "Comparison of disordered swallowing patterns in patients with recurrent cortical / subcortical stroke and first-time brainstem stroke COMPARISON OF DISORDERED SWALLOWING PATTERNS IN PATIENTS WITH RECURRENT CORTICAL / SUBCORTICAL STROKE AND FIRST-TIME BRAINSTEM STROKE," no. July 2014, 2005.

[15] G. N. Ali, K. L. Wallace, R. Schwartz, D. J. D. E. Carle, A. S. Zagami, and I. A. N. J. Cook, "Mechanisms of Oral-Pharyngeal Dysphagia in Patients With Parkinson's Disease," pp. 383–392, 1996.

[16] J. G. Kalf, B. J. M. De Swart, B. R. Bloem, and M. Munneke, "Parkinsonism and Related Disorders Prevalence of oropharyngeal dysphagia in Parkinson ' s disease : A meta-analysis," *Park. Relat. Disord.*, vol. 18, no. 4, pp. 311–315, 2012.

[17] A. Spychala, A. Potulska, A. Friedman, and L. Kro, "Swallowing disorders in Parkinson ' s disease," vol. 9, pp. 349–353, 2003.

[18] N. Chaumartin, M. Monville, and B. Lachaux, "Une ou des dysphagies lors d ' un traitement par neuroleptiques ? Dysphagia or dysphagias during neuroleptic medication ?," *Encephale.*, 2012.

[19] L. Kronenberg *et al.*, "Cortical Processing of Swallowing in ALS Patients

with Progressive Dysphagia – A Magnetoencephalographic Study," vol. 6, no. 5, 2011.

[20] C. Ertekin *et al.*, "AN ELECTROPHYSIOLOGICAL INVESTIGATION OF DEGLUTITION," 1995.

[21] G. Drost and D. F. Stegeman, "Clinical applications of high-density surface EMG : A systematic review," vol. 16, pp. 586–602, 2006.

[22] M. J. Zwarts and D. F. Stegeman, "MULTICHANNEL SURFACE EMG : BASIC ASPECTS AND CLINICAL UTILITY," vol. c, no. July, pp. 1–17, 2003.

[23] E. M. Maathuis, J. Drenthen, J. P. Van Dijk, G. H. Visser, and J. H. Blok, "Motor unit tracking with high-density surface EMG," *J. Electromyogr. Kinesiol.*, vol. 18, no. 6, pp. 920–930, 2008.

[24] D. Farina and R. Merletti, "Analysis of motor units with high-density surface electromyography," vol. 18, pp. 879–890, 2008.

[25] T. M. Vieira, A. Botter, S. Muceli, and D. Farina, "Specificity of surface EMG recordings for gastrocnemius during upright standing," *Sci. Rep.*, pp. 1–11, 2017.

[26] T. Fukuoka, T. Ono, K. Hori, Y. Wada, and Y. Uchiyama, "Tongue Pressure Measurement and Videofluoroscopic Study of Swallowing in Patients with Parkinson ' s Disease," *Dysphagia*, 2019.

[27] H. Taniguchi, T. Tsukada, S. Ootaki, Y. Yamada, and M. Inoue, "Correspondence between food consistency and suprahyoid muscle activity , tongue pressure , and bolus transit times during the oropharyngeal phase of swallowing," pp. 791–799, 2019.

[28] K. Schatz and N. Olson, "ENDOSCOPIC AND VIDEOFLUOROSCOPIC EVALUATIONS OF SWALLOWING AND ASPIRATION," pp. 678–681, 1991.

[29] T. Ozdemirkiran, Y. Secil, S. Tarlacı, and C. Ertekin, "An EMG screening method (dysphagia limit) for evaluation of neurogenic dysphagia in childhood above 5 years old," no. 12, 2007.

[30] A. Nacci, F. Ursino, R. La Vela, F. Matteucci, V. Mallardi, and B. Fattori, "Fiberoptic endoscopic evaluation of swallowing (fees): proposal for informed consent," pp. 206–211, 2008.

[31] B.-S. Susan E. Langmore, Ph.D., CCC-SLP, “Endoscopic evaluation of oral and pharyngeal phases of swallowing,” *GI Motil. online*, 2006.

[32] P. J. Kahriias, “TIMING OF GLOTTIC CLOSURE DURING NORMAL SWALLOW,” 1995.

[33] F. Townsend *et al.*, “Coordination of deglutition and phases of respiration : effect of aging , tachypnea , bolus volume , and chronic obstructive pulmonary disease,” 2018.

[34] R. J. Gilbert, “Dynamic Magnetic Resonance Imaging of Vocal Cord Closure During Deglutition,” pp. 843–849, 1995.

[35] M. Nolan, B. Madden, and E. Burke, “Accelerometer Based Measurement for the Mapping of Neck Surface Vibrations During Vocalized Speech,” pp. 4453–4456, 2009.

[36] D. C. B. Zoratto, “Hyolaryngeal excursion as the physiological source of swallowing accelerometry signals Hyolaryngeal excursion as the physiological source of swallowing accelerometry signals,” 2010.

[37] J. Lee, “Time and time – frequency characterization of dual- axis swallowing accelerometry signals Time and time – frequency characterization of dual-axis swallowing accelerometry signals,” 2008.

[38] T. Ono, K. Hori, and T. Nokubi, “Pattern of Tongue Pressure on Hard Palate During Swallowing,” vol. 264, pp. 259–264, 2004.

[39] G. L. Cerone, A. Botter, and M. Gazzoni, “A Modular , Smart , and Wearable System for High Density sEMG Detection,” *IEEE Trans. Biomed. Eng.*, vol. PP, no. c, p. 1, 2019.

[40] T. M. M. Vieira, R. Merletti, and L. Mesin, “Automatic segmentation of surface EMG images : Improving the estimation of neuromuscular activity,” *J. Biomech.*, vol. 43, no. 11, pp. 2149–2158, 2010.

[41] M. Vaiman and E. Eviatar, “Head & Face Medicine Surface electromyography as a screening method for evaluation of dysphagia and odynophagia,” vol. 11, pp. 1–11, 2009.

[42] A. Botter and T. M. Vieira, “Filtered Virtual Reference : A New Method for the Reduction of Power Line Interference With Minimal Distortion of Monopolar Surface EMG,” vol. 62, no. 11, pp. 2638–2647, 2015.

[43] D. A. Mendell and J. A. Logemann, “Temporal Sequence of Swallow Events During the Oropharyngeal Swallow,” vol. 50, no. October, 2007.

[44] K. H. O. Neil, M. Purdy, J. Falk, and L. Gallo, “The Dysphagia Outcome and Severity Scale,” vol. 145, pp. 139–145, 1999.